Physics Reports 679 (2017) 1–60

Contents lists available at ScienceDirect

Physics Reports

journal homepage: www.elsevier.com/locate/physrep

Quantum feedback: Theory, experiments, and applications

Jing Zhang [a,b,*], Yu-xi Liu [c,b], Re-Bing Wu [a,b], Kurt Jacobs [d,e,f], Franco Nori [g,h]

[a] Department of Automation, Tsinghua University, Beijing 100084, PR China

[b] Center for Quantum Information Science and Technology, Tsinghua National Laboratory for Information Science and Technology (TNList), Beijing 100084, PR China

[c] Institute of Microelectronics, Tsinghua University, Beijing 100084, PR China

[d] U.S. Army Research Laboratory, Computational and Information Sciences Directorate, Adelphi, MD 20783, USA

[e] Department of Physics, University of Massachusetts at Boston, Boston, MA 02125, USA

[f] Hearne Institute for Theoretical Physics, Louisiana State University, Baton Rouge, LA 70803, USA

[g] CEMS, RIKEN, Saitama 351-0198, Japan

[h] Physics Department, The University of Michigan, Ann Arbor, MI 48109-1040, USA

ARTICLE INFO

Article history:
Accepted 9 February 2017
Available online 6 March 2017
Editor: D.K. Campbell

Keywords:
Quantum control
Quantum feedback
Quantum optics
Cavity QED
Circuit QED
Optomechanics
Quantum nanoelectromechanics
Quantum information processing

ABSTRACT

The control of individual quantum systems is now a reality in a variety of physical settings. Feedback control is an important class of control methods because of its ability to reduce the effects of noise. In this review we give an introductory overview of the various ways in which feedback may be implemented in quantum systems, the theoretical methods that are currently used to treat it, the experiments in which it has been demonstrated to date, and its applications. In the last few years there has been rapid experimental progress in the ability to realize quantum measurement and control of mesoscopic systems. We expect that the next few years will see further rapid advances in the precision and sophistication of feedback control protocols realized in the laboratory.

Contents

* Corresponding author at: Department of Automation, Tsinghua University, Beijing 100084, PR China.
E-mail address: jing-zhang@mail.tsinghua.edu.cn (J. Zhang).

http://dx.doi.org/10.1016/j.physrep.2017.02.003
0370-1573/

1. Introduction

1.1. History and background

The subject of *control* is concerned with methods to manipulate the evolution of dynamical systems. As such it is relevant to many fields both inside [1–6] and outside [7,8] physics. Control has a long history, but it emerged as a modern scientific discipline only after the pioneering work of Norbert Wiener in the 1940s [9]. Up until the 1960s, control was largely studied by analyzing dynamical systems in the frequency domain (that is, the Laplace transform or the Fourier transform of the evolution). This was a reasonable approach because people were mainly interested in steady-state behavior. So long as the fluctuations about the steady state are sufficiently small, even nonlinear systems can be well-approximated by linear dynamics, and are thus amenable to frequency-domain methods. For networks of linear systems in which the outputs of some systems are connected to the inputs of others, frequency-space methods are also extremely useful, because complex exponentials are the eigenfunctions of all linear systems [10].

Frequency-domain methods were less helpful in understanding how control systems should make use of real-time information, and for this reason control theorists turned to the time domain. The techniques that were developed include the Kalman–Bucy filter [11] and the Hamilton–Jacobi–Bellman equation [12]. These are referred to as state-space methods, and are often referred to as "modern" control theory. Much of modern control theory is concerned with feedback control, in which a control system, or "controller" obtains a stream of information about the trajectory of the system, or "plant", and uses this information in real time to control it. The term "feedback" comes from the notion that the controller is "feeding" the information it obtains "back" to the system. Feedback control is also referred to as "closed-loop" control, because the flow of information to the controller, together with the action taken by the controller to affect the system is thought of as a loop that starts and ends at the system [13–16].

One usually speaks of a controller as trying to achieve some *objective*. This objective may be to have the system reach a given state at a given time, or to have it evolve in a precise way, despite the presence of noise in its inputs or slight errors

in its construction. Given an objective, the central problem in feedback control is to obtain a rule (or mapping) that the controller can use to select the action it should take based on the data it has received. Traditionally such a rule was referred to as a "feedback algorithm", but in quantum control theory the term "feedback protocol" is usually used instead, so as to avoid confusion with the algorithms of quantum computing [17].

The idea of controlling systems using feedback has been around for a long time; the first device on record employing feedback appears to have been the water clock of Ktesibios in the first half of the third century B.C. [18–20]. Another successful example of a feedback mechanism is the Watt governor developed in the 1780s. This centrifugal governor was a core component of the Watt steam engine which fueled the industrial revolution. Incidentally it was Maxwell who first performed a mathematical analysis of this control mechanism [21]. By introducing feedback control one can speed up transient processes, tune the stationary output of a system, and most importantly, reduce the effects of disturbances. The importance of using feedback in controlling a system is that it is the only way to reduce the effects of noise. Noise introduces uncertainty into the system dynamics, and the only way to reduce this uncertainty is to transfer it to another system. To understand this better, consider what happens if we make a measurement on a system. This reduces our uncertainty and allows us to correct the motion. In doing so, we reduce the spread in the state of the system, and thus the randomness in the system. But note that the measuring device must record the result of the measurement, and this result is necessarily as random as the quantity being measured. Thus the measurement and feedback transfers randomness, which is entropy, from the system to the memory of the measuring device. Now the fundamental forces (as we know them to date), and thus all fundamental physical processes, are reversible. While such processes can increase the entropy of a macroscopic system, whose individual states are not accessible, they cannot change the entropy of a microscopic system whose states are accessible (or reduce the entropy of a macroscopic system) without transferring this entropy to another system. The system to which entropy is ultimately transferred is usually a thermal bath. A transfer to a thermal bath would be accomplished, for example, when the memory of the controller is reset to its initial state. In the study of quantum feedback control, it is natural to refer to any process that transfers entropy from the system to the controller as a feedback process.

Feedback control was introduced into quantum dynamics in the early 1980s [22–27], but it was not until the 1990s that it began to be studied and applied in earnest. Naturally the prerequisite for describing continuous-time measurement-based feedback in quantum systems was a description of continuous quantum measurement.

In the 80s and early 90s, a number of authors independently derived equations describing the continuous measurement of quantum systems. Srinivas and Davies [28] appear to have been the first people to write down a formalism giving a complete description of the continuous measurement of a quantum system. They applied the continuous measurement theory developed by Davies [29–31] to obtain a trajectory theory for the continuous measurement of a cavity mode by detecting the photons that leak out of it using a photon counter. This continuous measurement theory for photon counting was the same as the "unraveling" of the master equation for a damped cavity as constructed later by Carmichael [32,33], Dalibard, Castin, and Molmer [34], and Hegerfeldt and Wilser [35]. Since photon counting involves discrete, instantaneous events, the evolution of the density matrix under this kind of continuous measurement is driven by a point process, being a generalization of a Poisson process.

A couple of years after Srinivas and Davies's work, Gisin [36] introduced a stochastic equation for a state vector that reproduced certain properties of measurement, and Diosi [37] introduced a stochastic equation for the quantum state of an open system, both of which were driven instead by Gaussian noise, also referred to as Weiner noise or "the Wiener process". At a similar time, Barchielli and Lupieri [38] obtained an equation describing continuous measurement in the Heisenberg picture, also using the Wiener process.

The stochastic equations introduced by the above authors, that involved Wiener noise, while connected in various ways with measurement, did not give the evolution of the state of knowledge of an observer who is making the measurement. It was Belavkin [39] (building on the work of Stratonovich), Diosi [40,41], and Wiseman and Milburn [42,43] (building on the "quantum trajectory" work of Carmichael [32,33]) who all independently obtained a stochastic differential equation of motion for an observer's state of knowledge for a measurement driven by Wiener noise. While Diosi considered only measurements of pure states, Belavkin, Wiseman, and Milburn considered also mixed states, and the result was the *stochastic master equation* (SME). The SME is the quantum equivalent of the Stratonovich equation that describes the evolution of the observer's state-of-knowledge for a Gaussian continuous measurement on a classical system [44]. (The Kalman–Bucy filter is the special case of the Stratonovich equation for linear systems, in which the measurement is restricted to linear functions of the dynamical variables.) While Diosi considered only measurements on pure states, the other authors considered also mixed states, which makes possible the description of inefficient measurements, and shows how the quantum measurement obtains classical information about the state, thus purifying it in a way that is closely analogous to the action of classical measurements.

It was Belavkin who first presented a mathematical theory of feedback control in quantum systems [45,46]. Since Belavkin had derived quantum continuous measurements as an extension of the theory of classical continuous measurements, where the latter are used heavily in control theory, it was natural for him to consider the application of continuous measurements to feedback control of quantum systems, and to consider adapting the techniques from classical control [39,47]. The highly mathematical nature of Belavkin's work, however, prevented it from being absorbed by the physics community, where applications for these ideas rose in the following decade.

Taking a very different approach to quantum feedback, in 1994 Wiseman and Milburn [48] showed that a Markovian master equation could be derived to describe continuous feedback in quantum systems, if the feedback was given by a

particularly simple function of the stream of measurement results (this kind of feedback is now referred to as Markovian feedback). In 1998, Yanagisawa and Kimura [49] and Doherty and Jacobs [50] introduced the notion of performing feedback using estimates obtained from the SME, in the control literature and physics literature, respectively. Both sets of authors [49,50] showed that for linear systems this class of feedback protocols was equivalent to modern classical feedback control, so that standard results for optimal control could be transferred to quantum systems. This method was in fact that proposed by Belavkin in 1983 in analogy to that used in classical control theory [39,47]. In quantum control, using estimates obtained from the SME is often referred to as Bayesian feedback to distinguish it from Markovian feedback. In the former the measurement results are processed ("filtered") to obtain an estimate of properties of the current state, whereas in the latter the measurement stream is fed back directly.

It is shown in Ref. [51] that feedback mediated by continuous measurements can in fact be implemented without measurements. To see how this works, let us consider two parallel mirrors between which a single mode of the electromagnetic field is trapped (the two mirrors are referred to as an "optical cavity"). The light that leaks out through one of the mirrors can be detected, and the information is used to manipulate the optical mode. Alternatively, the output light can be directed to a mirror of another optical cavity, and thus forms an input for this cavity. If we then connect an output from the second cavity back to the first we have a loop, and light can be made to travel only one way around the loop by the use of optical circulators [52]. For describing this situation the quantum input–output theory developed by Collett and Gardiner is invaluable [53,54]. The process of connecting quantum systems together via free-space one-way traveling-wave fields was first considered by Gardiner [55] and Carmichael [56], where the former called it a "cascade connection". Ref. [51] showed that cascade connections can implement the same feedback control processes as Markovian measurement-based feedback and can perform tasks that the latter cannot [51].

A second notion of feedback control without explicit measurements was introduced by Lloyd in 2000 [57]. He suggested that a unitary interaction between two quantum systems could be used to implement feedback control [57,58]. This can be achieved, for example, by choosing the interaction so as to correlate the two systems, i.e., the controlled system and the controller, whereby the state of the controller is dependent on the state of the system. One then chooses a second interaction in which the evolution of the system depends on the state of the controller. This particular process is equivalent to a measurement followed by a unitary feedback operation that depends upon the measurement result, although coherent feedback processes are not restricted to this form [59,60]. Both kinds of "measurement-free" feedback, that mediated by cascade connections and that which uses unitary interactions are now referred to as *coherent feedback control* (CFC), and the latter is often called "direct" coherent-feedback. All control involving explicit measurements is usually called *measurement-based* feedback control, or just *measurement feedback control* (MFC).

In the 2000s James and his collaborators [61] studied "feedback networks" of linear quantum systems connected by one-way fields, and Gough and James [62] built on input–output theory to construct a compact and convenient formalism to handle arbitrarily complex networks. More recently a number of authors [63–66] have considered the use of nonlinear coherent-feedback networks for various control tasks. In 2009, Nurdin, James, and Peterson [67] showed that linear coherent feedback networks could outperform linear measurement-based feedback, suggesting that measurement-based feedback was limited by the need to reduce the information about a system to classical numbers. It has also been shown quite recently that coherent feedback is able to generate quantum nonlinearities [65,66] and outperform measurement-based feedback in cooling linear resonators with linear controllers [68]. The relationship between measurement-based and coherent feedback is a topic of current research [59].

There are not only fundamental differences between measurement-based and coherent feedback, but also important practical differences. Making measurements on quantum systems, often possessing only a few quanta, usually requires a tremendous amplification of the signal. This is because the measurement results, by definition, are well-defined classical numbers [69]. To robustly store and manipulate such numbers requires states with energies much greater than a single quantum. Amplifying signals at the single-quantum scale without swamping them with noise is a great challenge, and is one major practical disadvantage of measurement-based feedback. A second disadvantage is the timescale required to obtain and then process the measurement results (usually on a digital device). On the other hand, measurement-based feedback has the advantage that the processing of the information is essentially noise-free. By contrast, if a quantum system is used as a controller it will likely be subject to noise processes from its environment. It may also be less clear how to use the quantum system to process the information to achieve a control objective.

It is important to note that the method of "adaptive feedback", in which the term "feedback" is used, is not the feedback control that we are concerned with in this review. Adaptive feedback [8] is a method for obtaining control protocols, not a class of protocols for controlling a system. In this method, one chooses an arbitrary control protocol, tries it out on the system, and based on the result make a modification to the protocol and tries it again. In this way one can use one of many search algorithms to look for a good protocol. People who refer to adaptive feedback as a feedback method distinguish the feedback control we consider here by calling it "real-time feedback control".

It is also important to note that we do not discuss in detail here all the ways in which feedback can be realized. One could, for example, perform a series of "single-shot" measurements with a discrete set of outcomes, and perform a unitary action on the system for each outcome. While there are certainly a range of interesting and non-trivial questions regarding such feedback, such as controlling thermal dynamics [70–74] and quantum error correction [75–81], the mathematical machinery required to analyze it does not require stochastic differential equations. This is also true of coherent feedback implemented via unitary interactions. This latter topic has only recently begun to be explored in earnest, and there are certainly many

open questions [82]. However in this review we focus on continuous-time measurement-based feedback control, coherent feedback mediated by continuous fields that carry the information between system and controller. Both of these require the use of stochastic (Ito) calculus, something that is less familiar to many researchers in quantum theory. While measurement-based feedback requires only the usual Ito stochastic calculus, field-mediated coherent feedback requires a quantum version of Ito calculus developed by Gardiner and Collett as part of their input–output theory [53,83]. The somewhat more general quantum stochastic calculus, that encompasses that of Collett and Gardiner, was also developed independently by Hudson and Parthasarathy in a more rigorous measure-theoretic way [84]. A readily accessible introduction to Ito calculus can be found in [85], and the quantum version is described in [53,54,86].

To distinguish between experiments that realize quantum feedback control rather than classical control, we apply the following criteria. Measurement-based feedback is *quantum* feedback if the dynamics of the system under the feedback loop cannot be explained merely by using Bayes' theorem. Another way to say this is that the *quantum back-action* from the measurement, which is the *dynamical* effect of the measurement on the system, plays a significant role in the system evolution. Coherent feedback is *quantum* feedback if the joint dynamics of the system and controller cannot be described by a classical model. For linear systems, the only distinction between quantum and classical motion is that the joint-uncertainty of position and momentum is limited by Heisenberg's uncertainty principle. A measurement introduces noise because a reduction in the uncertainty of one canonical variable tends to increase the uncertainty of the conjugate variable.

In the remainder of this section we give a brief introduction to classical feedback control. In Section 2 we discuss quantum continuous (weak) measurements and filtering, and their application to quantum measurement-based feedback. In particular we discuss the two ends of the spectrum of measurement-based feedback: the simplest in which the measurement signal is not processed at all before it is fed back to the system ("Markovian" feedback), and that in which the measurement signal is fully processed to obtain the observer's complete state-of-knowledge of the system as it evolves ("Bayesian" feedback). We complete Section 2 by giving an overview of most of the applications of measurement-based feedback that have been considered in the literature to date. In Section 3 we turn to coherent feedback. We discuss the two primary ways in which it can be implemented, and the formalism used to describe them. As with measurement-based feedback, we then review the majority of applications of coherent feedback that have been considered to date. In Section 4 we review two further topics that involve feedback, but not in the way envisioned in the traditional notion of feedback control. In Section 5 we turn to experiments, and give an overview of all experiments to date that have realized continuous feedback control in the quantum regime. These experiments cover a range of physical settings from quantum optics to superconducting circuits. Experiments implementing measurement-based feedback in the quantum regime were initially realized in quantum optics, where it first became possible to measure individual microscopic degrees of freedom with sufficient fidelity. These were followed by experiments involving trapped atoms and ions, and very recently it has become possible to realize measurement-based feedback control in mesoscopic superconducting circuits. Experiments involving continuous coherent feedback were performed prior to those realizing continuous measurement-based feedback, although at the time these experiments were not thought of as involving feedback. An example is the cooling of trapped ions using the "resolved sideband" cooling method [87,88]. In Section 6 we give a perspective on the current state of quantum feedback control and discuss some open questions.

1.2. A glance at classical feedback control

In the engineering discipline called *control theory*, a control system is always broken into three parts [89]:

- The system (or "plant"): the device we want to control, having inputs and outputs;
- The input(s) to the system (or "control"): the entity that we have freedom to choose to affect the system;
- The output(s) of the system (or "yield"): this includes the quantity we want to control, and any quantities we can measure to obtain information about the plant.

As explained above, the explicitly causal structure in which the control system first obtains information from a measurement and uses this to determine the input to the system, is a way of thinking about the interaction between two systems that is conceptually useful for feedback control. One can think about the interaction in this way even if this structure is not explicit in the mathematical description of the interaction. An example in which it is not explicit is in the Hamiltonian description of an interaction.

The usual objective of control is to steer one or more outputs of the plant towards a prescribed behavior against unknown disturbances or noises. As shown in Fig. 1, when the disturbance is known (or can be precisely measured), a feedforward controller can be used to cancel the effects of disturbances at the input side. Otherwise, if the disturbance is unknown (or cannot be precisely measured), a feedback controller must be introduced to adjust the input according to the outputs of the prescribed measurements imposed on the controlled system.

1.2.1. Classical model of a control system

We are concerned with dynamical systems that change continuously in time, and are therefore modeled by differential equations. The standard model of a control system can be written as

$$\dot{x}(t) = F[x(t), u(t)], \quad x(0) = x_0, \tag{1.1}$$

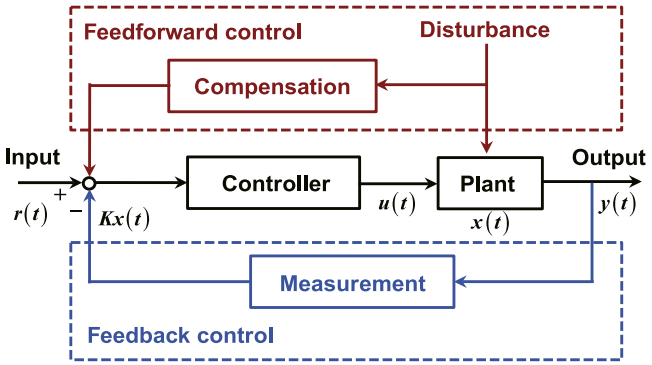

Fig. 1. Basic components in a control system with feedback (bottom loop, in blue) and feedforward (top branch, in red) controllers.

$$y(t) = G[x(t), u(t)], \tag{1.2}$$

where F and G are arbitrary vector-valued functions, the vector $x(t)$ is the state of the system, $u(t)$ is the control (set of inputs) that drives the system, and $y(t)$ is the set of outputs, which is allowed to be some algebraic function of both the state and the input.

In practice, the following linear control system model is favored by control engineers:

$$\dot{x}(t) = Ax(t) + Bu(t), \quad x(0) = x_0, \tag{1.3}$$

$$y(t) = Cx(t), \tag{1.4}$$

in which A, B, and C are constant matrices. This model can be solved analytically, which makes it convenient for design purposes. Many nonlinear systems can be transformed to a linear system under a proper nonlinear coordinate transformation [14]. Such a procedure is called linearization, which is broadly used in the literature. For those systems that cannot be precisely linearized, one can still often approximately linearize them in a small neighborhood of the "working point", using a perturbative technique [89].

The relation between the input and output of a linear control system can be alternatively characterized in the frequency domain by a transfer function obtained by taking the Laplace transform of Eq. (1.1):

$$Y(s) = G(s)U(s), \quad G(s) = C(sI - A)^{-1}B, \tag{1.5}$$

where $U(s)$ and $Y(s)$ are the Laplace transforms of the input $u(t)$ and the output $y(t)$, respectively, and $G(s)$ is the transfer function of the system. Transfer function models are popular in control engineering because they can be constructed directly from the input–output data without having to know the internal structure of the system. The corresponding analysis and design are conceptually simple and can be visualized using Nyquist or Bode plots, which require few computational resources [7].

1.2.2. System analysis and design

Consider the linear control system given by Eqs. (1.3) and (1.4). To implement feedback control, we make the control, $u(t)$, a function of the state $x(t)$, assuming that $x(t)$ can be determined from the measured outputs. To keep the system dynamics linear, we set $u(t) = -Kx(t) + r(t)$, where K is a constant matrix and $r(t)$ is the external input signal. The matrix K is called the feedback *gain*, and the function $r(t)$ is called the *reference signal* or *command signal*, which is sometimes chosen as the reference signal to be tracked by the system output under control. With this choice for $u(t)$, the dynamics of the resulting *closed-loop* system becomes

$$\dot{x}(t) = (A - BK)x(t) + Br(t), \quad y(t) = Cx(t). \tag{1.6}$$

Correspondingly, the closed-loop transfer function from the reference signal, $r(t)$, to the output we wish to control, $y(t)$, becomes

$$G_{\mathrm{CL}}(s) = C(sI - A - BK)^{-1}B. \tag{1.7}$$

The gain matrix and reference signal are together called the *control law*.

Two common control tasks are:

- Regulation: to find a control law that keeps $y(t)$ close to some predetermined function of time.
- Tracking: to find a control law that keeps $y(t)$ close to a time-varying signal that is not known beforehand.

A prerequisite for accomplishing these tasks is that the controlled system is *stable*, and the system's stability considered here is usually quantified by using the concept of *Lyapunov stability*. For linear systems, stability is ensured by choosing the gain matrix K so that the poles of the transfer function lie in the left half of the complex plane, and sufficiently far from the imaginary axis. A central result of control theory for linear systems, referred to as the *pole assignment theorem*, states that one can choose K to place the poles at arbitrary locations in the complex plane if and only if the system is fully controllable, meaning that it is possible to choose K and $r(t)$ to steer the system from any state to the origin. Note that controllability is a property of the control system which only depends on the matrices A and B in Eq. (1.3), and is independent of the control design, i.e., the matrix K and the external input $r(t)$.

1.2.3. Optimal control

In applications, one is often interested in obtaining a given output while using minimal resources [13]. We can formulate this goal as a typical constrained optimization problem. If we define a function that measures how far the output is to the desired output (the error incurred by the control law), and another function that quantifies the resource cost of the inputs, we can attempt to minimize the latter under a constraint on the former. The dynamics of the system is essentially another constraint in this optimization problem. We can alternatively define a single "cost" function that combines the error and resource cost, and attempt to minimize it. A well-motivated form for the cost function J is

$$J[u(t)] = \Phi[x(T)] + \int_0^{\mathrm{T}} L[x(t), u(t)]\,\mathrm{d}t, \tag{1.8}$$

where the differential equation given by Eq. (1.1) is the dynamical constraint.

The theory of optimal control is a beautiful part of modern control theory that can be analyzed with variational methods. In fact, with the above form for J, this theory has the same structure as that of Lagrangian and Hamiltonian mechanics. The reason for this is that the Lagrange equations give the conditions for the minimization of an action, which has the same form as J.

Subject to the restriction given by Eq. (1.1), one can introduce a Lagrangian multiplier $\lambda(t)$, and this turns out to be the "momentum coordinate" conjugate to $x(t)$ in the sense of Hamiltonian mechanics. The (pseudo) Hamiltonian to which this conjugate coordinate corresponds is

$$\mathbf{H}[x(t), u(t)] = L[x(t), u(t)] + \lambda(t)^{\mathrm{T}} F[x(t), u(t)]. \tag{1.9}$$

One can prove that the necessary condition for a control $u(t)$ to be optimal is

$$\left.\frac{\partial \mathbf{H}[x(t), u(t)]}{\partial u(t)}\right|_{u(t)=u_{\mathrm{opt}}(t)} = 0, \tag{1.10}$$

and $x(t)$ and $\lambda(t)$ can be obtained by solving the following conjugate equations

$$\dot{x}(t) = \frac{\partial \mathbf{H}[x(t), u(t)]}{\partial \lambda(t)}, \tag{1.11}$$

$$\dot{\lambda}(t) = -\frac{\partial \mathbf{H}[x(t), u(t)]}{\partial x(t)}. \tag{1.12}$$

From the viewpoint of Lagrangian mechanics, the evolution of the system under the control $u(t)$ minimizes the "action" J.

If the set of admissible controls $u(t)$ is not an open set, the condition (1.10) must be replaced by a more general condition, due to the fact that $u(t)$ can no longer be taken at any point in this set. In this case, the necessary condition under which $u(t)$ is optimal is that $u(t)$ minimizes $\mathbf{H}[x(t), u(t)]$. We can write this condition as

$$u_{\mathrm{opt}}(t) = \arg\left[\min_{u(t)} \mathbf{H}[x(t), u(t)]\right], \tag{1.13}$$

which is referred to as the "Maximum Principle". An alternative technique called dynamical programming can be used to locate the global optimal solutions for $u(t)$ by solving the so-called Hamiltonian–Jacobi–Bellman equation [86], but requires much higher computation resources than solving Eq. (1.10) or (1.13). All these approaches merely provide necessary conditions for optimality.

1.2.4. Fighting disturbances and uncertainties

So far we have not included the effects of uncertainty or noise in the system control model, but we have to do so if the controller is to combat them. If the system is driven by a noise of which the spectrum is known, we can include this noise in the model of the system, and explicitly calculate the observer's estimate of the system state derived from a measurement process in real-time. Feedback control can then be implemented based on this estimate. Sometimes it is possible to minimize

the noise in a subset of system variables at the expense of others, which is analogous to the squeezing of an optical beam or a quantum oscillator.

Alternatively, there may be uncertainties in the parameters that determine the dynamics of the system. If we consider a linear system whose equation of motion has the form $\dot{x} = Ax + f(t)$, there are two distinct ways to show the uncertainty in the system parameters. First, the driving term $f(t)$ may contain unknown or partially known parameters, such as the phase or amplitude of a sinusoidal drive. This is very similar to a time-variant noise driving the system, except that in this case a continuous measurement imposed on the system will provide sufficient information to estimate the values of the unknown parameters, and thus reduce the parametric uncertainty. Second, there may exist uncertainty in the system dynamical matrix A, due to which the oscillation frequencies of the system are partially unknown. Such parametric uncertainty is often referred to as *model uncertainty*. Once again a measurement can be used to extract information about A, and then one can implement a feedback control with a gain matrix K and reference signal $r(t)$ to minimize the effects induced by the model uncertainty. A control law that maintains a specific performance under (bounded) variations in the system parameters is referred to as being *robust*. Such robust control problems have stimulated a rich body of studies in the literature [90].

2. Quantum measurement-based feedback

As a first example we consider feedback based on the results of a von Neumann measurement. Each outcome of a von Neumann measurement projects a system into one of a set of basis states. For each of these states we are then able to perform a different unitary operation on the system. This form of measurement-based feedback does have important applications, an example of which is quantum error correction [75–81]. The simplest example of error-correction is the three-qubit "bit-flip" code, in which the state of a single logical qubit is encoded in three physical qubits by using the mapping $|0\rangle \rightarrow |\bar{0}\rangle = |000\rangle$ and $|1\rangle \rightarrow |\bar{1}\rangle = |111\rangle$. If any one of the physical qubits suffers from an error that flips the states $|0\rangle$ and $|1\rangle$, then this error can be corrected without otherwise disturbing the joint state of the three qubits. This correction is achieved by making a measurement that tells us about the total parity of each pair of adjacent qubits. To do this we make two measurements, one of which projects the state onto one of the eigenstates of $M_0 = \sigma_z \otimes \sigma_z \otimes I$ and the other onto the eigenstates of $M_1 = I \otimes \sigma_z \otimes \sigma_z$. From the two measurement outcomes we can determine which bit has flipped, and thus apply a σ_x operator to that qubit to correct the error. For example, if the two measurements return even and odd parity, respectively, then it is the third qubit that has flipped, and the feedback operation that corrects the error is the unitary operator $I \otimes I \otimes \sigma_x$ [75,91,92]. Since this error-correction code can correct a flip error on any single qubit, it is only if an error occurs on two or more of the physical qubits that the logical qubit will be corrupted. If the errors on each of the physical qubits are independent, and occur with a probability $p \ll 1$, then the probability of an error on two or more qubits is proportional to p^2, which is much less than p.

Maxwell's famous demon is another simple example of quantum feedback, and one that can be usefully analyzed in terms of von Neumann measurements. The "demon" is a device that makes measurements on a system and uses the information obtained to extract work [70–74].

2.1. Continuous quantum measurements

2.1.1. Quantum trajectories

A simple, albeit less rigorous way to represent continuous measurements is the "quantum trajectory" approach [33,93,94], a term coined by *Carmichael* [33]. In this approach, the evolution of the density matrix conditioned on the stream of measurement results (the "measurement record"). Before the development of the quantum trajectory approach, most of the initial studies involving quantum systems interacting with a bath considered only the ensemble description, in which one discards the measurement record, and thus calculates only the evolution of the system averaged over all possible records. This was all that was required before experimental techniques made it possible to observe single quantum systems in real-time. However, with the experimental progress, especially in optical systems and ion traps in the 1990s, it became necessary to describe the evolution of a system for an individual measurement record.

One of the early approaches to obtaining a quantum trajectory for a given measurement record was to express the quantum master equation as an average over a stochastic evolution for a pure quantum state [34,35]. This is equivalent to the use of a "Monte Carlo" method to simulate the master equation [95]. Carmichael referred to the process of expressing a master equation as the average of a stochastic evolution as *unraveling* it. For a single master equation there is more than one stochastic equation that will unravel it, and it can be unraveled by stochastic equations driven either by Gaussian white noise (Wiener noise) [94,96,97] or by a "point process" [28,34,93,98]. A point process consists of intervals of smooth (deterministic) motion, punctuated by instantaneous events in which the state of the system changes discontinuously. The Poisson process is an example of a point process. The different stochastic equations correspond to different ways in which the system can be continuously monitored.

1. *Quantum jumps:*

Before presenting the general form of quantum-jump continuous measurement, we first consider a simple example shown in Fig. 2(a). As shown in Fig. 2(a), the light that leaks out of an optical cavity is measured by a photon-counter [99,100]. Here, the electromagnetic field outside the cavity, into which the cavity light leaks, can be taken to be a white-noise

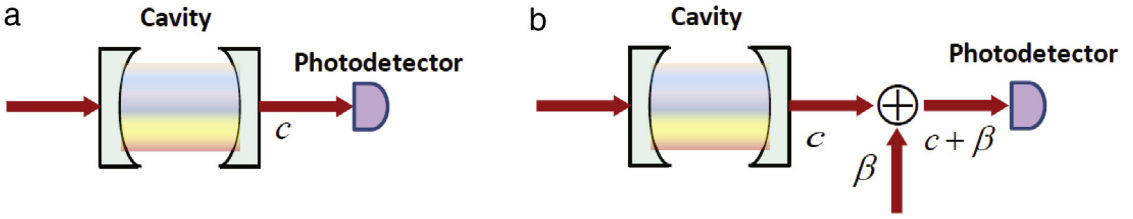

Fig. 2. (a) Diagram for the direct detection of an optical cavity: the optical field leaking out of the cavity carries the information of the intracavity field c and is then detected by a photodetector. (b) Diagram for the homodyne detection of an optical cavity: the output field from the cavity interferes with a laser (called "local oscillator") with complex amplitude β, and the strength of the laser is much stronger than the cavity output. The combined field is then detected by a photodetector.

bath. The optical cavity with free Hamiltonian H is coupled to this white-noise bath via its annihilation operator c. The white-noise bath can be represented by the bath operator $b_0(t)$ with δ-type commutation relation

$$[b_0(t), b_0(t')] = \delta(t - t'). \tag{2.1}$$

In this case, the total Hamiltonian of the cavity and the bath can be represented by

$$H_{\rm tot} = H - i\sqrt{\gamma}\left(c^\dagger b_0 - b_0^\dagger c\right), \tag{2.2}$$

where $\sqrt{\gamma}$ is the coupling strength between the cavity and the bath. Let us assume that the bath is initially in the vacuum state $|0\rangle\langle 0|$, and then introduce the Born approximation by which the state of the cavity at time t, i.e., $\rho(t)$, is disentangled from the bath. Let us redefine the bath operator as $a = \sqrt{dt}\, b_0$ which satisfies a normalized commutation relation and let dt be the infinitesimal time interval. By expanding our expressions up to the linear terms of dt, the state of the total system at time $t + dt$ can be calculated by

$$\begin{aligned}
R(t+dt) &= \exp\left(-iH_{\rm tot}\, dt\right) |0\rangle\langle 0| \otimes \rho(t) \exp\left(iH_{\rm tot}\, dt\right) \\
&= \exp\left[\left(a^\dagger c - c^\dagger a\right)\sqrt{\gamma dt} - iH dt\right] |0\rangle\langle 0| \otimes \rho(t) \exp\left[-\left(a^\dagger c - c^\dagger a\right)\sqrt{\gamma dt} + iH dt\right] \\
&= \left[1 + \left(a^\dagger c - c^\dagger a\right)\sqrt{\gamma dt} + \left(-iH - \frac{\gamma}{2} c^\dagger c a^\dagger a\right) dt\right] |0\rangle\langle 0| \\
&\quad \otimes \rho(t) \left[1 - \left(a^\dagger c - c^\dagger a\right)\sqrt{\gamma dt} + \left(iH - \frac{\gamma}{2} c^\dagger c a^\dagger a\right) dt\right] \\
&= |0\rangle\langle 0| \otimes \rho(t) + \sqrt{\gamma dt}\left[|1\rangle\langle 0| \otimes c\rho(t) + |0\rangle\langle 1| \otimes \rho(t) c^\dagger\right] - i\, dt\, |0\rangle\langle 0| \otimes [H, \rho(t)] \\
&\quad + \gamma dt \left\{|1\rangle\langle 1| \otimes c\rho(t)c^\dagger - |0\rangle\langle 0| \otimes \frac{1}{2}\left[c^\dagger c \rho(t) + \rho(t) c^\dagger c\right]\right\}.
\end{aligned} \tag{2.3}$$

Here $\otimes$ is the notation for the tensor product. If we ignore the output bath, the state of the cavity should be that obtained by taking an average over all possible states of the bath, and thus it should be

$$\rho(t+dt) = \langle 0|R(t+dt)|0\rangle + \langle 1|R(t+dt)|1\rangle = \rho(t) + dt\left\{-i[H, \rho(t)] + \gamma\left[c\rho(t)c^\dagger - \frac{1}{2}c^\dagger c\rho(t) - \frac{1}{2}\rho(t)c^\dagger c\right]\right\},$$

which leads to the following unconditioned master equation

$$\dot{\rho} = -i[H, \rho(t)] + \gamma\left[c\rho(t)c^\dagger - \frac{1}{2}c^\dagger c\rho(t) - \frac{1}{2}\rho(t)c^\dagger c\right]. \tag{2.4}$$

Let us then consider the system evolution conditioned on the state of the output bath. From Eq. (2.3), we can introduce the following operators

$$M_0(dt) = 1 - \left(iH + \frac{\gamma}{2}c^\dagger c\right) dt, \quad M_1(dt) = \sqrt{\gamma dt}\, c. \tag{2.5}$$

When the state of the output bath is $|0\rangle\langle 0|$, the state of the cavity is

$$\begin{aligned}
\rho_0(t+dt) &= \frac{M_0(dt)\rho_{\rm c}(t)M_0^\dagger(dt)}{{\rm tr}\left(M_0^\dagger(dt)M_0(dt)\rho_{\rm c}(t)\right)} = \frac{\rho_{\rm c}(t) - i[H, \rho_{\rm c}(t)] - \gamma\left[\frac{1}{2}c^\dagger c\rho_{\rm c}(t) + \frac{1}{2}\rho_{\rm c}(t)c^\dagger c\right] dt}{1 - \gamma\, {\rm tr}\left[c^\dagger c\rho(t)\right] dt} \\
&= \left\{\rho_{\rm c}(t) - i[H, \rho_{\rm c}(t)] - \left[\frac{\gamma}{2}c^\dagger c\rho_{\rm c}(t) + \frac{\gamma}{2}\rho_{\rm c}(t)c^\dagger c\right] dt\right\}\left\{1 - \gamma\, {\rm tr}\left[c^\dagger c\rho(t)\right] dt\right\} \\
&= \rho_{\rm c}(t) - i[H, \rho_{\rm c}(t)] - \left[\frac{\gamma}{2}c^\dagger c\rho_{\rm c}(t) + \frac{\gamma}{2}\rho_{\rm c}(t)c^\dagger c\right] dt + \gamma\, {\rm tr}\left[c^\dagger c\rho(t)\right]\rho_{\rm c}(t) dt.
\end{aligned} \tag{2.6}$$

Here the subscript "c" denotes the state conditioned on the measurement output. When the state of the output bath is $|1\rangle\langle 1|$, the state of the cavity is

$$\rho_1(t+dt) = \frac{M_1(dt)\rho_c(t)M_1^\dagger(dt)}{\mathrm{tr}\left(M_1^\dagger(dt)M_1(dt)\rho_c(t)\right)} = \frac{c\rho_c(t)c^\dagger}{\mathrm{tr}\left[c^\dagger c\rho_c(t)\right]}. \tag{2.7}$$

The final system state at time $t+dt$, conditioned on the state of the output bath, can be represented by

$$\begin{aligned}\rho_c(t+dt) &= [1-dN(t)]\rho_0(t+dt) + dN(t)\,\rho_1(t+dt)\\ &= \rho_c(t) + \left\{\frac{c\rho_c(t)c^\dagger}{\mathrm{tr}\left[c^\dagger c\rho_c(t)\right]} - \rho_c(t)\right\} dN(t) - i[H,\rho_c(t)] - \left[\frac{\gamma}{2}c^\dagger c\rho_c(t) + \frac{\gamma}{2}\rho_c(t)c^\dagger c\right]dt\\ &\quad + \gamma\,\mathrm{tr}\left[c^\dagger c\rho(t)\right]\rho_c(t)dt.\end{aligned} \tag{2.8}$$

Here $dN(t)$ is the stochastic increment of a point process, which takes one of the two values 0 or 1 at any given time, and thus satisfies $[dN(t)]^2 = dN(t)$. The times at which $dN = 1$ correspond to the detection of a photon by the photodetector. The above equation (2.8) leads to the following stochastic master equation

$$d\rho_c = \mathcal{G}[c]\,\rho_c dN(t) + \mathcal{H}\left[-iH - \frac{\gamma}{2}c^\dagger c\right]\rho_c dt. \tag{2.9}$$

The superoperators $\mathcal{G}[r]\,\rho_c$ and $\mathcal{H}[r]\,\rho_c$ are defined as

$$\begin{aligned}\mathcal{G}[r]\,\rho_c &= \frac{r\rho_c r^\dagger}{\mathrm{tr}\left[r\rho_c r^\dagger\right]} - \rho_c,\\ \mathcal{H}[r]\,\rho_c &= r\rho_c + \rho_c r^\dagger - \mathrm{tr}\left[\left(r+r^\dagger\right)\rho_c\right]\rho_c.\end{aligned} \tag{2.10}$$

When we take an average over the stochastic noise dN, the conditioned stochastic master equation (2.9) becomes the unconditioned master equation (2.4), and thus it can be shown that $E[dN(t)] = \gamma\mathrm{tr}[c^\dagger c\rho(t)]dt$, in which $E[\cdot]$ denotes the ensemble average over the stochastic noise.

Additionally, if the state of the cavity at time t is a pure state $|\psi_c(t)\rangle$, then the state of the cavity at time $t+dt$ is

$$\begin{aligned}|\psi_0(t+dt)\rangle &= \frac{M_0(dt)|\psi_c(t)\rangle}{\sqrt{\langle M_0^\dagger(dt)M_0(dt)\rangle}} = \frac{\left[1-\left(iH+\frac{\gamma}{2}c^\dagger c\right)dt\right]|\psi_c(t)\rangle}{\sqrt{1-\gamma\langle c^\dagger c\rangle dt}}\\ &= \frac{\left[1-\left(iH+\frac{\gamma}{2}c^\dagger c\right)dt\right]|\psi_c(t)\rangle}{1-\frac{\gamma}{2}\langle c^\dagger c\rangle dt} = \left[1-\left(iH+\frac{\gamma}{2}c^\dagger c\right)dt\right]\left(1+\frac{\gamma}{2}\langle c^\dagger c\rangle dt\right)|\psi_c(t)\rangle\\ &= |\psi_c(t)\rangle + \left[-iH+\frac{\gamma}{2}\left(\langle c^\dagger c\rangle - c^\dagger c\right)\right]|\psi_c(t)\rangle\,dt,\end{aligned}$$

when the state of the bath is $|0\rangle$. Here $\langle\cdot\rangle = \langle\psi_c(t)|\cdot|\psi_c(t)\rangle$. When the state of the bath is $|1\rangle$, the state of the cavity at time $t+dt$ is

$$|\psi_1(t+dt)\rangle = \frac{M_1(dt)|\psi_c(t)\rangle}{\sqrt{\langle M_1^\dagger(dt)M_1(dt)\rangle}} = \frac{c}{\langle c^\dagger c\rangle}|\psi_c(t)\rangle.$$

Thus, the final state of the cavity at time $t+dt$ can be written as

$$\begin{aligned}|\psi_c(t+dt)\rangle &= [1-dN(t)]\,|\psi_0(t)\rangle + dN(t)|\psi_1(t)\rangle\\ &= |\psi_c(t)\rangle + \left(\frac{c}{\langle c^\dagger c\rangle(t)} - 1\right)|\psi_c(t)\rangle\,dN(t) + \left[-iH+\frac{\gamma}{2}\left(\langle c^\dagger c\rangle(t) - c^\dagger c\right)\right]|\psi_c(t)\rangle\,dt,\end{aligned}$$

by which we can obtain the following stochastic master equation

$$d|\psi_c\rangle = \left[-iH+\frac{\gamma}{2}\left(\langle c^\dagger c\rangle(t) - c^\dagger c\right)\right]|\psi_c\rangle\,dt + \left(\frac{c}{\sqrt{\langle c^\dagger c\rangle(t)}} - 1\right)|\psi_c\rangle\,dN(t). \tag{2.11}$$

In the above discussion, we have assumed that the photodetector is ideal, meaning that it never misses a photon, and never clicks when there is no photon. Under this condition, an initially pure state remains pure, and the SSE is sufficient to describe the observer's state-of-knowledge as the measurement proceeds. But if the photodetector is not perfect, the observer no longer has full information about the quantum state as the measurement proceeds [101,102]. The observer's state-of-knowledge is then necessarily given by a density matrix, and we must use a stochastic master equation (SME), rather than a Schrödinger equation. We must also modify the master equation to include imperfect detection. If the photodetector

is inefficient, so that it records only a fraction η of the photons emitted by the cavity, and does not record any non-existent photons, then the SME in Eq. (2.9) should be modified as

$$d\rho_{\rm c} = \left\{ dN\mathcal{G}\left[\sqrt{\gamma\eta}a\right] + dt\mathcal{H}\left[-iH - \frac{\eta\gamma}{2}a^\dagger a\right] + dt\,(1-\eta)\,\mathcal{D}\left[\sqrt{\gamma}a\right]\right\}\rho_{\rm c}, \tag{2.12}$$

where

$$\mathcal{D}\left[c\right]\rho = c\rho c^\dagger - \frac{1}{2}c^\dagger c\rho - \frac{1}{2}\rho c^\dagger c. \tag{2.13}$$

For more general case of quantum-jump continuous measurement, let us consider the following measurement-induced unconditioned master equation

$$\dot{\rho} = -i[H,\rho] + \frac{1}{2}\sum_\mu \gamma_\mu \left(2c_\mu \rho c_\mu^\dagger - c_\mu^\dagger c_\mu \rho - \rho c_\mu^\dagger c_\mu\right). \tag{2.14}$$

The quantum continuous measurement represented by the above master equation can be written using the general representation of a quantum measurement that is often referred to as a positive-operator-valued-measure (POVM). A POVM is a set of measurement operators $\{M_{\tilde{\mu}}\}$ such that

$$\sum_{\tilde{\mu}} M_{\tilde{\mu}}^\dagger M_{\tilde{\mu}} = I, \tag{2.15}$$

where I is the identity operator. Each of the operators $M_{\tilde{\mu}}$ plays the role that a projector plays in a simple von Neumann measurement in projecting the system onto the final state. Let us denote the state of the system before and after the measurement as $\rho_{\rm before}$ and $\rho_{\rm after}$, respectively. If a measurement described by the above POVM is made, and the observer is ignorant of the measurement result $\tilde{\mu}$, then we have

$$\rho_{\rm after} = \sum_{\tilde{\mu}} M_{\tilde{\mu}}\ \rho_{\rm before}\ M_{\tilde{\mu}}^\dagger. \tag{2.16}$$

By taking a set of measurement operators

$$M_0(dt) = 1 - \left(iH + \frac{1}{2}\sum_{\tilde{\mu}}\gamma_\mu c_\mu^\dagger c_\mu\right)dt, \quad M_\mu(dt) = \sqrt{\gamma_\mu dt}\,c_\mu, \tag{2.17}$$

the quantum continuous measurement given by the master equation (2.14) can be seen as being given by an infinitesimal POVM, in the sense that

$$\rho(t+dt) = M_0(dt)\,\rho(t)\,M_0^\dagger(dt) + \sum_\mu M_\mu(dt)\,\rho(t)\,M_\mu^\dagger(dt), \tag{2.18}$$

where $\rho(t+dt)$ and $\rho(t)$ are the solutions of Eq. (2.14) at $(t+dt)$ and t.

A stochastic equation that unravels the master equation (2.14), and that is driven by a point process, is [100]

$$d|\psi_{\rm c}\rangle = \left[-iH + \frac{1}{2}\sum_\mu \gamma_\mu\left(\langle c_\mu^\dagger c_\mu\rangle(t) - c_\mu^\dagger c_\mu\right)\right]|\psi_{\rm c}\rangle\,dt + \sum_\mu\left(\frac{c_\mu}{\sqrt{\langle c_\mu^\dagger c_\mu\rangle(t)}} - 1\right)|\psi_{\rm c}\rangle\,dN_\mu. \tag{2.19}$$

The notation $\langle c_\mu^\dagger c_\mu\rangle = \langle\psi_{\rm c}|c_\mu^\dagger c_\mu|\psi_{\rm c}\rangle$ represents the average of $c_\mu^\dagger c_\mu$ over the state $|\psi_{\rm c}\rangle$ given by Eq. (2.19), which means that the Eq. (2.19) is a nonlinear stochastic differential equation and thus is different from usual Schrödinger equation which is a linear equation of the quantum state. That is one of the most interesting features of the stochastic differential equation (2.19) and leads to various effects such as state localization by quantum measurement. In Eq. (2.19), for each μ, the increment dN_μ is an increment of a point process, and takes only two values, either 0 or 1. The value 1 corresponds to an instantaneous event, and thus dN_μ is equal to 1 only at a set of discrete points. The rest of the time $dN_\mu = 0$. The events occur randomly and independently, and the probability per unit time that an event occurs for the process labeled by μ is $\gamma_\mu\langle c_\mu^\dagger c_\mu\rangle(t)$. This means that the probability for an event in the time interval $[t, t+dt]$ is $\gamma_\mu\langle c_\mu^\dagger c_\mu\rangle dt$. The point-process increments satisfy the relations

$$E\left[dN_\mu(t)\right] = \gamma_\mu\langle c_\mu^\dagger c_\mu\rangle dt, \qquad dN_\mu dN_\nu = dN_\mu\delta_{\mu\nu}, \tag{2.20}$$

where the average $E(dN_\mu)$ is in fact a conditional expectation of the classical stochastic process dN_μ conditioned on all the past-time measurement outputs. Since Eq. (2.19) is a stochastic equation for the state vector, it is usually called a *stochastic*

Schrödinger equation. We can alternatively write down a *stochastic master equation* for the density matrix $\rho_c = |\psi_c\rangle\langle\psi_c|$, which is [100]

$$d\rho_c = \sum_\mu \mathcal{G}\left[c_\mu\right]\rho_c dN_\mu(t) + \mathcal{H}\left[-iH - \frac{1}{2}\sum_\mu \gamma_\mu c_\mu^\dagger c_\mu\right]\rho_c dt. \tag{2.21}$$

2. *Quantum diffusion:*

The master equation given by Eq. (2.14) is also unraveled by the SSE [42,94,96,97,103]

$$d|\psi_c\rangle = -iH|\psi_c\rangle dt + \sum_\mu \gamma_\mu\left(\langle c_\mu^\dagger\rangle c_\mu - \frac{1}{2}c_\mu^\dagger c_\mu - \frac{1}{2}\langle c_\mu^\dagger\rangle\langle c_\mu\rangle\right)|\psi_c\rangle dt + \sum_\mu \sqrt{\gamma_\mu}\left(c_\mu - \langle c_\mu\rangle\right)|\psi_c\rangle dW_\mu, \tag{2.22}$$

where the dW_μ are a set of mutually independent Wiener noises satisfying

$$E\left(dW_\mu\right) = 0, \qquad dW_\mu dW_\nu = \delta_{\mu\nu}dt. \tag{2.23}$$

The equivalent stochastic master equation is

$$d\rho_c = -i\left[H, \rho_c\right]dt + \sum_\mu\left(\gamma_\mu \mathcal{D}\left[c_\mu\right]\rho_c dt + \sqrt{\gamma_\mu}\,\mathcal{H}\left[c_\mu\right]\rho_c\, dW_\mu\right). \tag{2.24}$$

Stochastic SSEs and SMEs driven by Wiener noise correspond to measurement techniques that are quite different from photon-counting. An important example is the measurement system shown in Fig. 2(b). In this case, instead of detecting the light from a cavity with a photodetector directly, one first interferes the light with a laser (traditionally called local oscillator in the literature) whose intensity is much greater than the cavity output. This measurement technique is sensitive to the phase of the cavity output, whereas direct photo-detection is not, and is called *homodyne detection* [42,99]. If we assume that the phase difference between the output light from the cavity and the local oscillator is zero, the SME describing homodyne detection can be obtained from Eq. (2.9) by replacing the operator c by $(c + \beta)$, giving

$$d\rho_c = \mathcal{G}\left[c + \beta\right]\rho_c\, dN(t) + \mathcal{H}\left[-iH - \beta\gamma c - \frac{\gamma}{2}c^\dagger c\right]\rho_c dt, \tag{2.25}$$

in which β is the amplitude of the local oscillator. In order to obtain a continuous stochastic master equation, we let $\beta \sim (dt)^{-2/3}$ by which we can see that $\beta \to \infty$ when $dt \to 0$. Note that dN is a stochastic noise, and in the limit in which β tends to infinity there are many jumps in a small interval dt. The result is that the number of jumps in this small interval becomes Gaussian due to the central limit theorem. The mean and variance of the number of jumps in an interval dt are

$$\mu = \gamma\,\langle(c^\dagger + \beta)(c + \beta)\rangle\, dt = \gamma\,\beta^2 dt + \sqrt{2}\gamma\beta\langle x\rangle dt,$$
$$\sigma^2 = \gamma\,\beta^2 dt.$$

Thus we can replace dN by the Gaussian process

$$dN = \gamma\beta^2 dt + \sqrt{2}\gamma\beta\langle x\rangle dt + \sqrt{\gamma}\beta dW(t), \tag{2.26}$$

where dW is a Wiener noise satisfying $E(dW) = 0$ and $(dW)^2 = dt$. The symbol $x = (c + c^\dagger)/\sqrt{2}$ denotes the normalized position operator of the cavity mode. By substituting dM in Eq. (2.26) for dN in Eq. (2.25) and omitting the higher-order products of infinitesimals that vanish, we obtain the following stochastic master equation

$$d\rho_c = -i\left[H, \rho_c\right]dt + \gamma\mathcal{D}\left[c\right]\rho_c + \mathcal{H}\left[\sqrt{\gamma}c\right]\rho_c dW. \tag{2.27}$$

The stream of measurement results for homodyne detection is given by

$$dy = \lim_{\beta\to\infty}\frac{dN(t) - \gamma\beta^2}{\sqrt{2}\gamma\beta} = \langle x\rangle dt + \frac{1}{\sqrt{2\gamma}}dW, \tag{2.28}$$

where dW is the same Wiener noise increment that appears in the SME.

If the initial state of the cavity mode is a pure state, then the dynamical equation for the cavity under homodyne detection can be obtained by replacing the operator c in Eq. (2.11) by the displacement operator $c + \beta$

$$d|\psi_c\rangle = \left[-iH + \frac{\gamma}{2}\left(\langle c^\dagger c\rangle(t) - c^\dagger c + \frac{\gamma}{2}\langle c^\dagger\beta + \beta c\rangle - \beta c\right)\right]|\psi_c\rangle\, dt$$
$$+ \left(\frac{c + \beta}{\sqrt{\langle(c^\dagger + \beta)(c + \beta)\rangle(t)}} - 1\right)|\psi_c\rangle\, dN(t). \tag{2.29}$$

By substituting Eq. (2.26) into Eq. (2.29), it can be shown that

$$d|\psi_c\rangle = -iH|\psi_c\rangle dt + \gamma\left(\langle c^\dagger\rangle c - \frac{1}{2}c^\dagger c - \frac{1}{2}\langle c^\dagger\rangle\langle c\rangle_c\right)|\psi_c\rangle dt + \sqrt{\gamma}\,(c - \langle c\rangle)\,|\psi_c\rangle dW. \tag{2.30}$$

If the photo-detector is inefficient, then the SME becomes

$$d\rho_c = -i\,[H,\,\rho_c]\,dt + \gamma\,\mathcal{D}\,[c]\,\rho_c + \mathcal{H}\left[\sqrt{\eta\gamma}\,c\right]\rho_c dW, \tag{2.31}$$

and the measurement output is

$$dy = \langle x\rangle dt + \frac{1}{\sqrt{2\eta\gamma}}dW, \tag{2.32}$$

where η is the detection efficiency. Continuous measurements containing Wiener noise are also sometimes referred to as weak measurements. We prefer to call them continuous measurements because (i) weak measurements are not necessarily continuous, and (ii) it can lead to confusion with the "weak values" of Aharonov, Albert and Vaidman [104–106].

More generally, a continuous measurement of the quantum variables A_l ($l = 1, \ldots, m$) can be expressed as the stochastic master equation [94]

$$d\rho_c = -i\,[H,\,\rho_c]\,dt + \sum_{l=1}^{m}\left(\Gamma_l\,\mathcal{D}\,[A_l]\;\rho_c\,dt + \sqrt{\eta_l\Gamma_l}\,\mathcal{H}\,[A_l]\,\rho_c\,dW_l\right), \tag{2.33}$$

and output equation

$$dy_l = \langle A_l\rangle\,dt + \frac{1}{\sqrt{2\eta_l\Gamma_l}}\,dW_l, \tag{2.34}$$

where Γ_l and η_l represent the measurement strengths and measurement efficiencies. Note that the measurement strengths of continuous measurements have units of inverse time [see, e.g., Γ_l in Eq. (2.33)], as well as the inverse square of the observable being measured. It can be thought of as the rate at which the inverse variance of the observable is increased (and thus the variance reduced) by the measurement. The stochastic master equation (2.33) and the equation for the stream of measurement results, Eq. (2.34), are just the quantum filtering equations (Eqs. (2.56) and (2.55)).

As mentioned above, we can simultaneously make more than one continuous measurement on a system, and we can simultaneously measure observables that do not commute. Since the respective dynamics induced by the continuous measurements of two different observables commute to first order in dt, we can think of the measurements of the two observables as being interleaved—the process alternates between infinitesimal measurements of each observable. Note that a von Neumann measurement cannot simultaneously project a system onto the eigenstates of two noncommuting observables, but continuous measurements do not perform instantaneous projections. The effect of simultaneously measuring the position and momentum of a single particle, for example [107,108], is to feed noise into both observables. Measuring noncommuting observables therefore in general introduces more noise into a system than is necessary to obtain a given amount of information. The optical measurement techniques of heterodyne detection [22] and eight-port homodyne detection [109] are very similar to simultaneous measurements of momentum and position [99].

2.1.2. Another point of view: quantum filtering

When we make a continuous measurement on a quantum system, if we know the dynamics of the system, then we can derive an equation of motion for our full state-of-knowledge of the system determined by the continuous stream of measurement results. For a classical system, an observer's state-of-knowledge is given by a probability distribution over the state-space. For a quantum system, it is the density matrix that captures all the information that an observer has about a system. Control theorists refer to the process by which an observer calculates his or her state-of-knowledge of a system from a series of measurement results *filtering*, and the quantum version of this *quantum filtering* [45,46,110]. In classical control theory, when we can only obtain partial information of the system state from the measurement output (e.g., we can measure the position but not the momentum of a mechanical system), we can introduce a dynamical system called a filter, using the measurement results as inputs to recover the whole system dynamics. However, quantum filtering is not just a trivial extension of classical filtering. In quantum filtering, we feed the measurement output (which is a classical signal) into a classical system to generate an estimated state of the measured quantum system. Thus, we use a classical system to mimic a quantum system, and some particular quantum effects, such as quantum coherence, may be lost during this process by the action of the measurement on the system. Quantum filtering is a bridge between a quantum system and a classical controller, since the classical controller can use the resulting state-of-knowledge to decide how to apply control forces to the system. For certain systems, results for optimal control from classical control theory can be directly applied to obtain optimal protocols for quantum system [50,111].

There is a way to formulate quantum theory as a non-commutative generalization of the measure-theoretic formulation of classical probability. We discuss this now because it tends to be used by control theorists and mathematicians who

work on quantum feedback control. While traditional quantum theory deals with operators in a Hilbert space, quantum probability deals with quite different objects, such as a (non-commutative) sigma-algebra of events in a probability space. A set of quantum observables that are mutually commuting are then described by a subset of the full probability space that is merely a classical probability space. To the authors' knowledge there is no practical advantage in using one formulation of quantum mechanics or the other; control theorists use the quantum probability formulation since it is an extension of something that is part of their training, whereas physicists use the traditional formulation because it is part of their training. Interestingly, however, in quantum probability theory it is simpler to show the equivalence between the measurement record as described by the SME and the statistics of the measurement record as described by input–output theory.

We now introduce the quantum probability formulation of quantum mechanics, and then present continuous measurement theory (the theory of quantum filtering) in terms of this formulation. The main difference between classical and quantum mechanics is that quantum mechanics is *noncommutative*, by which we mean that the operators that represent different physical variables do not always commute with each other. Heisenberg's uncertainty principle, for example, is a direct result of the commutation relation $[x, p] = i\hbar$, between the position x and the momentum p of a quantum degree of freedom. Because of this, quantum probability theory is a noncommutative version of classical probability theory. Recall that classical probability theory consists of the triple, $(\Omega, \mathcal{F}, \mathbb{P})$, referred to as a probability space. Here Ω is the sample space which is the set of all elementary, mutually exclusive outcomes. For example, for the probability experiment of throwing a coin, the sample space is the set $\Omega = \{\text{head, tail}\}$. The second item in the triple, $\mathcal{F}$, is the set of "events", where each event is some subset of the possible outcomes (a subset of the set Ω). This makes $\mathcal{F}$ a so-called σ-algebra, which satisfies the following conditions: (i) the empty set $\emptyset$ belongs to $\mathcal{F}$; (ii) $\mathcal{F}$ is closed under complement: $\Omega \setminus A \in \mathcal{F}$ if $A \in \mathcal{F}$; and (iii) $\mathcal{F}$ is closed under countable unions: $\bigcup_{n=1}^{\infty} A_n \in \mathcal{F}$ if all $A_n \in \mathcal{F}$. The elements of $\mathcal{F}$ can also be equivalently expressed as a function defined on Ω (that is, something that associates a value with every outcome), which is called a random variable. In fact, for any $A \in \mathcal{F}$, we can define a random variable $\chi_A : \Omega \to \mathcal{R}$ such that $\chi_A(\omega) = 1$ if $\omega \in A$, and $\chi_A(\omega) = 0$ if it is not. The final item in the triple is the probability measure $\mathbb{P}$, which is a function that associates a probability with every subset of $\mathcal{F}$: $(\mathbb{P} : \mathcal{F} \to [0, 1])$ such that: (i) $\mathbb{P}$ is countably additive, i.e., $\mathbb{P}\left(\bigcup_{n=1}^{\infty} A_n\right) = \sum_{n=1}^{\infty} \mathbb{P}(A_n)$ for any sequence $A_1, A_2, \ldots, A_n$ of disjoint sets in $\mathcal{F}$, and (ii) the measure of the whole sample space Ω is normalized so that $\mathbb{P}(\Omega) = 1$.

Quantum probability theory, developed in the 1980s [45,46,50,84,110,111] is a non-commutative analog of classical probability theory. In quantum probability theory, there is no longer an underlying sample space, and so the quantum probability model can be described by a pair $(\mathcal{N}, \mathbb{P})$. The first item, $\mathcal{N}$, is an algebra, and is defined as the set of all Hermitian operators on the Hilbert space of the system. An element $A \in \mathcal{N}$ is an observable of the quantum system which can be seen as the quantum version of the random variable. The "events" of quantum probability are defined as all the projection operators $P \in \mathcal{N}$. These project onto the subspaces of the Hilbert space. Thus each possible set of outcomes is given by a subspace of the Hilbert space. This is simply the projection postulate of quantum measurement theory. The function $\mathbb{P} : \mathcal{N} \to \mathcal{C}$, where $\mathcal{C}$ is the complex space, is called a state on $\mathcal{N}$. In fact, we can always find a system density operator ρ such that $\mathbb{P}(A) = \mathrm{tr}(A\rho)$ for any $A \in \mathcal{N}$.

By comparing the classical probability model $(\Omega, \mathcal{F}, \mathbb{P})$ and the quantum probability model $(\mathcal{N}, \mathbb{P})$, the main difference is that the algebra $\mathcal{N}$, called the von Neumann algebra, is noncommutative (the Hermitian operators may not commute with each other) while the σ-algebra $\mathcal{F}$ in classical probability is a commutative algebra. As an example, let us consider a quantum measurement of the observable A. Before this measurement, the quantum system can be described by the quantum probability model $(\mathcal{N}, \mathbb{P})$. After this measurement, the quantum state collapse occurs. The measurement output corresponds to a classical probability model $(\mathcal{A}, \mathbb{P})$, where

$$\mathcal{A} = \{X : X = f(A), f : \mathcal{R} \to \mathcal{C}\} \tag{2.35}$$

forms a commutative algebra. Thus, the quantum measurement of the observable A converts a quantum probability model into a classical probability model. More generally, in the following discussions, we will show that the quantum filtering process, which is based on quantum measurement, is merely a bridge between a quantum probability model and a classical probability model.

To better understand quantum filtering, let us consider an indirect quantum measurement, which is achieved by interacting the measured system with a bath via a system operator L, and then making a measurement on the bath. The bath is a continuum of harmonic oscillators of different frequencies. The bath also describes a field, such as the electromagnetic field, in which the oscillators are the modes of the field. The Hamiltonian of the total system composed of the measured system and the bath is given by

$$\begin{aligned} H &= H_s + H_b + H_{\text{int}}, \\ H_b &= \int_{-\infty}^{+\infty} d\omega\, \omega\, b^{\dagger}(\omega)\; b(\omega), \\ H_{\text{int}} &= i\int_{-\infty}^{+\infty} d\omega \left[\kappa(\omega)\, b^{\dagger}(\omega)\, L - \text{h.c.}\right], \end{aligned} \tag{2.36}$$

where H_s is the free Hamiltonian of the measured system, $b^{\dagger}(\omega)$ and $b(\omega)$ are the creation and annihilation operators of the bath mode with frequency ω, and satisfy

$$\left[b(\omega), b^{\dagger}(\tilde{\omega})\right] = \delta(\omega - \tilde{\omega}). \tag{2.37}$$

The bath mode with frequency ω interacts with the system via the system operator L, where $\kappa(\omega)$ is the corresponding coupling strength. Hereafter we set $\hbar = 1$. The total Hamiltonian H can be re-expressed in the interaction picture as

$$H_{\text{eff}} = \exp(iH_b t)(H_s + H_{\text{int}})\exp(-iH_b t) = H_s + i\int_{-\infty}^{+\infty} d\omega \left[\kappa(\omega) e^{i\omega t} b^\dagger(\omega) L - \text{h.c.}\right]. \tag{2.38}$$

We now introduce the Markovian assumption. In probability theory, the term "Markovian" refers to the memoryless property of a stochastic process: a process is said to be Markovian if the conditional probability distribution of the future states of this process, in general conditional on both past and present states, depends only upon the present state. In short, given the present, the future does not depend on the past. Given the following assumption

$$\kappa(\omega) = \sqrt{\frac{\gamma}{2\pi}}, \tag{2.39}$$

it will be presented in the following discussions that the output field and the dynamical equation of the system do not depend on the past. We thus refer to Eq. (2.39) as the Markovian assumption. Under this assumption, the Hamiltonian H_{eff} can be expressed as

$$H_{\text{eff}} = H_s + i\sqrt{\gamma}\left[b_{\text{in}}^\dagger(t) L - L^\dagger b_{\text{in}}(t)\right], \tag{2.40}$$

where

$$b_{\text{in}}(t) = \frac{1}{\sqrt{2\pi}}\int_{-\infty}^{+\infty} d\omega\, e^{-i\omega t}\, b(\omega) \tag{2.41}$$

is the Fourier transform of the bath modes. The operator $b_{\text{in}}(t)$ is, in fact, the time-varying field that is incident on, and thus the input to, the system, and satisfies [53,54,86]

$$\left[b_{\text{in}}(t), b_{\text{in}}^\dagger(\tilde{t})\right] = \delta(t - \tilde{t}). \tag{2.42}$$

We now define a new bath operator

$$B_{\text{in}}(t) = \int_0^t b_{\text{in}}(\tau)\, d\tau \tag{2.43}$$

which is called a *quantum Wiener process*. If we assume that the bath is initially in a vacuum state, the increment of the quantum Wiener process dB_{in} and its conjugate $dB_{\text{in}}^\dagger$ satisfy the following algebraic conditions:

$$dB_{\text{in}}\, dB_{\text{in}}^\dagger = dt, \qquad dB_{\text{in}}^\dagger\, dB_{\text{in}} = dB_{\text{in}}^\dagger\, dB_{\text{in}}^\dagger = dB_{\text{in}}\, dB_{\text{in}} = 0. \tag{2.44}$$

These constitute the quantum version of the so-called classical *Ito rule* [84]

$$\left(d\tilde{W}\right)^2 = dt, \tag{2.45}$$

where $d\tilde{W}$ is the increment of the classical Wiener process $\tilde{W}(t)$, which has zero mean, and the above equality is defined in the root-mean-square sense. The unitary evolution operator $V(t)$ of the total system composed of the controlled system and the input field satisfies the following dynamical equation

$$dV(t) = \left(\sqrt{\gamma}\, dB_{\text{in}}^\dagger L - \sqrt{\gamma}\, L^\dagger\, dB_{\text{in}} - \frac{\gamma}{2} L^\dagger L\, dt - iH_s dt\right) V(t) \tag{2.46}$$

with initial condition $V(0) = I$. In the Heisenberg picture, an arbitrary system operator $X(t) = V^\dagger(t) X V(t)$ satisfies the following quantum stochastic differential equation [53,54]

$$dX(t) = -i[X(t), H_s]\, dt + \frac{\gamma}{2}\left\{L^\dagger[X(t), L] + \left[L^\dagger, X(t)\right] L\right\} dt + \sqrt{\gamma}\left\{dB_{\text{in}}\left[L^\dagger, X(t)\right] + [X(t), L]\, dB_{\text{in}}^\dagger\right\}, \tag{2.47}$$

which can be derived by applying the quantum Ito rule (2.44) and expanding the unitary operator to second order in the quantum Wiener increment. In fact, it can be calculated that

$$\begin{aligned} dX(t) &= dV^\dagger(t) X V(t) + V^\dagger(t) X dV(t) + dV^\dagger(t) X dV(t) \\ &= \sqrt{\gamma}\, dB_{\text{in}} L^\dagger X(t) - \sqrt{\gamma}\, L X(t)\, dB_{\text{in}}^\dagger - \frac{\gamma}{2} L^\dagger L X(t) dt + iH_s X(t) dt \\ &\quad + \sqrt{\gamma}\, X(t) L\, dB_{\text{in}}^\dagger - \sqrt{\gamma}\, dB_{\text{in}} X(t) L^\dagger - \frac{\gamma}{2} X(t) L^\dagger L\, dt - iX(t) H_s dt + \gamma L^\dagger X(t) L dt \\ &= -i[X(t), H_s]\, dt + \frac{\gamma}{2}\left\{L^\dagger[X(t), L] + \left[L^\dagger, X(t)\right] L\right\} dt + \sqrt{\gamma}\left\{dB_{\text{in}}\left[L^\dagger, X(t)\right] + [X(t), L]\, dB_{\text{in}}^\dagger\right\}. \end{aligned} \tag{2.48}$$

It is then possible to define an output field $B_{\text{out}}(t)$ which describes the field leaving the system after it has interacted with it by

$$B_{\text{out}}(t) = V^{\dagger}(t) B_{\text{in}}(t) V(t).$$

The celebrated input–output relation for the system can then be written in the increment form as [53,54]

$$dB_{\text{out}} = dB_{\text{in}} + \sqrt{\gamma}\, L(t), \tag{2.49}$$

which can also be derived by applying the quantum Ito rule (2.44) and expanding the unitary operator to second order in the quantum Wiener increment. In fact, it can be shown that

$$\begin{aligned} dB_{\text{out}} &= V^{\dagger}(t)\, dB_{\text{in}}\, V(t) + dV^{\dagger}(t)\, dB_{\text{in}}\, V(t) + V^{\dagger}(t)\, dB_{\text{in}}\, dV(t) \\ &= dB_{\text{in}} + 0 + \sqrt{\gamma}\, V^{\dagger}(t)\, L\, V(t) = dB_{\text{in}} + \sqrt{\gamma}\, L(t). \end{aligned} \tag{2.50}$$

If homodyne detection is performed [99] on the output field $B_{\text{out}}(t)$, and we set the phase of the local oscillator to zero, then the operator corresponding to the output of the homodyne measurement is

$$dY_{\text{out}} = \frac{1}{\sqrt{\gamma}} \left(dB_{\text{out}} + dB_{\text{out}}^{\dagger} \right),$$

and satisfies the following equation

$$dY_{\text{out}} = \left(L + L^{\dagger} \right) dt + \frac{1}{\sqrt{\gamma}} \left(dB_{\text{in}} + dB_{\text{in}}^{\dagger} \right). \tag{2.51}$$

With the above preparation, we can now present the main results of quantum filtering theory [110]. The purpose of quantum filtering is to provide an estimate $\pi(X)$ of the value of the system observable X, at time t, given the stream of measurement results up until that time. We will define this estimate as the expectation value of X given the measurement results. To obtain $\pi(X)$ we first define the event set generated by the measurement output signals up to the current time t as

$$\mathcal{Y}_{\text{out}} = \{ Y(t) \mid Y(t) = f\left[Y_{\text{out}}(\tau) : 0 \le \tau \le t \right] \} \tag{2.52}$$

where $f(\cdot)$ is an arbitrary function, and denote $\mathbb{P}$ as the probability measure on $\mathcal{Y}_{\text{out}}$. The estimate $\pi_t(X)$ is then the conditional expectation of $X(t)$ on $\mathcal{Y}_{\text{out}}$

$$\pi_t(X) = \mathbb{P}\left(X(t) | \mathcal{Y}_{\text{out}} \right). \tag{2.53}$$

From the definition of $\pi_t(X)$ given in Eq. (2.53), it can be proved (see, e.g., the derivations in Ref. [110]) that we can obtain the following dynamical equation for $\pi(X)$ and the corresponding output equation from Eqs. (2.47) and (2.51)

$$d\pi_t(X) = \pi_t\left[\mathcal{L}(X) \right] dt + \sqrt{\gamma} \left[\pi_t\left(L^{\dagger} X + X L \right) - \pi_t\left(L + L^{\dagger} \right) \pi_t(X) \right] dW, \tag{2.54}$$

$$dY_{\text{out}} = \pi_t\left(L + L^{\dagger} \right) dt + \frac{1}{\sqrt{\gamma}}\, dW, \tag{2.55}$$

where $\mathcal{L}(X)$ is the Liouville superoperator of the system defined as

$$\mathcal{L}(X) = -i\left[X, H_s \right] + \gamma \left(L^{\dagger} X L - \frac{1}{2} L^{\dagger} L X + \frac{1}{2} X L^{\dagger} L \right).$$

The process $W(t)$ in Eqs. (2.54) and (2.55) is called the innovation process of quantum filtering, and has been shown to be a classical Wiener process [110]. The increment of $W(t)$, i.e., dW, satisfies the classical Ito rule given by Eq. (2.45). The dynamical equation (2.54) of $\pi(X)$ is called the *quantum filtering equation*. The filtering equation (2.54) and the output equation (2.55) are the main results of quantum filtering theory.

Additionally, we can rewrite the filtering equation (2.54) as a stochastic equation for the evolution of the density operator. To show this, we use the fact that the density operator $\rho_c(t)$ satisfies $\pi_t(X) = \text{tr}\left(X \rho_c(t) \right)$, where X is the corresponding system observable at $t = 0$. Substituting Eq. (2.54) into the above relation, the system density operator $\rho_c(t)$ evolves according to the following stochastic master equation [110]

$$\begin{aligned} d\rho_c(t) &= -i\left[H_s, \rho_c(t) \right] dt + \frac{1}{2} \left(2 L \rho_c(t) L^{\dagger} - L^{\dagger} L \rho_c(t) - \rho_c(t) L^{\dagger} L \right) dt \\ &\quad + \left\{ L \rho_c(t) + \rho_c(t) L^{\dagger} - \text{tr}\left[\left(L + L^{\dagger} \right) \rho_c(t) \right] \rho_c(t) \right\} dW. \end{aligned} \tag{2.56}$$

The stochastic master equation (2.56) is also often referred to as *quantum filtering equation*.

To summarize, the quantum stochastic differential equation (2.47) and the output equation (2.51) give the dynamics of the operators that describe the measured quantum system. These equations are driven by the quantum Wiener noise dB_{in}, and are thus defined on a quantum probability space. As a comparison, the quantum filtering equation (2.54) [or the

stochastic master equation (2.56)] and the output equation (2.55) give the observer's state-of-knowledge of the measured quantum system based on the information extracted by the quantum measurement. These equations are driven by the classical Wiener noise dW and thus defined on a classical probability space. Thus, in quantum filtering theory we use a classical stochastic system to mimic the dynamics of a quantum stochastic model, which is why we refer to quantum filtering as a bridge between a quantum probability model and a classical probability model.

2.2. Markovian quantum feedback

The continuous collapse of the quantum state in continuous quantum measurement means that we can execute real-time quantum feedback control before the quantum state collapses to a completely classical state. That is the starting point of continuous measurement-based feedback control. The key questions in feedback control are usually (i) what observable should we measure? and (ii) how should we choose the feedback forces as a function(al) of the stream of measurement results? Optimal feedback strategies can always be obtained by using the SME to determine the observer's full state of knowledge (the density matrix) given the stream of measurement results up to the present time, and using this to determine the choice of Hamiltonian at each time. But solving the SME can take significant numerical resources, and it may not be possible to do so in real-time. In that case, one can attempt to approximate the SME with a simpler differential equation, which may be possible depending on the dynamics of the system [112–114]. Alternatively we can take the opposite approach, and see what can be achieved with quantum feedback when we perform no processing of the measurement results, and merely engineer a term in the Hamiltonian of the system that, at each time, is proportional to the measurement result at that time. This is the kind of feedback protocols that were introduced by Wiseman and Milburn [42,43,48], and are now referred to as Markovian feedback. The reason for this name is that for this kind of feedback, if we average the evolution over all trajectories, the result is a Markovian master equation. This is not usually true for feedback protocols.

Let us consider a quantum continuous measurement of the operator A with efficiency η. From Eqs. (2.33) and (2.34), the measurement and output equations of this measurement can be expressed as

$$d\rho_c = -i\left[H, \rho_c\right] dt + \Gamma_A \mathcal{D}\left[A\right] \rho_c \, dt + \sqrt{\eta \Gamma_A}\, \mathcal{H}\left[A\right] \rho_c \, dW, \tag{2.57}$$

and

$$dy = \langle A \rangle \, dt + \frac{1}{\sqrt{2\eta\Gamma_A}} \, dW. \tag{2.58}$$

The main objective of measurement-based quantum feedback is to use the output signal $dy\,(t)$ to engineer the system dynamics given by Eq. (2.57). The most general form of the system dynamics, modified based on the output signal $dy\,(t)$, can be expressed as [22]

$$d\rho_f = \mathcal{F}\left[t, \{dy\,(\tau)\,|\tau \in [0, t]\}\right] \rho_c, \tag{2.59}$$

where $\mathcal{F}\left[t, \{dy\,(\tau)\,|\tau \in [0, t]\}\right]$ is a superoperator that depends on the output signal $dy\,(t)$ for all past times. ρ_f is the system state modified by the feedback control.

For most of the existing studies, quantum feedback control is introduced by varying the parameters in the system Hamiltonian based on the output signals $\{dy\,(\tau)\,|\tau \in [0, t]\}$. The simplest case is Markovian quantum feedback in which the control is applied by adding a Hamiltonian that is proportional to the measured signal $dy(t)/dt$. This Hamiltonian generates the dynamics

$$d\rho_f = \left[\exp(\mathcal{K} dy) - 1\right] \rho_c, \tag{2.60}$$

where the superoperator $\mathcal{K}$ is defined by $\mathcal{K}\rho_c = -i[F, \rho_c]$ for some Hermitian operator F. Combining the measurement equation (2.57) and the feedback equation (2.60), we can obtain the following modified closed-loop stochastic master equation [22]

$$d\rho_f = \left\{-i\left[H, \rho_f\right] + \Gamma_A \mathcal{D}\left[A\right] \rho_f - i\left[F, A\rho_f + \rho_f A\right] + \frac{1}{\eta}\mathcal{D}\left[F\right] \rho_f\right\} dt + \mathcal{H}\left[\sqrt{\eta}A - \frac{i}{\sqrt{\eta}}F\right] \rho_f \, dW. \tag{2.61}$$

By averaging over the noise term dW, we can derive the following Wiseman–Milburn master equation [22] from Eq. (2.61):

$$\dot{\rho} = -i\left[H, \rho\right] + \Gamma_A \mathcal{D}\left[A\right] \rho - i\left[F, A\rho + \rho A\right] + \frac{1}{\eta}\mathcal{D}\left[F\right] \rho, \tag{2.62}$$

where $\rho = E(\rho_f)$. The effects induced by the feedback loop are clearer in this form: (i) the first feedback term $-i\left[F, A\rho + \rho A\right]$ plays a positive role to steer the system dynamics to achieve the desired effects; and (ii) the second feedback term $\mathcal{D}\left[F\right] \rho/\eta$ represents the decoherence effects induced by feedback, which tends to play a negative role for purposes of control. The master equation (2.62) can be reexpressed as the traditional Lindblad form [22,48]

$$\dot{\rho} = -i\left[H + \frac{(AF + FA)}{2}, \rho\right] + \mathcal{D}\left[A - iF\right] \rho + \frac{1 - \eta}{\eta}\mathcal{D}\left[F\right] \rho. \tag{2.63}$$

Although the Markovian quantum feedback given by Eq. (2.62) is the simplest measurement-based quantum feedback approach, it can be used to solve various problems by choosing A and F appropriately. Markovian quantum feedback has been used to stabilize arbitrary one-qubit quantum states [115–117], manipulate quantum entanglement [118–131], generate and protect Schrödinger cat states [132–136], and induce optical, mechanical, and spin squeezing [137–145].

2.3. Feedback via time-averaging

Markovian quantum feedback is simple to describe analytically, but is also rather limited. Further, feeding back the measurement signal at each instant of time does not make optimal use of the information extracted by the measurement. To do that we must process the measurement results using the SME. It is worth pausing at this point to understand a little more how the measurement results, given by Eq. (2.34), provide information about the measured operator and the state of the system. If we process the measurement results so that we know ρ_c at each time, then we also know the expectation value of the measured operator, $\langle A\rangle$, at each time. The first term in Eq. (2.34) is therefore already known, and provides no new information about the system. It is the noise term dW that carries the new information, and that modifies our state-of-knowledge. In fact, by definition we always know the expectation value $\langle A\rangle = \mathrm{tr}(A\rho_c)$ at the start of the continuous measurement, because ρ_c is our state-of-knowledge. But the system might really be in some pure state $|\psi\rangle$, so that the true mean value of A is $\bar{A} = \langle\psi|A|\psi\rangle$. As the measurement proceeds, the conditional expectation value $\langle A\rangle$ tends to $\bar{A}$ and ρ_c tends to $|\psi\rangle$.

Now consider what happens if A is a Hermitian observable, and $|\psi\rangle$ is an eigenstate of both the system Hamiltonian and A. In this case, assuming that the system is not driven by other noise sources, it remains in the state $|\psi\rangle$ as the measurement proceeds, and $\bar{A}$ is constant. In that case we can obtain an estimate of $\bar{A}$ of ever increasing accuracy without solving the SME. All we need to do is to average the measurement results obtained so far, and divide by the total time [146]. If we define

$$Y_A(t) = \frac{1}{t}\int_0^t dy = \frac{1}{t}\int_0^t \langle A\rangle dt' + \frac{1}{t\sqrt{2\eta\Gamma_A}}\int_0^t dW, \tag{2.64}$$

then as $t\to\infty$ the second term tends to zero and $Y_A(t)\to\bar{A}$. The reason that the second term, being the average of the noise, tends to zero is that it has equally positive and negative fluctuations and these average to zero over time.

The mean value of the measured observable, $\bar{A}$, is usually not constant for a system that we are trying to control. Nevertheless we can still use an averaging procedure to obtain an estimate of $\bar{A}$ and use this to choose our feedback forces. This method is not as complex as processing the measurements using the SME, but more complex than Markovian feedback [147–150]. To do this we average the signal over a time T that is long enough to reduce the noise but not so long that $\bar{A}$ changes too much during T. We can also include a weighting function, $f(t)$, to smoothly reduce the dependence on our estimate of A on measurement results that are too far in the past. For example, if we use an exponential weighting function, our estimate of $\bar{A}$ at time t is

$$\tilde{Y}_A(t) = \frac{1}{T}\int_{t-T}^t \exp\left(-\gamma_f t'\right)\left(\langle A\rangle dt' + \frac{1}{\sqrt{2\eta\Gamma_A}}dW\right). \tag{2.65}$$

When $T \ll 1/\gamma_f$, the estimate converges as

$$\tilde{Y}_A(t) - \bar{A}(t) = \exp\left(-\gamma_f t\right)\left[\tilde{Y}_A(0) - \bar{A}(0)\right]. \tag{2.66}$$

Such an exponentially-convergent filter has been introduced in the literature to stabilize two-qubit entanglement [151,152] and a three-qubit GHZ state [153] both in optical systems and in superconducting circuits. It has also been applied experimentally to the adaptive estimation of the optical phase [154].

2.4. Bayesian quantum feedback

To make full use of the information provided by the measurement, we must process the measurement results using the SME [Eq. (2.33)] to obtain the conditional density matrix. Since this density matrix, along with the knowledge of the dynamics of the system, determines the probabilities of the results of any measurement on the system at any time in the future, any optimal strategy for controlling the system can ultimately be specified as a rule for choosing the Hamiltonian at time t as a function of the density matrix at that time and possibly the time itself: $H(t) = f(\rho_c(t), t)$. Feedback control in which the feedback protocol is specified in this way is sometimes referred to as "Bayesian feedback" because the SME is the quantum equivalent of processing the measurement record using Bayes' theorem [155].

As we have mentioned above, the SME, since it requires simulating the full dynamics of the system, may be impractical to solve in real-time. Sometimes it is possible to approximately, or even exactly, reduce the computational overhead by choosing an ansatz for ρ_c that contains only a small number of parameters. The SME then reduces to a stochastic differential equation for these parameters. Two examples in which an approximate ansatz provides an effective control protocol can be found in [112–114]. There is one class of systems in which an ansatz with a small number of parameters provides an *exact* solution to the SME, that of linear systems. A quantum system is referred to as linear if its Hamiltonian is no more than

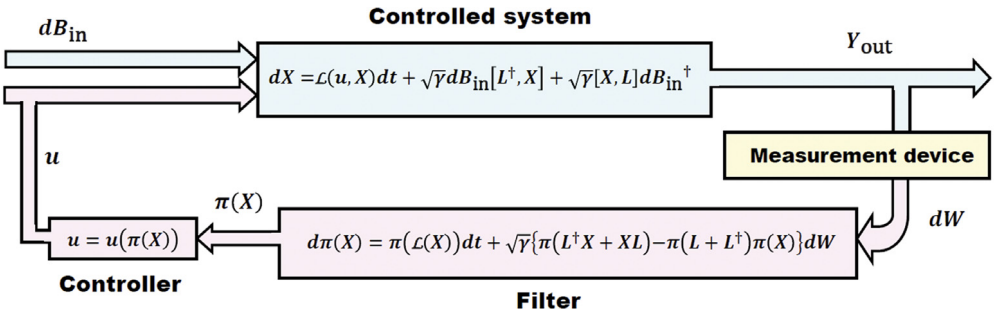

Fig. 3. Diagram for state-based quantum feedback. The controlled system (top branch, in blue) is described by a quantum stochastic differential equation driven by the quantum Wiener noise $dB_{\rm in}$. Part of the quantum output field $Y_{\rm out}$ from the controlled system is converted into a classical signal dW by a measurement device (shown in yellow) and then fed into the filter. The dynamics of the filter is determined by the quantum filtering equation driven by the classical Wiener noise, i.e., the innovation process dW. The estimated quantum state $\pi(X)$ is fed into a classical controller to obtain a control signal u, which is then fed back to steer the dynamics of the controlled system. The filter and controller which form the classical control loop (in pink) can be realized by a classical digital signal processor.

quadratic in the position and momentum operators, any Lindblad operators that describe the noise driving the system are linear in the position and momentum operators, and any measurements are (i) driven by Wiener noise, and (ii) of operators that are linear in the position and momentum.

If we further assume that the initial states of the noise-driven linear systems are Gaussian states (states that are Gaussian in the position and momentum bases, and thus have Gaussian Wigner functions), then the states of the system will remain Gaussian under the evolution. This fact is not difficult to show, and implies immediately that if the state of a linear system is Gaussian, the SME reduces to a stochastic differential equation for the means and (co-)variances of the position and momentum [50]. What is more, the dynamics of these variables are exactly reproduced by those of a classical linear system driven by Gaussian noise, and subjected to continuous measurements of the same observables. To correctly reproduce the quantum dynamics, for each continuous measurement made on the system a noise source must be added to the classical system to mimic Heisenberg's uncertainty principle.

Consider a linear quantum system with N degrees of freedom [156–160], and write the N position and momentum operators, denoted respectively by q_n and p_n, in the vector

$$\mathbf{x} = (q_1, p_1, \ldots, q_N, p_N)^{\rm T}. \tag{2.67}$$

We scale these operators so that $[q_n, p_n] = i$. If x_m is the mth element of the vector $\mathbf{x}$, then we have $[x_n, x_m] = i\Sigma_{nm}$, where

$$\Sigma = \bigoplus_{n=1}^{N} \begin{pmatrix} 0 & 1 \\ -1 & 0 \end{pmatrix}.$$

For linear quantum systems, the system Hamiltonian H_s and the dissipation operator L in Eq. (2.47) can be written as [156–158]

$$H_s = \frac{1}{2}\mathbf{x}^{\rm T} G\,\mathbf{x} - \mathbf{x}^{\rm T}\Sigma\,\mathbf{b}\,u, \qquad L = \mathbf{l}^{\rm T}\mathbf{x}, \tag{2.68}$$

where G is a real and symmetric matrix, and $\mathbf{b}$, $\mathbf{l}$ are real and complex vectors, respectively. The second term in H_s, including the time-dependent function $u(t)$, describes the force applied by the feedback controller (see Fig. 3). This feedback Hamiltonian must be linear in the conditional mean values of the position and momentum operators, in order to ensure that the system remains linear. This also means that there is a linear map from the measurement output $Y_{\rm out}$ to $u(t)$, and thus a linear input–output relation for the controlled system. From Eq. (2.47), the dynamics of the controlled system can be expressed as the following linear quantum stochastic differential equation:

$$d\mathbf{x} = A\,\mathbf{x}\,dt + \mathbf{b}\,u\,dt + i\sqrt{\gamma}\,\Sigma\left[\mathbf{l}\,dB_{\rm in}^\dagger - \mathbf{l}^*\,dB_{\rm in}\right], \tag{2.69}$$

where the matrix $A = \Sigma\left[G + {\rm Im}\left(\mathbf{l}^*\mathbf{l}^{\rm T}\right)\right]$. The output equation (2.51) can be written as

$$dY_{\rm out} = F\,\mathbf{x}\,dt + \frac{1}{\sqrt{\gamma}}\left(dB_{\rm in} + dB_{\rm in}^\dagger\right), \qquad F = \mathbf{l}^{\rm T} + \mathbf{l}^\dagger. \tag{2.70}$$

After quantum measurement, the dynamics of this linear quantum system can be fully described by the conditional means $\pi(\mathbf{x})$ and variances $V_t = \mathbb{P}(P_t|\mathcal{Y}_{\rm out})$, where P_t is the covariance matrix of the position and momentum variables with the (i,j)-element being $P_{ij} = \left(\Delta x_i \Delta x_j + \Delta x_j \Delta x_i\right)/2$, and $\Delta x_i = x_i - \pi(x_i)$. The conditional mean values $\pi(\mathbf{x})$ obey the filtering equation

$$d\pi(\mathbf{x}) = A\,\pi(\mathbf{x})\,dt + B\,u\,dt + \left[V_t F^{\rm T} + \Sigma^{\rm T}\,{\rm Im}(l)\right] \times \left[dY - F\pi(\mathbf{x})\,dt\right], \tag{2.71}$$

and the conditional covariance matrix satisfies the deterministic Riccati differential equation

$$\dot{V}_t = A\,V_t + V_t\,A^{\mathrm{T}} + D - \left[V_t\,F^{\mathrm{T}} + \Sigma^{\mathrm{T}}\,\mathrm{Im}\,(l)\right] \times \left[F\,V_t + \mathrm{Im}\left(l^{\mathrm{T}}\right)\,\Sigma\right], \tag{2.72}$$

where $D = \Sigma\,\mathrm{Re}\left(l^{*}l^{\mathrm{T}}\right)\,\Sigma^{\mathrm{T}}$. Thus, the filtering equation (2.54) or (2.56) is equivalent to the closed set of filtering equations (2.71) for the first-order quadrature and the Riccati differential equation (2.72), which is finite-dimensional and thus simulated with relative ease. The quantum filter given by Eqs. (2.71) and (2.72) is called a quantum Kalman filter [50,111,156–158].

For linear quantum feedback control systems, many objectives, such as cooling and squeezing, can be reduced to the optimization of the following quadratic cost function of the system state $\mathbf{x}$

$$J_q = \frac{1}{2}\mathbf{x}_T^{\mathrm{T}}\,S\,\mathbf{x}_T + \frac{1}{2}\int_0^T \left[\mathbf{x}_\tau^{\mathrm{T}}\,Q\,\mathbf{x}_\tau + u_\tau^{\mathrm{T}}\,R\,u_\tau\right] d\tau. \tag{2.73}$$

To obtain a closed-form control problem, we should first take the expectation value over the conditioned state and then average over all the stochastic trajectories to define a new quadratic cost function $J = E\left(\mathbb{P}\left(J_q|\mathcal{Y}_{\mathrm{out}}\right)\right)$, where $E(\cdot)$ is the average taken over the classical Wiener noise dW. From Eq. (2.73) we have

$$J = E\left(\frac{1}{2}\int_0^T \left[\pi\left(\mathbf{x}_\tau\right)^{\mathrm{T}}\,Q\,\pi\left(\mathbf{x}_\tau\right) + \mathrm{tr}\left(QV_\tau\right) + u_\tau^{\mathrm{T}}\,R\,u_\tau\right] d\tau\right) + E\left(\frac{1}{2}\pi\left(\mathbf{x}_T\right)^{\mathrm{T}}\,S\pi\left(\mathbf{x}_T\right) + \frac{1}{2}\mathrm{tr}\left(SV_T\right)\right). \tag{2.74}$$

Here the control $u_t = u\left(\pi\left(\mathbf{x}_t\right), V_t\right)$ is a function of the conditional means and variances $\pi\left(\mathbf{x}_t\right)$ and V_t. The optimization of the quadratic cost function (2.74) subject to the quantum filtering equations (2.71) and (2.72) is a standard classical Linear–Quadratic–Gaussian (LQG) control problem which can be solved by the Kalman filtering theory well developed in the field of classical control.

2.5. Applications

2.5.1. Noise reduction and quantum error correction

Similar to classical feedback, one of the most important applications of quantum feedback is to suppress the effects of noise, which in quantum systems causes decoherence. Markovian quantum feedback can be used to suppress the decoherence of macroscopic-superposition states (so-called "Schrödinger cat" states) [132–136] if we measure the output channel that is causing the decoherence. As an example, if we prepare the following superposition of two coherent states,

$$|\psi\rangle = \frac{|\alpha_0\rangle + |-\alpha_0\rangle}{\sqrt{2}}, \tag{2.75}$$

in an optical cavity, then by making a homodyne measurement of the light that leaks out of the cavity we can use Markovian feedback to extend the time over which the coherence survives. Without quantum feedback, the timescale over which the coherence between the two coherent states survives is $\tau = 1/\left(2\gamma|\alpha_0|^2\right)$, where γ is the decay rate of the cavity [161]. If the signal from the homodyne measurement is used to control the transmissivity of an electro-optic modulator (EOM), as depicted in Fig. 4, then the timescale over which the coherence survives is [133]

$$\tau_{\mathrm{fb}} = \frac{\tau}{(1 - g\,\sin\theta)^2}, \tag{2.76}$$

where ϕ and g are the phase shift and gain of the feedback, respectively.

Another example of the use of Markovian quantum feedback is to reduce the phase noise in an atom laser [162,163]. The primary source of this phase noise is collisions between atoms. A single-mode atom laser can be described by the master equation

$$\dot{\rho} = -i[C(a^{\dagger})^2a^2,\,\rho] + \kappa\,\mu\,\mathcal{D}[a^{\dagger}]\,\mathcal{A}[a^{\dagger}]^{-1}\rho + \kappa\,\mathcal{D}[a]\,\rho, \tag{2.77}$$

where as usual a is the annihilation operator for the mode, κ, $\mu \gg 1$ are respectively the damping rate and the stationary mean number of atoms in the laser mode, and the superoperator $\mathcal{A}[\cdot]$ is defined by

$$\mathcal{A}[r]\rho = \frac{1}{2}\left\{r^{\dagger}r,\,\rho\right\}.$$

The nonlinear Hamiltonian

$$H_{\mathrm{coll}} = \hbar C(a^{\dagger})^2a^2$$

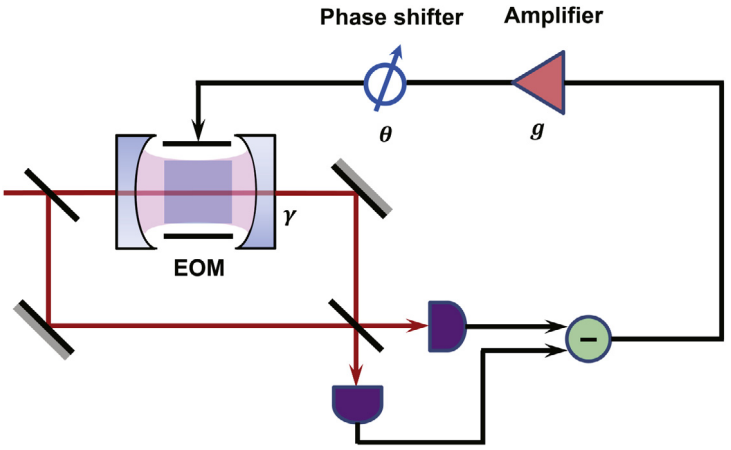

Fig. 4. Diagram of a proposal by Goetsch et al. [133] to extend the lifetime of superpositions of macroscopically distinguishable coherent states. Such a "Schrödinger-cat" state is initially prepared inside an optical or superconducting cavity. The output field from the cavity is measured by homodyne detection and then the homodyne photocurrent is fed back to control the transmissivity of an electro-optic modulator. The feedback gain and phase are denoted by g and θ, respectively. The negative sign in the circle indicates that the two signals are subtracted.

describes the collisions between atoms at a rate C. From Eq. (2.77) the linewidth of the atom laser without feedback can be shown to be

$$l = \begin{cases} \dfrac{\kappa}{2\mu}\left(1+\chi^2\right), & \chi \ll \sqrt{\mu}, \\ \dfrac{\kappa\chi}{\sqrt{\pi\mu/2}}, & \chi \gg \sqrt{\mu}, \end{cases} \tag{2.78}$$

where $\chi = 4\mu C/\kappa$ is a dimensionless atomic interaction strength. We now make a quantum nondemolition measurement of the atomic number, and use the photocurrent (the stream of measurement results) from this measurement to modulate the external field applied to the condensate of atoms to generate the output of the laser. With this feedback the linewidth of the atom laser becomes

$$l = \frac{\kappa}{2\mu}\left(1+\frac{\chi}{\sqrt{\eta}}\right), \tag{2.79}$$

where η is the detection efficiency. The feedback is thus capable of eliminating the effect of atomic collisions on the linewidth of the laser [162,163].

Continuous-time feedback has also been applied to quantum error correction, a technique that is able to slow the decoherence of unknown quantum states [91,92,164–168]. By "unknown", we mean that the controller is able to preserve the initial state without knowing what the state is. This requires that the state is initially encoded in a larger Hilbert space before the error-correction can be applied. As an example, we return to the three-qubit bit-flip code given in the beginning of this section. The idea is to replace the projective measurements that extract the error syndrome with continuous measurements [91]. Recall that the state of a single logical-qubit is encoded (stored) in three physical qubits. To extract the information about the error, we make a continuous measurement of the three operators ZZI, IZZ, and ZIZ, all with the same measurement strength, κ. We also apply three control Hamiltonians, $H_1 = \hbar\lambda_1 XII$, $H_2 = \hbar\lambda_2 IXI$, and $H_3 = \hbar\lambda_3 IIX$. These three Hamiltonians apply the corrections for the three possible errors, and thus the rates λ_1, λ_2, and λ_3 are to be determined by the measurement results. Recall that Bayesian feedback involves integrating the stochastic master equation, which in this case is

$$\begin{aligned} d\rho_c = &-i[\lambda_1 XII + \lambda_2 IXI + \lambda_3 IIX, \rho_c]dt + \gamma\left(\mathcal{D}[XII] + \mathcal{D}[IXI] + \mathcal{D}[IIX]\right)\rho_c dt \\ &+ \kappa\left(\mathcal{D}[ZZI] + \mathcal{D}[IZZ] + \mathcal{D}[ZIZ]\right)\rho_c dt + \sqrt{\kappa}\left(\mathcal{H}[ZZI]dW_1 + \mathcal{H}[IZZ]dW_2 + \mathcal{H}[ZIZ]dW_3\right)\rho_c. \end{aligned} \tag{2.80}$$

By minimizing a cost function, which is defined as the distance between the conditional density matrix and the space in which the logical qubit should reside (the codespace), the optimal feedback is determined to be

$$\begin{aligned} \lambda_1 &= \lambda\,\mathrm{sgn}\langle YZI + YIZ\rangle_c, \\ \lambda_2 &= \lambda\,\mathrm{sgn}\langle ZYI + IYZ\rangle_c, \\ \lambda_3 &= \lambda\,\mathrm{sgn}\langle ZIY + IZY\rangle_c, \end{aligned} \tag{2.81}$$

where λ is the maximum available feedback strength. Here, $\mathrm{sgn}(x) = +1$ if $x > 0$, $\mathrm{sgn}(0) = 0$, and $\mathrm{sgn}(x) = -1$ if $x < 0$. It is shown in Ref. [91] that this quantum error-correction protocol can efficiently increase the fidelity of the encoded

quantum states beyond that achieved by traditional projective-measurement-based error-correction, so long as the time delay induced by the feedback loop is small enough.

It was shown in [164] that averaging the stream of measurement results is sufficient to perform quantum error-correction, thus replacing the highly complex Bayesian feedback with time-averaged feedback. Further efficient methods for continuous-time quantum error-correction are presented in [165].

A simpler situation occurs if the environment that is causing the errors can itself be measured. An example of this is when the light that leaks out of an optical cavity is detected. In this case the measurement provides direct information about what error has occurred, reducing the resources required for quantum error correction. It is shown in [92] that when the bath that causes the errors is detected, Markovian feedback is all that is required to perform error-correction, and only $n+1$ physical qubits are required to encode n logical qubits.

Quantum feedback has been combined with open-loop control protocols to reduce errors in quantum systems. The open-loop technique of dynamical decoupling allows errors to be reduced if they are due to noise that has a sufficiently long correlation time [169–172]. In [173], feedback and dynamical decoupling are combined by feeding the output of a dynamical decoupling protocol to a feedback controller. It is shown that for a single qubit the combination of quantum feedback and dynamical decoupling outperforms either method when used alone.

2.5.2. State reduction and stabilization

In the previous section we discussed the use of feedback to protect quantum states temporarily. We refer to the indefinite protection of a quantum state as stabilization. Unknown states cannot be stabilized, but known states certainly can be. Sometimes open-loop control can be used to stabilize states, but only in certain circumstances, for example when an effectively zero-temperature environment is available [115]. Markovian quantum feedback can be used to stabilize the states of a single two-level atom when the source of decoherence is detected [115–117]. In Ref. [115] it is shown that for a two-level atom, states in an ellipsoid in the lower hemisphere of the Block sphere can be stabilized by open-loop control under the damping process. However, when we introduce Markovian quantum feedback and carefully choose the feedback gain and the strength of the driving field, it is only states on the equator of the Bloch sphere that cannot be stabilized.

More generally, Bayesian feedback has been applied to the stabilization of quantum states in a variety of mesoscopic systems [174–198]. These include nano-mechanical resonators [176–178], quantum-dots [179–190,196–198], and superconducting qubits [191–195].

Immediately before a stabilization feedback process starts, the system to be controlled will likely be in some steady state determined by the noise processes that drive it, and this state is often significantly mixed. When we first apply measurement-based feedback, the measurement will reduce the entropy of the system, a process often called *purification*. If the state towards which the measurement projects the system is not one of the eigenstates of the initial density matrix, then the measurement necessarily also induces a "collapse" of the wave-function, a process often called "state-reduction". Thus purification may or may not involve state-reduction, although often these terms are used interchangeably.

If we make a continuous measurement of an observable, and perform no feedback, then the measurement will continually try to project the system onto one of the eigenstates of the observable, where the choice of eigenstate is random. In the absence of noise that interferes with the reduction process, the final state of the system will be one of these eigenstates. As shown in [199–203], if we perform feedback control during the state-reduction process, we can control which eigenstate that the measurement projects onto.

To examine this process further, we consider the single-qubit state-reduction protocol presented in Ref. [199]. As shown in Fig. 5, a single two-level system, such as an atom, is inserted into an optical cavity, and the output of the cavity is measured by a homodyne detection. When the cavity damping rate is much faster than the dynamics of the qubit, this measurement procedure realizes a continuous measurement of the σ_z operator of the two-level system.

The stream of measurement results is fed into a digital controller and then back to control a classical field that allows us to rotate the two-level system around the y-axis. The control Hamiltonian is thus $H = B(t)\,\sigma_y$, where $B(t)$ is the control parameter that we can vary. Writing the state of the two-level system using the Bloch vector $\mathbf{v} = \left(v_x, v_y, v_z\right)^{\mathrm{T}} = \left(\langle\sigma_x\rangle, \langle\sigma_y\rangle, \langle\sigma_z\rangle\right)^{\mathrm{T}}$, the dynamics under the feedback process is

$$\begin{aligned} dv_x &= \left[B(t)\,v_z - \frac{\Gamma_z}{2}v_x\right]dt - \sqrt{\Gamma_z}\,v_x v_z\,dW, \\ dv_y &= -\frac{\Gamma_z}{2}v_y\,dt - \sqrt{\Gamma_z}\,v_y v_z\,dW, \\ dv_z &= -B(t)\,v_x\,dt + \sqrt{\Gamma_z}\left(1-v_z^2\right)dW. \end{aligned} \tag{2.82}$$

If we assume that $v_y = 0$, the control field $B(t) = Gv_x$ with $G > 0$ can steer the system to the spin-up state with unit probability. This method is extended in Ref. [203] to systems with any fixed total angular momentum J, such as a dilute gas of two-level atoms. In this work a piecewise-continuous control protocol is designed to stabilize any selected eigenstate of the J_z operator, and can also be used to stabilize the symmetric and antisymmetric states in a system with two qubits.

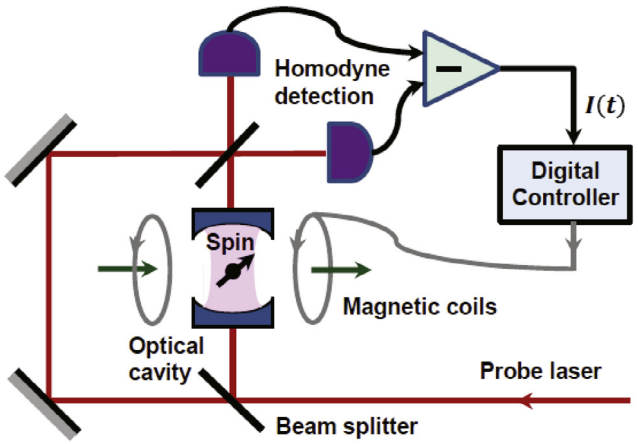

Fig. 5. Diagram of a proposal by van Handel et al. [199] for the stabilization of qubit states. The information of the spin inside the cavity is continuously extracted by an optical probe field and then detected by homodyne measurement. The electric output signal $I(t)$ of the homodyne measurement is fed into a digital controller and then fed back to control the magnetic field (shown in green) imposed on the spin.

As our final example of stabilization, we now present the approaches introduced in [204–206] in which feedback is used to stabilize a particular dressed state in a strongly-coupled cavity-QED system. For a weakly-driven single-cavity mode strongly coupled to N atoms with coupling strength g, the steady state is

$$|\psi_{ss}\rangle = |0,g\rangle + \lambda\left(|1,g\rangle - \frac{2g\sqrt{N}}{\gamma}|0,e\rangle\right) + O\left(\lambda^2\right). \tag{2.83}$$

Here γ is the damping rate of the atom, and $\lambda \ll 1$ is proportional to the ratio ε_d/κ, where ε_d and κ are the driving strength and damping rate of the cavity, respectively. The state $|j,g\rangle$ denotes j photons in the cavity mode, and all the atoms in the their ground states, while $|j,e\rangle$ denotes j photons in the cavity mode and all but one of the atoms are in their ground states.

Since the steady state has almost no photons, photon detections are relatively rare. When a photon is detected, the conditional state changes abruptly, and evolves as

$$|\psi_c(\tau)\rangle = |0,g\rangle + \lambda\left[\xi(\tau)|1,g\rangle + \theta(\tau)|0,e\rangle\right], \tag{2.84}$$

where $\xi(\tau)$ and $\theta(\tau)$ are oscillatory functions of time. It turns out that by adjusting the driving field at a specific time after the detection, the state of the system can be frozen indefinitely. Once the driving field has returned to its original value, the evolution of the conditioned state continues as if it had never been interrupted, and returns to the steady state. This feedback scheme was realized experimentally in Ref. [204].

It has also been shown that the same atom–cavity system can be stabilized in the opposite regime of strong-driving [205]. In this case one of the dressed states is stabilized by flipping the atomic state using a π-pulse when a measurement-induced quantum jump is observed. The signature of this stabilization process appears in the atomic fluorescence spectrum as the enhancement of one sideband.

Not all feedback involves changing the Hamiltonian of a system conditional upon the measurement stream. If the purpose is to engineer a specific kind of measurement, for example, one may change the *measurement* conditional on the stream of measurement results. The result of this feedback-modified measurement is referred to as an *adaptive* measurement. We will give examples of adaptive measurements below. In Refs. [207,208], the authors consider how to design an adaptive measurement to minimize the classical memory required to track the state of the measured system. They show that a d-dimensional system can be tracked by a classical k-state machine where $k \geq (d-1)^2 + 1$, and a special case shows that a qubit can be tracked by a classical bit.

2.5.3. Squeezing via feedback

A quantum harmonic oscillator obeys Heisenberg's uncertainty principle, meaning that the momentum variance can only be reduced below $\hbar m\omega/2$ at the expense of increasing the position variance above $\hbar/(2m\omega)$. Here m and ω are respectively the mass and frequency of the oscillator. For an optical mode, the equivalent conjugate variables are referred to as the amplitude quadrature X and phase quadrature Y. A state in which the variance of one conjugate variable is decreased at the necessary expense of the other is called a *squeezed* state. For a single mode of an optical or microwave cavity it is not only the state of the mode that is of interest, but the state of the traveling-wave light or electrical signal that is emitted from the cavity. We may want to squeeze either the oscillator or this output. Methods for squeezing both have been investigated quite extensively [209–211].

Assuming that the thermal noise on an oscillator is negligible, its state can be squeezed merely by modulating its frequency ω at 2ω. This is called *parametric amplification* because it amplifies one quadrature, and because ω is a "parameter" in the Hamiltonian [212]. If we want to squeeze the oscillator in the presence of thermal noise, then we need to reduce this noise, for which measurement-based feedback is one option. Neither measuring a single quadrature, nor making a homodyne measurement are sufficient for this purpose [137]. There are two methods presently known to do this. One is to make a measurement of a single quadrature, but do so in the rotating frame of the oscillator. Braginsky et al. [213] were the first to devise a method to do this, which effectively involves making a measurement of an oscillator's position, and turning the measurement off and on at the frequency 2ω (see also [143,177,214]). This "strobing" of the measurement can be achieved merely by modulating the interaction with the measuring device sinusoidally at this frequency. In the interaction picture the quadrature variables are unchanging, so that Braginsky's measurement is a *quantum nondemolition* (QND) measurement. Other methods for making QND measurements of the quadratures have be devised [137–141], but Braginsky's is probably still the most practical. A QND measurement produces a squeezed conditional state—a squeezed state from the point of view of someone who is able to have processed the measurement record to determine the means and the variances of the quadratures. Since the means fluctuate, without this information the state is not squeezed. But since a linear feedback force can be used to stabilize the means, we can use feedback from the QND measurement to produce an unconditional squeezed steady state [177,214].

The second method to produce squeezed states in the presence of significant thermal or other noise is to combine a parametric drive with a standard (unmodulated) measurement of position. Here the parametric drive creates the squeezing and the measurement is much weaker, and extracts the entropy injected by the thermal noise [215,216]. This method of producing squeezing has been realized, although not in the quantum regime, in Refs. [144,217,218].

We note that QND measurements have also been used to generate squeezing in the collective spin state of a gas of two-level atoms, both theoretically [145] and experimentally [219–221].

2.5.4. Controlling mechanical resonators

In the previous section we discussed the use of feedback to squeeze oscillators, mechanical or otherwise. We now focus on mechanical oscillators, and consider the creation of other states. The first task in bringing a mechanical resonator into the quantum regime is to suck out all the thermal noise so as to put the resonator in its ground state. From there we can use purely open-loop control protocols to place it in a more interesting nonclassical state. To make it possible to cool a mechanical resonator to the ground state (see, e.g., Refs. [222–224]), it must have a very high frequency so as to reduce the thermal noise, even when placed in a dilution refrigerator. To attain the required frequencies the resonators must have a very small mass, and there are a number of ways to realize such microscopic and mesoscopic resonators. One can merely make them small [225–237], in which case their frequencies are still a little low to enter the quantum regime. One can go even smaller by fabricating resonators on layered structures using lithography, and these are usually referred to as nano-resonators [238–244]. One can also use microscopic systems such as trapped ions [245], electrons [246], laser-trapped nano-particles [247], or a gas of neutral atoms trapped in an optical lattice [248–253]. Quite recently, quantum feedback has also been applied to Bose–Einstein condensates (BECs) for feedback-cooling an ultra-cold atomic ensemble undergoing continuous weak measurement [254,255]. It is shown that, in certain regimes, full quantum-field simulations and more exotic feedback controls are required in order to successfully cool the BEC close to the ground state [256], and the robustness of a control scheme to corruption of the measurement signal by classical noise, detector inefficiencies, parameter mismatches and a time delay is considered [257].

State-of-the-art cooling schemes for nano- and micro-mechanical resonators currently use coherent feedback, to be discussed in Section 3. Nevertheless measurement-based cooling methods for mechanical resonators have been investigated quite extensively. When the resonator is far from the quantum regime, feedback cooling of resonators can be considered classical [258–260]. The primary obstacle to cooling resonators to the ground state using measurement-based feedback is the requirement that the measurement has an efficiency near unity. At the time of writing, measurements on nano-resonators do not have the required efficiency, but we expect this to change in the near future. Cooling via measurement has been investigated both for Markovian feedback [261–263] and Bayesian feedback [112,113,176,177,264]. Feedback can also be used to create and control highly nonclassical states of resonators [114].

2.5.5. Controlling transport in nano-structures

In principle, measurement-based quantum feedback can be used to control the quantum transport process in nanostructures [265–268]. This can be thought of as stabilizing the quantum state of the transport device. The proposal in Ref. [267] shows that a classical feedback control can freeze the fluctuations of quantum transport by changing parameters in the Hamiltonian conditional to the number of tunneled particles. This feedback method can be further used to reconstruct the full counting statistics of the transport device from the frozen distribution. In [268], this proposal was applied to nonequilibrium-electron-transport through a double-quantum-dot, which for this purpose can be treated as a two-level system. The feedback is able to purify the transport state, represented by the full counting statistics of the electron flow through the device, and it is shown that half of the quantum states on the Bloch sphere of the double-quantum-dot can be stabilized. The feedback is also able to stabilize the coherent delocalized states of the electrons.

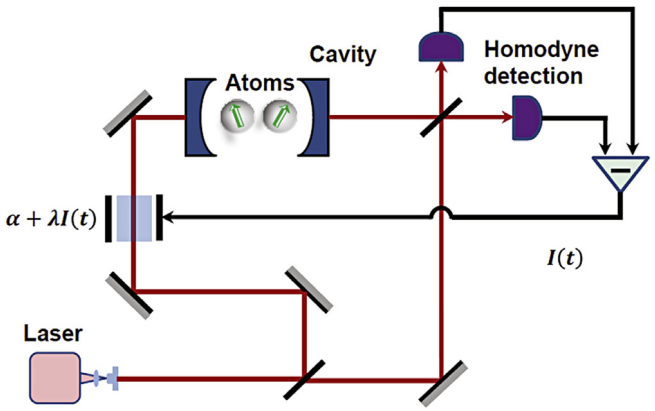

Fig. 6. Diagram of a theoretical proposal by Wang et al. [118] for two-atom entanglement creation by homodyne-mediated feedback. The homodyne current $I(t)$ from the damped cavity is directly fed back to generate a control signal $\alpha + \lambda I(t)$, which is converted into an optical signal by an electro-optic modulator and then used to resonantly drive the cavity coupled to the two atoms. These two atoms are entangled in the steady state.

2.5.6. Entanglement creation and control

It is shown theoretically in Ref. [269] that when a cavity containing two two-level atoms is resonantly driven, the steady state of the atoms can be entangled. More specifically, if (i) the cavity damping rate κ is much faster than all other timescales, so that the cavity can be adiabatically eliminated, and (ii) the collective damping rate of the atoms induced by the cavity is much larger than the atoms' spontaneous emission rates, then one can recover a Dicke model for the atoms. The steady state of this Dicke model can be written in the angular momentum basis and analyzed in terms of the symmetric and antisymmetric subspaces. When the initial state of the atoms is symmetric, the stationary state is entangled, although this entanglement, measured by the Wootters' concurrence [270], is only about 0.11 [269]. Additionally, it is shown that more complex and interesting "entangled-state cycles" can be observed in which N effective two-level atoms driven by laser and cavity fields switch between entangled states conditioned on the detections of the cavity output field [271].

It turns out that Markovian quantum feedback can be used to increase the steady state entanglement of the atoms [118–131]. It has been shown that this is possible using both feedback based on photon detections (quantum jumps) [125–131], and feedback using homodyne detection (trajectories driven by Gaussian noise) [118–122].

In Ref. [118] the authors show that for homodyne detection the stationary entanglement can be increased from 0.31 under feedback that is symmetric for the two atoms (see Fig. 6). This stationary entanglement can be increased further to 0.82 if local asymmetric feedback is introduced [119]. Feedback based on photon detections is even better at maintaining entangled states, and for symmetric feedback is able to achieve a concurrence of 0.49 [126]. This stationary entanglement is reduced by spontaneous emission, but can be increased further by the use of local asymmetric feedback. Feedback based on photon-detections is also robust against fluctuations in various parameters, such as the detection efficiency, especially in the adiabatic regime [126]. Bayesian feedback has also been used to generate and protect entanglement in the above system [146,272]. Although the computational complexity for this kind of control is high, it can also potentially produce higher entanglement.

As an extension of the above feedback schemes, the stabilization of multipartite entanglement via feedback has also been considered [273,274]. Due to the lack of a measure for multipartite entanglement, these studies have focussed on stabilizing particular multipartite entangled states, such as Dicke states [146] or GHZ states [153]. More recently, the control of entanglement via feedback has been discussed for solid-state systems, especially superconducting circuits [151–153], and has been demonstrated experimentally both in superconducting circuits [275] and cavity QED systems [276].

Continuous-variable entanglement of optical beams, which is closely related to multi-mode optical squeezing, can, and usually is, produced by using a nondegenerate parametric oscillator in an optical cavity. This method is limited by the strength of the optical nonlinearity employed, which is usually very weak, and is further reduced by the cavity damping. It has been shown that feedback can be used to increase the continuous-variable entanglement [277–285] generated in this way.

Consider two optical modes with quadrature operators X_1, Y_1 and X_2, Y_2, respectively. In Ref. [277] it is shown that a single-loop Markovian feedback scheme can be used to reduce the variance of the operator $(X_1 - X_2)$ while preserving the variance of the operator $(Y_1 + Y_2)$, thus improving the steady-state entanglement of the two modes. However, the entangled state in this case is a mixed state. A modified proposal in Refs. [278,279] is able to produce a pure steady-state two-mode entangled state by using two independent feedback loops to control the variances of $(X_1 - X_2)$ and $(Y_1 + Y_2)$ simultaneously.

It has been shown that the problem of finding the optimal homodyne measurement and Markovian feedback to produce two-mode intracavity Einstein–Podolsky–Rosen correlations for both a vacuum environment [280] and a thermal bath [281] is a semidefinite programming problem [286]. This means that a global optimum can be found numerically in a systematic way. A general upper bound for the generation of steady-state entanglement for multi-mode bosonic fields via feedback has

also been obtained [282]. Quantum feedback has been applied to the problem of generating deterministic entanglement at the single-photon level [283], to avoid entanglement sudden death [284], and to enhance entanglement distributed between cavities including propagation delays and photon loss [285].

2.5.7. Quantum state discrimination

The efficient discrimination of nonorthogonal quantum states has various applications in quantum and classical communications and quantum-enhanced metrology. For discrete-variable quantum systems, such as qubits, it has been shown theoretically [287] and experimentally [288] that continuous measurement and feedback can efficiently discriminate two nonorthogonal states of a single qubit, as well as correct these states against dephasing noise. It has also been demonstrated experimentally that adaptive local measurement and feedback performs much better than non-adaptive measurements for discriminating non-orthogonal states of qubits, given multiple copies, and can efficiently suppress noise [289].

Quantum feedback has also been used for the discrimination of coherent states of oscillators or traveling-wave fields. Such discrimination is useful for communication, because coherent states are easy to prepare and manipulate. Adaptive measurement schemes can maximize the information rate so as to achieve Holevo's bound [290], and allow for long-distance communication. It has been shown both theoretically [291] and experimentally [292–294] that joint-detection and adaptive feedback with pulse-position-modulation codewords reduces the error probability for both conditioned and unconditioned coherent-state discrimination, compared with traditional direct detection methods (e.g., homodyne detection). This method can also beat the standard quantum limit to approach the Helstrom limit [295], being the minimum achievable average probability of error for discriminating quantum states.

2.5.8. Quantum parameter estimation

High-precision phase measurements of optical beams, especially those in the quantum regime, have various important applications, such as interferometric gravity-wave detection or quantum communication. However, the phase of the electromagnetic field mode is not a directly-measurable quantity, and phase measurement protocols always measure some other quantity that introduces excess uncertainty and noise into the estimation process.

The traditional method for measuring phase was to use heterodyne detection, in which the field mode to be measured is combined with a far-detuned strong local oscillator field. It is well known that phase measurements based on heterodyne detection can reach the standard quantum limit, in which the phase sensitivity, being the variance of the measured phase $(\delta\phi)^2$, scales as N^{-1} when a state with an average of N photons is fed into the input port to be measured. But this is not the fundamental limit to phase estimation. The latter is the Heisenberg limit, which gives a scaling of N^{-2}. Theoretically, the Heisenberg limit could be achieved with a perfect measurement of canonical phase [296,297], but experimentally this is not easy.

Wiseman and collaborators [298–306] have shown that by using an adaptive measurement it is possible to realize a measurement of phase that is very close to the Heisenberg limit [296,297,307,308]. There are primarily two approaches. One can use an adaptive homodyne measurement [298–303] or an adaptive interferometric measurement [304–306] (see Fig. 7). As shown in Fig. 7(a), the key element of an adaptive homodyne phase measurement is to feed back the output of the homodyne detection to control the phase of a local oscillator, and thus track the phase quadrature to be estimated. It is shown in Ref. [299] for a semiclassical model and in Ref. [300] for a full quantum analysis that an excess phase uncertainty scaling as $N^{-3/2}$ can be reached. A modified approach in Ref. [302] shows that a more sophisticated feedback protocol can reach a better theoretical limit, scaling as $\ln N/N^2$.

The adaptive interferometric phase measurement can perform even better than the adaptive homodyne method. In an adaptive interferometry phase measurement, a Mach–Zehnder interferometer is introduced with the unknown phase to be estimated in one arm and the controllable phase used to track the unknown phase in the other arm. This achieves a phase sensitivity very close to the Heisenberg limit [304,305]. It has also been shown that both the adaptive homodyne method [303] and the interferometric method [306] can be used to estimate a stochastically-varying phase. More complex feedback designs, such as those based on time-symmetric smoothing [309–311], can also be used in adaptive phase measurement. A number of adaptive phase-measurement schemes have been demonstrated in experiments [154,312–318].

More generally, we may wish to estimate one or more numbers that parameterize the state, Hamiltonian, or overall evolution of a system. Such parameters can be estimated by making a continuous measurement on an evolving system and processing the measurement results [319–324]. Such a procedure has applications to metrology, such as the detection of weak force by monitoring a harmonic oscillator [323], or estimating the Rabi frequency of a two-level atom [320]. Feedback control can be used to make the estimation process more robust to the uncertainty in the system parameters [324]. The basic method involved in parameter estimation and metrology via continuous measurements to use a "hybrid" master equation that evolves the observer's knowledge of the system as well as their knowledge of the parameters [323], or an equivalent quantum particle filtering equation [322].

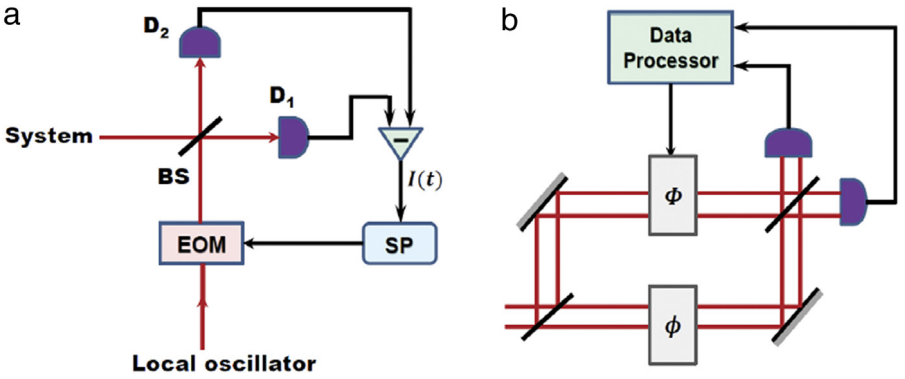

Fig. 7. (a) Theoretical proposal by Wiseman [298] for adaptive homodyne phase measurement. The output $I(t)$ of the homodyne detection is processed by a Signal Processor (SP) which then controls the phase of the local oscillator by an electro-optic modulator (EOM). (b) Theoretical proposal [305] for adaptive interferometry phase measurements. The figure shows a Mach–Zehnder interferometer with the unknown phase ϕ to be estimated in one arm and the controllable phase Φ (used to track the unknown phase ϕ) in another arm.

2.5.9. Rapid state-purification and measurement

It is possible to use quantum feedback to speed up the rate at which a continuous measurement purifies, or provides information about a quantum system [183,325–337]. To understand this further, let us consider a continuous measurement of a qubit which provides information about the basis $\{|0\rangle, |1\rangle\}$. The dynamics of this measurement is given by the SME

$$d\rho = \mathcal{D}[\sigma_z]\,\rho\,dt + \mathcal{H}[\sigma_z]\,\rho\,dW. \tag{2.85}$$

In order to study how one can reduce the observer's uncertainty of the measured quantum system, an algebraically simple measure of the observer's uncertainty, called "linear entropy", $s = 1 - \mathrm{tr}\left[\rho^2\right]$, is useful. If we assume without loss of generality that $y = 0$, we can obtain from Eq. (2.85) that [327]

$$ds = -\left(8s^2 + 4x^2 s\right)dt - 4zs\,dW, \tag{2.86}$$

where $\alpha = \mathrm{tr}\left[\sigma_\alpha \rho\right]$, $\alpha = x, y, z$. It can be seen that s will decrease more rapidly when x is maximized. If we introduce an ideal Hamiltonian feedback that rotates the qubit at each time step to maintain $z = 0$, then ds is maximized and given by $ds = -4sdt$. As shown in Ref. [325], if we start from a maximally mixed state, then under this feedback, and in the long time limit, the time required to achieve a purity of $1 - \epsilon$ is $\tau_q = \ln\left(\epsilon^{-1}\right)/4$, which is half the time taken for the average purity to reach this level without feedback. Here $\epsilon \ll 1$ denotes the error threshold value. Such an increase in the rate of purification is a purely quantum effect, and cannot be realized for an equivalent measurement on a classical bit.

Although the above analysis shows that using feedback to continually rotate the quantum state onto the plane orthogonal to the measurement axis will speed up purification, Ref. [327] shows that keeping the quantum states parallel to the measurement axis can reduce the average time for the measured quantum system to reach a given purity.

As an extension of the results in Ref. [325], a more general study in Ref. [326] shows that Hamiltonian feedback can speed up the rate of purification, or state reduction, by at least a factor of $2(d+1)/3$ for an observable with d equispaced eigenvalues. However, the quantum feedback methods in these studies concentrate only on maximizing the purity of the measured quantum states, and do not care about how to obtain information about the initial state of the system. That is why they are referred to as rapid purification protocols rather than rapid measurement protocols.

In contrast to quantum rapid purification, in Ref. [332] the authors show that quantum feedback can increase the rate of information gain about the initial preparation. It is found that the information-extraction rate for a d-dimensional system can be increased by a factor that scales as d^2. More exact bounds for rapid measurement protocols are given in [334], in which it is shown that feedback can increase the rate of information extraction by a factor R by

$$\frac{2}{3}(d+1) \le R \le \frac{d^2}{2} \tag{2.87}$$

for an observable with d equispaced eigenvalues. Further results on quantum rapid purification and measurement can be found in Ref. [335].

2.5.10. Control-free control

The term "control-free control" refers to measurement-based feedback control in which the state of the system is controlled without modifying the Hamiltonian of the system, but merely by changing the measurement with time. This is an adaptive measurement process designed to control the system. Control-free control exploits the fact that, in general, quantum measurements affect the dynamics of a system in ways that classical measurements do not. Several approaches

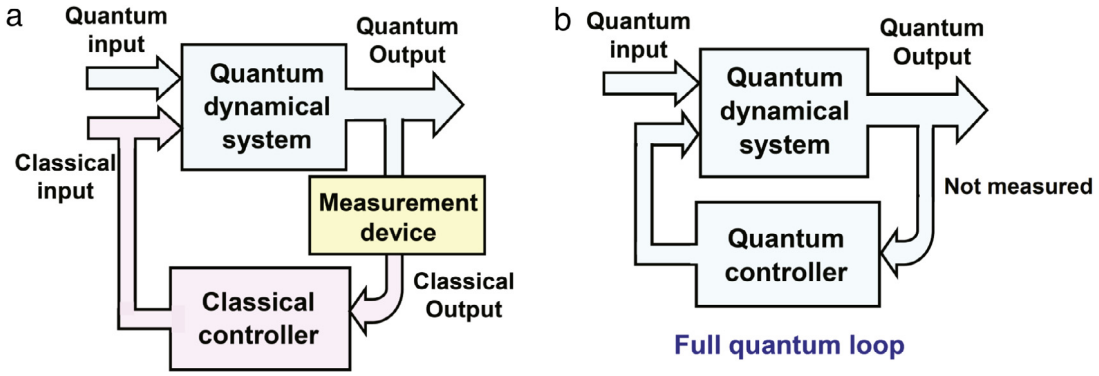

Fig. 8. Comparison of (a) measurement-based feedback and (b) coherent feedback. In measurement-based feedback in (a), the system (in blue) is controlled by a classical feedback loop (in pink); while in coherent feedback (b) the system is coherently controlled by a fully quantum feedback loop.

for control-free control have been discussed to date. In one of these, the quantum anti-Zeno effect is used to drag the system in the direction of one of the states onto which the measurement projects [338,339]. However, this requires rather strong measurements.

In another approach, a small set of measurements [340–342] is able to prepare a state by alternating between the measurements [343,344]. This process is able to stochastically drive the system towards a final pure state with unit probability. The control-free control protocols [343] have been realized in recent experiments. For example, in Ref. [345], measurement-only state manipulations are realized on a nuclear spin qubit in diamond by adaptive partial measurements. By combining a quantum nondemolition readout on the electron ancilla qubit with real-time adaptation of the measurement strength, the nuclear spin can be steered to a target state by measurements alone. This interesting work [345] shows that it is possible to implement measurement-based quantum computing by quantum feedback.

A third method [346] involves making a continuous measurement, and exploiting the fact that when the measurement-basis is chosen in the right way, the measurement generates diffusion of the state in Hilbert space. By changing the measurement basis with time, a diffusion gradient can be created in Hilbert space. This diffusion gradient will then stochastically drive the system towards a single pure state [346].

3. Coherent quantum feedback

As explained above, measurement-based feedback involves using the results of measurements on a quantum system to direct its motion. When we make a measurement on a quantum system, we obtain classical information. But we necessarily obtain only partial information about the dynamical variables, and in general we disturb the state at the same time. It is therefore interesting to consider a feedback loop in which classical information is not extracted. This concept, now referred to as *coherent feedback*, was first introduced by Lloyd in 2000 [57], and it can be seen as the more general case of the all-optical feedback proposed earlier, in 1994, in quantum optical systems by Wiseman and Milburn [51]. The idea is that instead of having a classical controller that makes a measurement on the system, the controller is a quantum system, and the control is achieved simply by having the two systems interact. To understand this better, it is worth examining the Watt governor, which has a very simple feedback mechanism. The purpose of the Watt governor is to control the speed of an engine. To do this, the engine is connected to a simple mechanical device so that it spins the device. The device is designed so that the centrifugal force from the spinning causes it to expand, so that the faster the engine spins, the more it expands. This expansion is then used to reduce the fuel supply to the engine, thus stabilizing the engine at some chosen speed. The nice thing about this simple feedback system is that we can think of it as a loop in which the control device obtains information from the engine, and uses this to control it. It is also clear that the engine and controller are merely two coupled mechanical systems. In the Hamiltonian description of the joint system, there is therefore no loop, but merely an interaction between the two systems. A quantum controller can therefore act in the same way, performing feedback control even though the description of the system may not involve an explicit loop.

In fact, there is a way to make the loop explicit for a quantum controller in which there are no measurements. This is done by coupling the system to a traveling-wave electrical (optical) field that propagates in one direction from the system to the controller. We then use a second traveling-wave field that propagates from the controller to the system, thus closing the loop. To do this, the two traveling fields must continue propagating after they interact with the systems, and this introduces an irreversible element to the dynamics. However, since control systems are usually intended to introduce some kind of damping to the system, this irreversibility need not be detrimental. In what follows, we first discuss feedback control that employs a unitary (Hamiltonian) interaction between the system and controller, often referred to as *direct coherent feedback*, and then turn to feedback in which the interaction is mediated by traveling-wave fields, often referred to as *field-mediated* feedback (see Fig. 8).

3.1. Direct coherent feedback

In general, the action of a controller that is coupled to a system via a unitary interaction may not break down into clearly defined processes which involve the extraction of information and use of this information to apply forces to the system. Nevertheless, it is interesting to construct an interaction that does perform these individual processes. As an example, let us consider the control of a single qubit by a controller that is also a qubit. The qubit to be controlled (the primary) is initially in some unknown state $|\phi\rangle = \alpha|0\rangle + \beta|1\rangle$, and we want to place it in the state $|1\rangle$. If the state of the primary is completely unknown, then from the point of view of any observer, and the controller, the state of the qubit is the density matrix $\rho = (1/2)|0\rangle\langle 0| + (1/2)|1\rangle\langle 1|$. We cannot do this by executing a unitary operation on the system, because to choose the right unitary we would need to know the initial state. If we were using measurement-based feedback, then we could perform a projective measurement on the primary, at which point we would know what unitary to apply and execute a unitary operation according to the measurement output. Note, however, that if we did this we would have destroyed the initial state, so that no other information can be extracted from it.

To use a unitary interaction to prepare the primary in the state $|1\rangle$, we need the controller to be in a pure state. Starting the controller in the state $|0\rangle$, we turn on an interaction that will transform the controller to the state $|1\rangle$ only if the primary is in state $|1\rangle$. If we write the states of the primary on the left of the tensor product, and those of the controller on the right, then the unitary operator required is

$$U_{\text{corr}} = |0\rangle\langle 0| \otimes I + |1\rangle\langle 1| \otimes (|0\rangle\langle 1| + |1\rangle\langle 0|), \tag{3.1}$$

where "$\otimes$" is the tensor product. This unitary transforms the state of the two systems as

$$U_{\text{corr}}\,|\psi\rangle \otimes |0\rangle = U_{\text{corr}}\,(\alpha|0\rangle + \beta|1\rangle) \otimes |0\rangle = \alpha|0\rangle \otimes |0\rangle + \beta|1\rangle \otimes |1\rangle. \tag{3.2}$$

The two qubits are now correlated, since the controller is in state $|1\rangle$ if and only if the primary is in state $|1\rangle$. The controller now "knows" the state of the system, and can act accordingly. To do this, we need an interaction that performs a different action on the primary for each of the states of the controller. In particular, we need to transform the state of the primary from $|0\rangle$ to $|1\rangle$ only if the state of the controller is $|0\rangle$. The unitary that does this is

$$U_{\text{fb}} = (|0\rangle\langle 1| + |1\rangle\langle 0|) \otimes |0\rangle\langle 0| + I \otimes |1\rangle\langle 1|. \tag{3.3}$$

Acting on the joint state in Eq. (3.2) with this unitary produces the final state

$$U_{\text{fb}}\,(\alpha|0\rangle \otimes |0\rangle + \beta|1\rangle \otimes |1\rangle) = |1\rangle \otimes (\alpha|0\rangle + \beta|1\rangle) = |1\rangle \otimes |\psi\rangle. \tag{3.4}$$

This completes the feedback procedure, placing the primary in the state $|1\rangle$ for every value of α and β. Interestingly the initial state of the primary has not been destroyed. This state, and thus the "quantum information" in the primary has been transferred to the controller.

In the above example, the controller in the measurement-free feedback procedure performs essentially the same action as a measurement that projects the primary onto the basis $\{|0\rangle, |1\rangle\}$. The controller becomes correlated with the system in the basis $\{|0\rangle, |1\rangle\}$, and then performs an action depending on whether the system is in state $|0\rangle$ or $|1\rangle$, just as the measurement-based feedback would. But because the projection is not actually performed, and the whole process is "coherent", the quantum information in the primary is not destroyed. We note that direct coherent feedback was experimentally demonstrated in a nuclear magnetic resonance (NMR) system shortly after it was proposed [58].

3.2. Field-mediated coherent feedback

To explain how traveling-wave fields can mediate interactions between quantum systems, it may be simplest to begin with an example. As mentioned in the introduction, feedback mediated by fields was first introduced in the setting of quantum optics [51]. In Fig. 9, we show the configuration considered in [51]. In this scheme, there are two optical cavities, one of these is horizontal in the figure (cavity 1), and the other is vertical (cavity 2). The two cavities are coupled directly by a nonlinear crystal, but this is not the field-mediated part of the coupling. The output beam from the horizontal cavity is fed through a combination of a polarization beam splitter and a Faraday rotator, and then into cavity 2. This combination breaks time-reversal symmetry, and acts differently depending on the direction that a beam passes through it. Because of this, it is able to separate the input beam to cavity 2 from the beam that comes back out in the reverse direction, so that this output beam does not go back into cavity 1. The output field from cavity 1 thus travels to cavity 2 but does not travel in the reverse direction, and, because of this, it is referred to as a unidirectional, one-way, or cascade coupling between the cavities. The combination of the polarization beam splitter and Faraday rotator is called a unidirectional coupler, or isolator, and the equivalent exists for electrical (microwave) circuits.

In the feedback scheme in Fig. 9, cavity 1 is the primary system, and cavity 2 is the controller. The controller obtains information about the system from the one-way field, and applies feedback via the direct coupling. Wiseman and Milburn [51] considered three kinds of interaction Hamiltonian V. If we define A to be an arbitrary observable of the mode in cavity 1, B an arbitrary operator of this mode, and c_2 is the annihilation operator for cavity 2, then the three interactions are (i) $V = c_2^\dagger c_2 A$, (ii) $V = (c_2 + c_2^\dagger)A$ and (iii) $V = c_2^\dagger B + c_2 B^\dagger$. The first interaction is obtained by using a nonlinear crystal

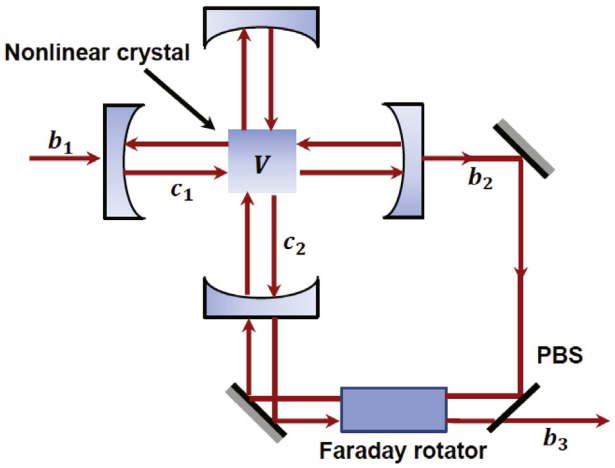

Fig. 9. Diagram of a theoretical proposal by Wiseman and Milburn [51] for an all-optical feedback scheme used to reproduce feedback via photon counting. An external input field b_1 is first fed into the horizontal cavity c_1 (the primary system), and then the output field b_2 is directed back to be fed into another vertical cavity c_2 (controller) via an all-optical feedback loop. The vertical cavity (controller) and the horizontal cavity (system) are coupled to each other by a nonlinear crystal which induces a nonlinear coupling, denoted by the interaction Hamiltonian $V = c_2^\dagger c_2 A$, where A is an arbitrary observable of the mode in cavity 1. The Faraday rotator and the Polarization-sensitive Beam Splitter (PBS) are introduced to generate a unidirectional feedback loop.

with a $\chi^{(2)}$ nonlinearity, and can be used to reproduce feedback via photon counting. The second interaction can be realized by a $\chi^{(2)}$-nonlinear crystal and one additional field which may be treated classically. It can be used to mimic feedback via homodyne detection. The third interaction provides feedback for which there is no equivalent measurement-based feedback protocol, and can generate nonclassical states in the primary mode. For example, if we choose $B = i\lambda(c_1 + \mu c_1^\dagger)$ where λ is real and positive and μ is real, the resulting feedback produces squeezed states of the primary mode for $0 < |\mu| < 1$. However, it is not easy to realize this interaction experimentally. One possibility, discussed in [51], would be to combine mode conversion using a polarization rotator with a $\chi^{(2)}$ nonlinear crystal.

3.2.1. Networks of quantum systems

The configuration of the feedback system in Fig. 9 has a unidirectional connection from the system to controller, which replaces the measurement in measurement-based feedback, but does not use a unidirectional coupling for the feedback part of the loop. We can, however, use a cascade connection for both, in which case we have a complete unidirectional loop. What we now need to know is how to describe these cascade connections mathematically. To do this, we use the input–output, or "quantum noise" formalism of Collett and Gardiner (CG) [53,83], also known as the Hudson–Parthasarathy (HP) model. In fact, Hudson and Parthasarathy independently derived a somewhat more general quantum stochastic calculus in a mathematical context, using the rigorous formalism of quantum probability theory. The formalism uses Heisenberg equations of motion for the operators of the systems, with input operators that drive these equations in a similar way to that in which Wiener noise drives classical stochastic equations. The formalism also contains output operators, and systems are then easily connected together by setting the input of one system equal to the output of another.

In the CG/HP formalism, each system is described by a Hamiltonian, along with the operators through which it is coupled to the input/output fields. Further, the fields can be coupled to each other using beam splitters, which take two inputs and produce two outputs that are linear combinations of the inputs. By describing a single "unit" as having a Hamiltonian H, a vector of input coupling operators $\mathbf{L}$, and a linear transformation between inputs and outputs codified by a matrix $\mathbf{S}$, Gough and James [62] elucidated a set of rules that covered the ways in which these units, or network elements, could be combined into networks. We now describe the CG/HP formalism, and the Gough–James rules [62] for combining circuit elements.

The dynamics of a system coupled to input fields is given by the quantum Langevin equations, i.e., Eq. (2.11), and the output fields that correspond to each input are given by Eq. (2.12). As mentioned above, we describe each unit by a tuple

$$G = (\mathbf{S}, \mathbf{L}, H)\,, \tag{3.5}$$

where H is the internal Hamiltonian of the system;

$$\mathbf{S} = \begin{pmatrix} S_{11} & \cdots & S_{1n} \\ \vdots & \ddots & \vdots \\ S_{n1} & \cdots & S_{nn} \end{pmatrix} \tag{3.6}$$

Table 1
Quantum Ito rule for quantum stochastic calculus.

dX/dY	$d\mathbf{B}$	$d\boldsymbol{\Lambda}$	$d\mathbf{B}^\dagger$	dt
$d\mathbf{B}$	0	$d\mathbf{B}$	dt	0
$d\boldsymbol{\Lambda}$	0	$d\boldsymbol{\Lambda}$	$d\mathbf{B}^\dagger$	0
$d\mathbf{B}^\dagger$	0	0	0	0
dt	0	0	0	0

is a scattering matrix with operator entries satisfying $\mathbf{S}^\dagger\mathbf{S} = \mathbf{S}\mathbf{S}^\dagger = \mathbf{I}$ and $\mathbf{S}^\dagger$ is defined by

$$\mathbf{S}^\dagger = \begin{pmatrix} S_{11}^\dagger & \cdots & S_{n1}^\dagger \\ \vdots & \ddots & \vdots \\ S_{1n}^\dagger & \cdots & S_{nn}^\dagger \end{pmatrix}; \tag{3.7}$$

$\mathbf{L} = (L_1, \ldots, L_n)^{\mathrm{T}}$ is a vector of operators through which the system couples to the inputs, with one for each input. We denote the inputs to the system by $\mathbf{b}_{\mathrm{in}}(t) = [b_1(t), \ldots, b_n(t)]^{\mathrm{T}}$ in which each of the $b_i(t)$, $(i = 1, \ldots, n)$ are separate input fields, all initially in the vacuum state. The notation given in Eq. (3.7) can be used to describe a wide range of dynamical and static systems. A single quantum input–output system given by Eqs. (2.47) and (2.49) can be written as $G_{\mathrm{LH}} = (I, \mathbf{L}, H)$, and a quantum beam splitter is given by $G_{\mathrm{BS}} = (\mathbf{S}, 0, 0)$. Many examples of the use of this formalism can be found in Refs. [62,347–352]. We now present the Langevin equations describing input–output systems in more generality. To begin, we introduce a vector of quantum Wiener processes $\mathbf{B}(t)$ and a matrix of quantum Poisson processes $\boldsymbol{\Lambda}(t)$ as

$$\mathbf{B}(t) = \begin{pmatrix} B_1 \\ \vdots \\ B_n \end{pmatrix}, \qquad \boldsymbol{\Lambda}(t) = \begin{pmatrix} B_{11} & \cdots & B_{1n} \\ \vdots & \ddots & \vdots \\ B_{n1} & \cdots & B_{nn} \end{pmatrix}. \tag{3.8}$$

These noise processes are integrals of the input fields:

$$B_i(t) = \int_0^{\mathrm{T}} b_i(\tau)\, d\tau, \qquad B_{ij}(t) = \int_0^{\mathrm{T}} b_i^\dagger(\tau)\, b_j(\tau)\, d\tau. \tag{3.9}$$

The increments of these processes $\mathbf{B}(t)$ and $\boldsymbol{\Lambda}(t)$ satisfy the quantum stochastic calculus relations given in Table 1. Let $V(t)$ be the unitary evolution operator of the total system composed of the controlled system and the input field, then the evolution equation of the total system can be written as [62]

$$dV(t) = \left\{ \mathrm{tr}\left[(\mathbf{S} - I)\, d\boldsymbol{\Lambda}^{\mathrm{T}}\right] + d\mathbf{B}^\dagger \mathbf{L} - \mathbf{L}^\dagger \mathbf{S}\, d\mathbf{B} - \frac{1}{2}\mathbf{L}^\dagger \mathbf{L}\, dt - iH dt \right\} V(t) \tag{3.10}$$

with initial condition $V(0) = I$. Note that $d\mathbf{B}^\dagger$ is defined by

$$d\mathbf{B}^\dagger = \left(dB_1^\dagger, \ldots, dB_n^\dagger\right). \tag{3.11}$$

In the Heisenberg picture, the system operator $X(t) = V^\dagger(t) X V(t)$ satisfies the following quantum stochastic differential equation

$$\begin{aligned} dX(t) = {} & \left\{\mathcal{L}_{\mathbf{L}(t)}[X(t)] - i[X(t), H(t)]\right\} dt + d\mathbf{B}^\dagger(t)\, \mathbf{S}^\dagger(t)\, [X(t), \mathbf{L}(t)] + \left[\mathbf{L}^\dagger(t), X(t)\right] \mathbf{S}(t)\, d\mathbf{B}(t) \\ & + \mathrm{tr}\left\{\left[\mathbf{S}^\dagger(t) X(t) \mathbf{S}(t) - X(t)\right] d\boldsymbol{\Lambda}^{\mathrm{T}}(t)\right\}, \end{aligned} \tag{3.12}$$

where the Liouville superoperator $\mathcal{L}_{\mathbf{L}}(\cdot)$ is defined by

$$\mathcal{L}_{\mathbf{L}}(X) = \frac{1}{2}\mathbf{L}^\dagger [X, \mathbf{L}] + \frac{1}{2}\left[\mathbf{L}^\dagger, X\right] \mathbf{L} = \sum_{j=1}^{n} \left\{ \frac{1}{2} L_j^\dagger \left[X, L_j\right] + \frac{1}{2}\left[L_j^\dagger, X\right] L_j \right\}, \tag{3.13}$$

which is of the standard Lindblad form. Similar to Eq. (2.49), the output fields corresponding to the inputs $\mathbf{B}(t)$ and Poisson process $\Lambda(t)$ are given by

$$\mathbf{B}_{\mathrm{out}}(t) = V^\dagger(t)\, \mathbf{B}(t)\, V(t), \qquad \boldsymbol{\Lambda}_{\mathrm{out}}(t) = V^\dagger(t)\, \boldsymbol{\Lambda}(t)\, V(t),$$

from which we obtain the following input–output relation

$$\begin{aligned} d\mathbf{B}_{\mathrm{out}}(t) &= \mathbf{S}(t)\, d\mathbf{B}(t) + \mathbf{L}(t)\, dt, \\ d\boldsymbol{\Lambda}_{\mathrm{out}}(t) &= \mathbf{S}^*(t)\, d\boldsymbol{\Lambda}(t)\, \mathbf{S}^{\mathrm{T}}(t) + \mathbf{S}^*(t)\, d\mathbf{B}^*(t)\, \mathbf{L}^{\mathrm{T}}(t) + \mathbf{L}^*(t)\, d\mathbf{B}^{\mathrm{T}}(t)\, \mathbf{S}^{\mathrm{T}}(t) + \mathbf{L}^*(t)\, \mathbf{L}^{\mathrm{T}}(t)\, dt. \end{aligned} \tag{3.14}$$

For the matrix $\mathbf{M} = \{m_{ij}\}$ with operator entries m_{ij}, the notations in the above equation are defined by

$$\mathbf{M}^\dagger = \{m_{ji}^\dagger\}, \quad \mathbf{M}^* = \{m_{ij}^\dagger\}, \quad \mathbf{M}^{\mathrm{T}} = \{m_{ji}\}. \tag{3.15}$$

It can be verified that the increments $d\mathbf{B}_{\mathrm{out}}$ and $d\boldsymbol{\Lambda}_{\mathrm{out}}$ of the output processes also satisfy the rules of quantum stochastic calculus shown in Table 1.

For linear quantum systems, the quantum Langevin equations can be solved directly. In order to perform calculations for nonlinear quantum systems, one must transform the Heisenberg equations of the input–output formalism to master equations. The corresponding master equations are

$$\dot{\rho} = -i\,[H, \rho] + \sum_j \left(L_j \rho L_j^\dagger - \frac{1}{2} L_j^\dagger L_j \rho - \frac{1}{2} \rho L_j^\dagger L_j \right). \tag{3.16}$$

Although the scattering matrix $\mathbf{S}$ does not appear in the master equation (3.16), it affects the input–output relation of the system as shown in Eq. (3.14) and thus will affect the dynamics of more complex quantum input–output systems, such as the quantum cascade systems which will be specified below.

To connect the outputs of one unit to the inputs of another, so as to form an arbitrary network, we need only two rules. The first is merely a rule that says how to represent a universe that contains more than one separate unit, none of which are connected. If we have the two units $\mathbf{G}_1 = (\mathbf{S}_1, \mathbf{L}_1, H_1)$ and $\mathbf{G}_2 = (\mathbf{S}_2, \mathbf{L}_2, H_2)$, the larger unit that describes both of these units with no connections between them is

$$\mathbf{G}_1 \boxplus \mathbf{G}_2 = \left(\begin{pmatrix} \mathbf{S}_1 & 0 \\ 0 & \mathbf{S}_2 \end{pmatrix}, \begin{pmatrix} \mathbf{L}_1 \\ \mathbf{L}_2 \end{pmatrix}, H_1 + H_2 \right). \tag{3.17}$$

Gough and James [62] refer to this rule as the *concatenation product*.

The second rule for combining circuit elements tells us how to determine the unit that describes a network in which the outputs of a unit $\mathbf{G}_1$ are connected to the inputs of a unit $\mathbf{G}_2$. This rule is

$$\mathbf{G}_2 \lhd \mathbf{G}_1 = \left(\mathbf{S}_2\mathbf{S}_1, \mathbf{L}_2 + \mathbf{S}_2\mathbf{L}_1, H_1 + H_2 + \frac{1}{2i}\left(\mathbf{L}_2^\dagger \mathbf{S}_2 \mathbf{L}_1 - \mathbf{L}_1^\dagger \mathbf{S}_2^\dagger \mathbf{L}_2 \right) \right), \tag{3.18}$$

and is called the *series product*. The concatenation and series products can also be used to decompose a given system into subsystems, and are thus fundamental to feedforward and feedback control.

3.2.2. Quantum transfer-function model

The Collett–Gardiner/Hudson–Parthasarathy cascade connections can be used to model essentially any network. However, for linear systems, time delays and quantum amplifiers can be modeled more easily in frequency space. If we specialize the network formalism of Gough and James [62] so that all the systems are linear, and transform the equations of motion to frequency space, then we have the method of quantum transfer functions [347–350].

A general linear quantum network described by the tuple $(\mathbf{S}, \mathbf{L}, H)$ satisfies the following conditions [349]: (i) the scattering matrix $\mathbf{S}$ is now a matrix of numbers rather than operators; (ii) the dissipation operators L_j are linear combinations of the a_k and $a_k^\dagger$; and (iii) the system Hamiltonian H is a quadratic function of the a_k and $a_k^\dagger$. To elucidate the transfer-function method further, we consider a useful special case, in which each system is a harmonic oscillator, and the field coupling operators are linear combinations of only the annihilation operators. In this case, the Langevin equations for the annihilation operators are not coupled to those for the creation operators. The annihilation operators for the n oscillators, $\{a_j : j = 1, \ldots, n\}$, satisfy the commutation relations

$$\left[a_j, a_k^\dagger\right] = \delta_{jk}, \qquad \left[a_j, a_k\right] = \left[a_j^\dagger, a_k^\dagger\right] = 0.$$

For our special case, the total Hamiltonian is $H = \sum_{ij} \omega_{ij} a_i^\dagger a_j$ and the coupling operators $L_j = \sum_{jk} c_{jk} a_k$, and so we can simplify the SLH formalism, writing the tuple as

$$G = (\mathbf{S}, C, \Omega), \tag{3.19}$$

where

$$C = \begin{pmatrix} c_{11} & \cdots & c_{1n} \\ \vdots & \ddots & \vdots \\ c_{n1} & \cdots & c_{nn} \end{pmatrix}, \quad \Omega = \begin{pmatrix} \omega_{11} & \cdots & \omega_{1n} \\ \vdots & \ddots & \vdots \\ \omega_{n1} & \cdots & \omega_{nn} \end{pmatrix}.$$

If we now introduce an operator vector, which we will call the state vector of the system, $\mathbf{a} = (a_1, \ldots, a_n)^{\mathrm{T}}$, then from Eqs. (3.12) and (3.14), we can obtain the following Langevin equation and input–output relation:

$$\dot{\mathbf{a}}(t) = A\,\mathbf{a}(t) - C^\dagger \mathbf{S}\,\mathbf{b}_{\mathrm{in}}(t), \tag{3.20}$$

$$\mathbf{b}_{\mathrm{out}} = \mathbf{S}\,\mathbf{b}_{\mathrm{in}}(t) + C\,\mathbf{a}(t), \tag{3.21}$$

where $A = -C^\dagger C/2 - i\Omega$.

We can now transform these equations to frequency space by taking either the Laplace transform or the Fourier transform. Using the Fourier transform, defined as

$$R(\nu) = \int_0^\infty \exp(-i\nu t)\ R(t)\, dt, \tag{3.22}$$

the Langevin equations can be rearranged to obtain

$$\mathbf{a}(\nu) = -(i\nu I_n - A)^{-1} C^\dagger \mathbf{S}\, \mathbf{b}_{\text{in}}(\nu), \tag{3.23}$$

$$\mathbf{b}_{\text{out}}(\nu) = \mathbf{S}\, \mathbf{b}_{\text{in}}(\nu) + C\mathbf{a}(\nu), \tag{3.24}$$

where I_n is $n \times n$ identity matrix. From Eqs. (3.23) and (3.24), we can obtain the input–output relation of the whole system or network

$$\mathbf{b}_{\text{out}}(\nu) = \Xi(i\nu)\ \mathbf{b}_{\text{in}}(\nu), \tag{3.25}$$

where $\Xi(\cdot)$ is the transfer function of the linear quantum system which can be calculated by

$$\Xi(i\nu) = \mathbf{S} - C(i\nu I_n - A)^{-1} C^\dagger\, \mathbf{S}. \tag{3.26}$$

The input–output relation (3.25) show the linear map between the input and output of the linear quantum system given by Eqs. (3.20) and (3.21).

The quantum transfer function approach is useful for a number of reasons. While the time-domain network formalism can describe essentially any network, it cannot be used to incorporate static models of non-conservative elements, such as quantum amplifiers, and such components must be treated as dynamical systems. In frequency space, a static model of a quantum amplifier is simply a Bogoliubov transformation [350]. Time delays are also much simpler to include in frequency space, and of course frequency space has the advantage that the transfer function of two cascaded systems is merely the product of the transfer functions of each.

3.3. Applications

3.3.1. Noise-reduction in linear systems

Like measurement-based quantum feedback, the main merit of quantum coherent feedback is that it can be used to suppress sources of entropy, such as external noise, uncertainty in the parameters that define the system, and even to some extent errors in the modeling of the system. In general, the problem of noise-reduction can be captured by asking how to minimize the effect of a set of inputs on a set of outputs. For linear networks, this problem has been studied by a number of authors. James, Nurdin, and Petersen developed linear–quadratic–Gaussian control [67] and H-infinity (H_∞) control [61]. Control of linear systems with squeezers and phase-shifters has been explored by Zhang et al. [352], and Zhang and James [351] have investigated the relationship between direct and field-mediated coupling in networks. The extension of the Collett and Gardiner input–output formalism to non-Markovian field couplings has been developed by Diosi [353] and Zhang et al. [354], and noise suppression via non-Markovian coherent feedback has been analyzed by Xue et al. [355]. For non-Markovian input–output systems, the Markovian assumption (2.39) may not be valid, which will lead to input fields with colored noises rather than white noises [353]. The output fields and the dynamical equations of these systems not only depend on the current-time states of the systems but also depend on the past-time information [354], and thus these systems are non-Markovian. These kind of non-Markovian coherent feedback models can be useful when considering the control of solid-state quantum systems such as superconducting circuits or quantum dots. Coherent noise-reduction for a single cavity was demonstrated experimentally by Mabuchi in [356]. It was also shown quite recently that coherent feedback can be used to control the quantum-transport properties of a mesoscopic device and optimize the conductance of a chaotic quantum dot [357].

3.3.2. Optical squeezing

Squeezing as an application of coherent feedback was considered in Ref. [51]. More recently, a coherent protocol for squeezing was devised by Gough and Wildfeuer [358] which is simpler and allows more control of the amount squeezing. This protocol [358] has now been experimentally realized by Furusawa's group in a linear optical system [359]. We depict the protocol in Fig. 10, in which we see that the coherent feedback loop is composed of a squeezing component, such as a degenerate parametric amplifier in the strong-coupling regime, and a beam splitter whose reflectivity can be adjusted. By tuning this reflectivity, the effective damping rate of the cavity is modified, and the squeezing effects are enhanced or suppressed.

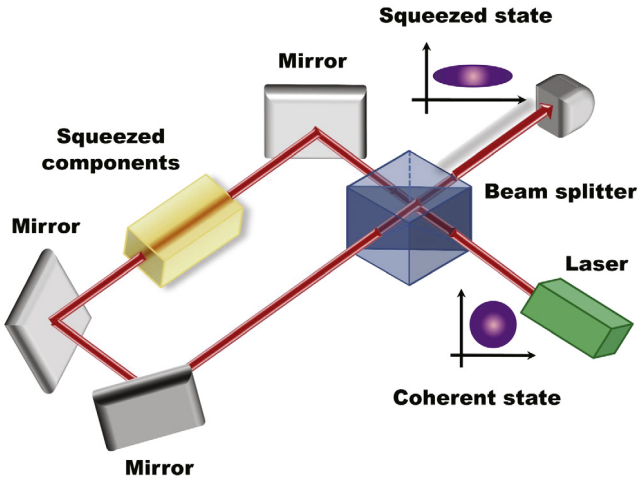

Fig. 10. Diagram of a theoretical proposal by Gough and Wildfeuer [358] for tunable optical squeezing by coherent feedback. The optical squeezing output produced by a squeezing device can be enhanced and suppressed by tuning the reflectivity of a control beam splitter within the coherent feedback loop.

3.3.3. Quantum error correction

Coherent quantum feedback has been used to implement continuous quantum error-correction (see the start of Section 2 for a brief introduction to quantum error correction) [360,361]. In Ref. [360], the authors propose a three-qubit error correction method to correct single-qubit bit-flip or phase-flip errors using coherent feedback. As shown in Fig. 11, the atoms in cavities Q_1, Q_2, and Q_3 are the three physical qubits that code for, and thus allow, the single logical qubit to be corrected. The blue lines are the optical beams for error detection and the red lines are the laser beams that apply the bit flips or phase flips. The central components of this autonomous error correction network are the two relays R_1 and R_2, which work as controlled quantum switches [362,363]. When the "Reset" ("Set") input port of the relay receives a coherent input signal, the input from the "Power in" port will be transferred to the "Out" ("$\overline{\text{Out}}$") port. The operating principle of the quantum error correction network can be summarized as follows. If the qubits Q_1 and Q_2 have even (odd) parity, the "Set" ("Reset") input port of the relay R_1 receives a signal, while the "Reset" ("Set") input port remains in the vacuum. The same relationship exists between the relay R_2 and the qubits Q_2 and Q_3. This detected signal controls the power transfer of the relay from the "Power in" port to the "Out" or "$\overline{\text{Out}}$" port, which is then directed back to the qubits. When a qubit is simultaneously stimulated by two feedback signals from the output ports of the relays, the Raman resonance process will lead to a coherent Rabi oscillation of the qubit and thus correct the errors. Otherwise, the control signal will only introduce an ac Stark shift for the qubit. Such a coherent feedback network can thus automatically correct the bit-flip or phase-flip errors. In Ref. [361], the authors extend this method to perform corrections for Shor's nine-bit error-correcting code, which concatenates two three-bit codes so as to correct an arbitrary error.

3.3.4. Controlling mechanical resonators

Mechanical resonators can be built with sufficiently high frequencies that they will behave quantum mechanically at a temperature of a few milliKelvin, only an order of magnitude from temperatures that can be reached with dilution refrigerators. These mechanical resonators can be coupled to optical modes ("optomechanics") or cryogenic superconducting circuits (nanoelectromechanics) for potential use in more complex devices. To prepare highly nonclassical states, or for the purpose of using mechanical resonators for quantum technologies, it is useful to prepare them in the ground state. This is usually referred to as cooling.

As far as experiments are concerned, the present state of the art in cooling mechanical resonators is a version of "resolved-sideband" cooling [87,88]. This method is, in fact, an example of coherent feedback. The mechanical resonator is linearly coupled to another "auxiliary" harmonic oscillator, a mode of an optical or superconducting cavity. These auxiliary resonators have such high frequencies that they sit in their ground states at cryogenic temperatures. The coupling is modulated at the difference frequency of the two resonators, which allows them to exchange excitations as if they were on resonance. The auxiliary oscillator is arranged to have a higher damping rate than the mechanical resonator, and because the former is in its ground state at the ambient temperature, it sucks the energy out of the mechanical resonator [86,364–367]. The coupling can be direct or field-mediated. Sideband cooling is limited by the linear interaction: to transfer energy without heating the strength of the interaction must be much smaller than the frequency of the mechanical resonator, so that the rotating-wave approximation is valid. It has been shown that if the interaction strength is modulated in a more complex way, then this limitation can be overcome, and energy (or quantum information) can be transferred between the resonators within a single period of the mechanical resonator [368].

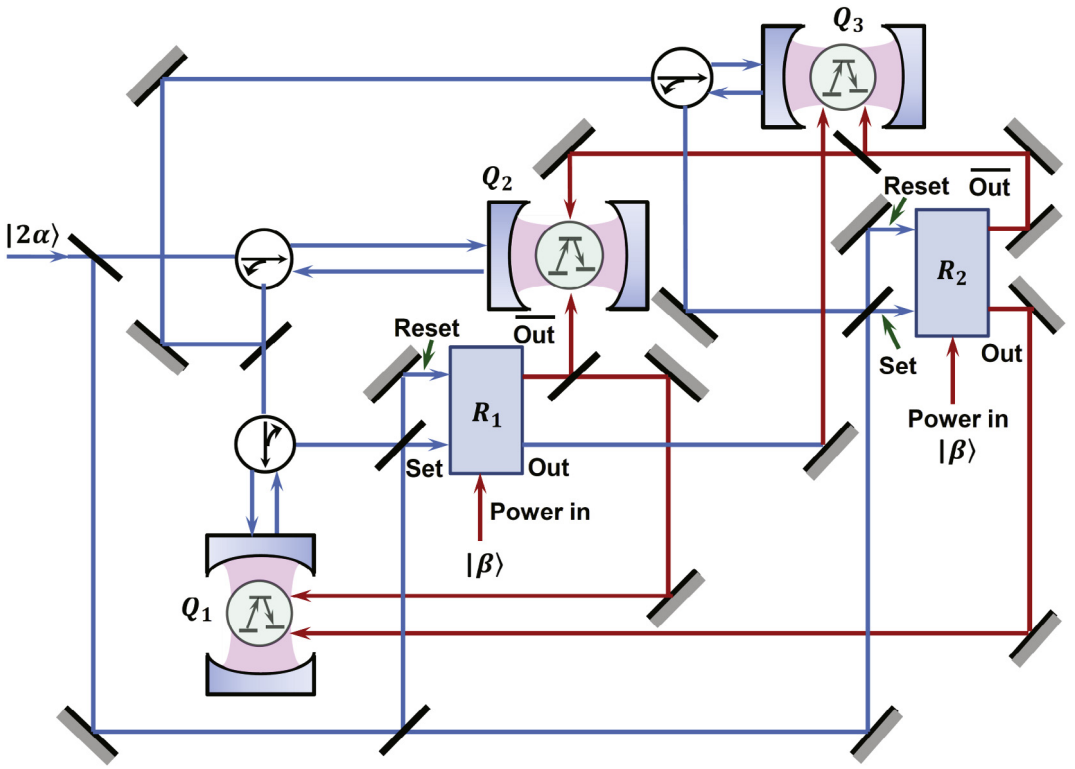

Fig. 11. Diagram of a theoretical proposal by Kerckhoff et al. [360] for an autonomous three-qubit quantum error correction network. This scheme has been proposed to correct single-qubit bit-flip or phase-flip errors, which includes register qubits $Q_{1,2,3}$, beam splitters, circulators, and the relays R_1 and R_2. The blue lines and red lines represent the probe beam and the feedback correction beam, respectively. The relays are quantum switches introduced in Ref. [362]. R_1 and R_2 have two outputs denoted by Out and $\overline{\text{Out}}$.

It has been shown that if one is restricted to a linear interaction with a resonator, then coherent feedback performs much better than measurement-based feedback in the quantum regime, including the regime of ground-state cooling [68,369]. The superiority of coherent feedback in this case can be traced to the projection noise from the position measurement [370]. This noise is the change in the quantum state induced by the measurement, which is the term proportional to the Wiener noise in the stochastic master equation.

A recent experiment by Kerckhoff et al. has shown that coherent feedback can be used as a practical method to tune the damping rate of a superconducting oscillator [369].

3.3.5. *Quantum nonlinear optics*

As is well known, it is not easy to deterministically generate nonclassical optical states due to the absence of strong optical nonlinearities. To solve this problem, an interesting study by Yanagisawa in Ref. [371] showed that nonclassical optical states can be produced via linear optical components by introducing a multiple-feedback structure. It is first shown how a quantum-nondemolition output of x^2 can be constructed by reading out the x quadrature of the optical field and feeding it back to adjust the system–environment coupling strength. In this way one can produce eigenstates of x^2, which are superpositions of two eigenstates of position with eigenvalues of equal magnitude. A further feedback loop is then introduced in which the Hamiltonian of the controlled system is adjusted by the quantum nondemolition output of x to increase the probability to obtain a desired superposition state. However, in this method the first form of feedback is hard to realize experimentally. To solve this problem, Zhang et al. [65,66] proposed a method which they called "quantum feedback nonlinearization". This enables strong nonlinear effects in a linear plant by the use of a weak-nonlinear component and a quantum amplifier. With this method it is possible to generate strong Kerr effects that are four or five orders of magnitude stronger than the initial nonlinearity, and can demonstrate nonclassical optical phenomena such as sub-Poisson photon counting statistics and photon antibunching effects.

Another potential application of coherent feedback in nonlinear optical systems is classical information processing. An optical Kerr-nonlinear resonator in a nanophotonic device can exhibit dispersive bistability effects, and these can be used for all-optical switching in the attojoule regime [372–375]. However, in this regime, the optical logic states are separated by only a few photons and thus suffer from random switching due to quantum noise [376,377]. In Ref. [378], Mabuchi proposed a coherent feedback method to avoid the quantum noise. In this scheme, a Kerr-nonlinear ring resonator works as an optical

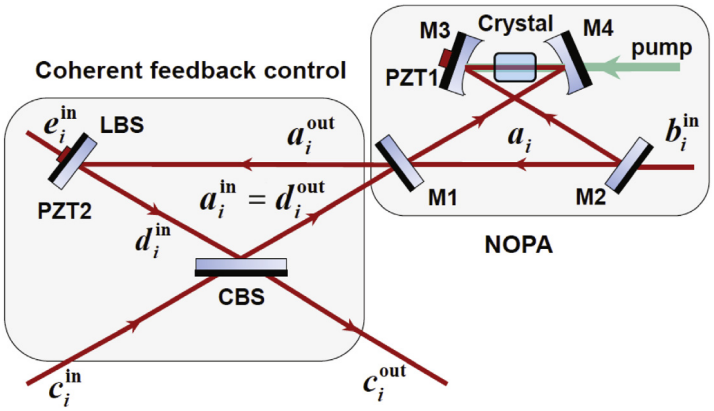

Fig. 12. Schematic diagram of a theoretical proposal by Yan et al. [380] for continuous-variable multipartite entanglement control. A multipartite entangled state is generated by a nondegenerate optical parametric amplifier (NOPA) and enhanced by a coherent feedback loop. The amount of entanglement that is generated can be tuned by adjusting the transmissivity of the control beam splitter (CBS).

switch in which the two states have differing numbers of photons. This switch is connected to a second Kerr-nonlinear ring resonator, which acts as a controller that suppresses the spontaneous switching, in a feedback configuration. Since the effective cavity detuning of a Kerr resonator varies with the driving strength, the controller induces an amplitude-dependent phase shift ϕ on the optical beam. This leads to a ϕ-dependent effective detuning, and a ϕ-dependent effective cavity decay rate for the switch (the controlled resonator). One chooses the control parameter ϕ in an optimal way so that the overall feedback phase is close to π when the switch is in the "low" state and close to zero when it is in the "high" state. In this way, the spontaneous switching between the "low" and "high" states can be efficiently suppressed.

The proposal of Ref. [378] was extended in Ref. [63] to implement photonic sequential logic by using optical Kerr resonators, in which interference effects enable the binary logic gates. Binary logic elements, such as single-output AND gate and NOT gates with an output fan-out of two, can be generated in this way [379]. This theoretical proposal has been experimentally realized in superconducting circuits by Kerckhoff et al. [64], in which the emergent bistable and astable states were used to realize a latch.

3.3.6. Controlling entanglement

A proposal in Ref. [380] shows that coherent feedback can be used to generate and control continuous-variable multipartite optical entangled states. As shown in Fig. 12, in this scheme the multipartite entangled state generated by a nondegenerate optical parametric amplifier (NOPA), denoted by the output fields a_i^{out}, are fed into a coherent feedback control loop. The optical beam d_i^{in} is split into two branches by a controlled beam splitter (CBS). One branch, denoted by $a_i^{\text{in}} = d_i^{\text{out}}$, is fed back to the NOPA to couple with the intracavity optical modes a_i and the other branch, c_i^{out}, provides the multipartite entangled output. Here, the subscripts $i = 1, \ldots, N$ denote different longitude output modes with different frequencies, which are entangled with each other via the nonlinear medium inside the NOPA and thus constitute the multipartite entangled state. The multipartite entanglement can be controlled by adjusting the transmissivity t of the CBS. The NOPA in Fig. 12 is composed of a nonlinear crystal and a bow-tie type ring cavity. The fields b_i^{in} and e_i^{in} are vacuum fields introduced to model the loss in the NOPA and the coherent feedback loop. The piezoelectric transducers (PZTs) are used to lock the cavity length for resonance. The authors evaluated the multipartite entanglement that is generated by the scheme between longitude output modes c_i^{out}. More specifically, they calculated the quantum correlation variances of the quadrature amplitude and phase components of c_i^{out} and used the nonseparability criterion developed in Ref. [381] to evaluate the multipartite entanglement. They found that the coherent feedback loop can efficiently enhance the multipartite entanglement generated by the NOPA in particular parameter regimes that can be reached by tuning the transmissivity of the CBS.

4. Other kinds of quantum feedback

4.1. Adaptive feedback

"Adaptive feedback" is a term that was coined by Judson and Rabitz in 1992 in a now famous paper [382]. This term does not refer to feedback in the sense used by the classical control community, in which a measured signal is fed back as it is received to control a dynamical system. Instead, adaptive feedback, also known as a "learning control loop", refers to an iterative method for searching open-loop control protocols. The idea is to start with some arbitrary control protocol, try it out on a real system to see how well it does, modify the protocol in some way based on its performance, and repeat this process many times to obtain increasingly better protocols. One way to do this is to use a "genetic algorithm", in which one

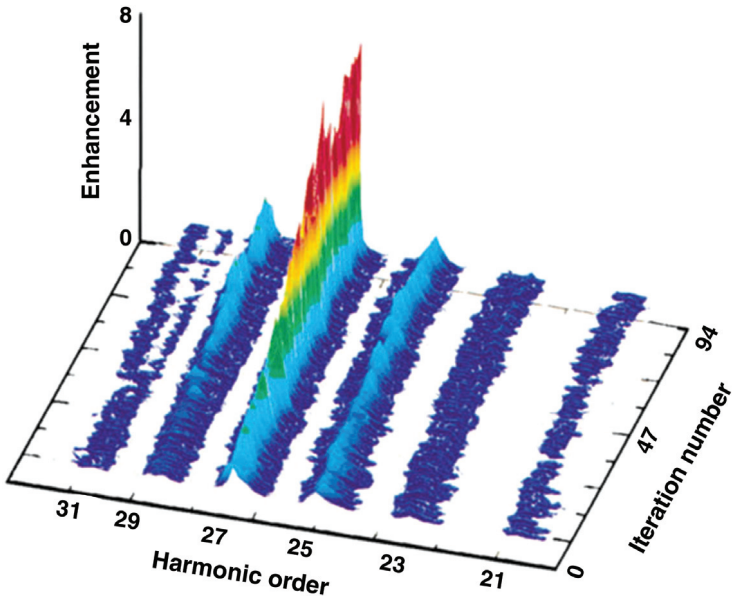

Fig. 13. The improved yield from a High-Harmonic Generation (HHG) experiment by Bartels et al. [383]. The adaptive-feedback-control (AFC) guided search found a control that can selectively enhance the 27th-order harmonic mode.
Source: This figure is from Ref. [383].

tries not one, but N randomly chosen protocols. One then selects from these the M protocols that perform the best, creates a new set of N protocols by making random changes to these M protocols, and repeats the process. This is the same procedure that is used for numerical searches to find optimal protocols. The essential point is that when the system to be controlled is too complex to simulate on a computer, replacing the computer simulation with the real system can be a fast and effective way to obtain good control protocols. We also note that adaptive control has also proved to be an effective way to obtain protocols that are robust against imperfections in the control pulse [8]. This means that the pulse, or protocol, can sustain a certain level of noise without significantly affecting its performance.

The adaptive feedback method for designing control protocols has been successfully applied to a range of tasks in the control of molecules and chemical reactions, such as the discrimination of similar molecules, ionization, and molecular isomerization. It has also been applied to ultrafast optical switching in semiconductors [8], and the production of X-rays through high-harmonic generation (HHG) [383]. While second-order harmonics are easily generated, the production of X-rays requires harmonics to tenth order or higher, which in turn requires a very high optical nonlinearity and an intense laser. In the experiment reported in Ref. [383], a shaped ultrafast and intense laser pulse (with a duration of only 6-8 optical cycles) is shot into an atomic gas. The authors used an adaptive feedback loop to shape the laser pulse, and in doing so improved the efficiency of X-ray generation by an order of magnitude. As shown in Fig. 13, adaptive feedback can be also used to find pulse shapes that will selectively generate specific high-order harmonics. To date, over 150 successful adaptive feedback control experiments have been reported, and the number applications is still growing [384].

4.2. Quantum self-feedback

While the term "self-cooling" has been used to refer to scenarios that are now understood as coherent feedback [227], similar terms have been used to refer to a situation that is distinct from coherent feedback, and yet involves a feedback mechanism. This is the method of cooling a mechanical resonator by using photothermal pressure [385] (as opposed to the radiation pressure of resolved-sideband cooling [227]). In photothermal cooling [386], the motion of the resonator affects a thermal bath to which the resonator is coupled, and the resulting effect of the bath back on the resonator is what produces the cooling. The effect is therefore feedback, but it is not feedback from a coherent and controllable system that is envisaged in coherent feedback, but from a many-body environment. For this reason, we feel that it is reasonable to give this situation another name, and here we choose to call it "self-feedback".

Another setting in which feedback from a many-body environment can facilitate control is that in which the system to be controlled interacts with a bath consisting of many nuclear spins [387–398]. One example of this is the spin of a single electron trapped in a "quantum dot", and a second is a cantilever (a mechanical oscillator) that interacts with the nuclear spins via a magnet attached to it. The ability to use the spin bath for control comes from the fact that the nuclear spins have a long coherence time. By driving the system (the electron spin or the cantilever), one can polarize the nuclear spins so that they act on a single coherent spin, and this coherence lasts for a time that is long compared to the timescale on which we

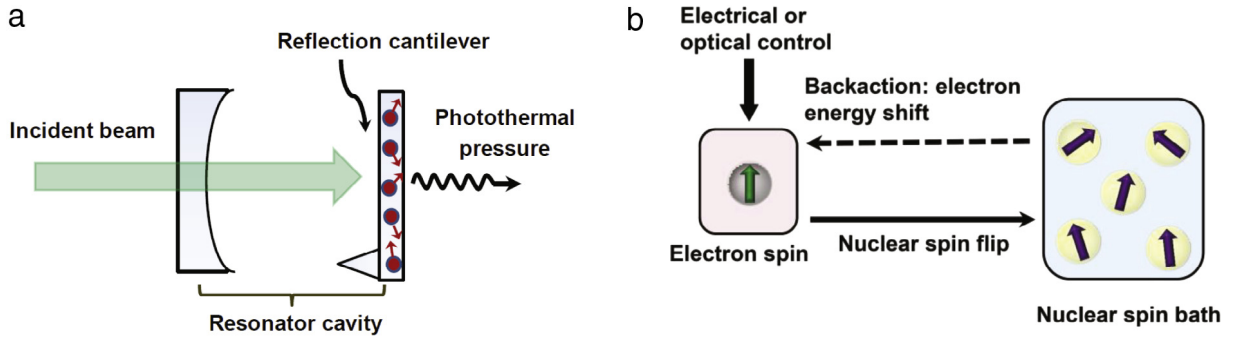

Fig. 14. Schematic diagram of self-feedback: (a) Passive cooling by photothermal pressure in optomechanical systems and (b) Feedback from a nuclear spin bath to an electron spin in a quantum dot.

Table 2
Characteristic parameters for feedback in various physical settings.

	Linear optics	Optomechanics	Cavity QED	Superconducting circuits
System energy scale	1 THz	0.1–100 MHz	1 THz	1–10 GHz
Feedback bandwidth	1 MHz	1 MHz	1 MHz	10 MHz
Decoherence rate	1 MHz	10–100 Hz	1 MHz	10–100 kHz
Measurement efficiency	0.9	0.9	0.8	0.4
Measurement rate	Photon flux	10 Hz–1 kHz	10 Hz–1 kHz	100 kHz
Feedback delay	0.1–10 μs	0.1–10 μs	1 μs–1 ms	250 ns
Ambient temperature	300 K	30 mK	300 K	30 mK

wish to control the system. Since the noise from the nuclear spin bath comes only from unpolarized spins, we can greatly reduce this noise in this way.

It is also possible to use the nuclear spin bath to cool a cantilever, in a process similar to resolved-sideband cooling. By polarizing the spins, or merely by using their steady-state thermal polarization, and driving the electron spin at the appropriate (blue-detuned) frequency, we can create a net transfer of excitations from the cantilever to the spin bath [391] (see Fig. 14).

5. Experiments realizing quantum feedback

We now give an overview of the experiments that have been performed to date realizing feedback in the quantum regime, both measurement-based and coherent. Feedback has now been realized in a range of distinct physical settings: atom optics and cavity QED, optomechanics, superconducting circuits, and quantum dots. For measurement-based feedback, the measurement efficiency is a crucial factor in determining to what extent control can be realized in the quantum regime, and the fidelity of this control. Before we begin, we present a table that shows various key parameters in current experiments on feedback control, and how they compare across the various physical realizations. Some of these parameters, such as the measurement efficiency, represent the state of the art that we expect will be continually improved. Other parameters, such as the feedback bandwidth, are merely what is typically being used in current experiments. The feedback bandwidth gives the fastest rate at which the control force applied to the system can change. Thus the timescale of the feedback control process is necessarily limited by the feedback bandwidth.

As discussed following Eq. (2.34), the *measurement rate* of a continuous measurement, also referred to as the "measurement strength", has units of inverse time as well as the inverse square of the observable being measured. It can be thought of as the rate at which the inverse variance of the observable is increased (and thus the variance reduced) by the measurement. The measurement rates given in the table are a result of choosing units that are natural in each case. For example, if one is measuring the position of a harmonic oscillator, then the natural unit of position is the uncertainty in the position for the ground state of the oscillator. For linear optics, the "system" being measured is often a continuous-wave laser beam, and the measurement rate in this case is merely the photon flux. Since it is possible to vary this flux over many orders of magnitude, we have left the entry in the table simply as "photon flux". Note that since the continuous measurements are mediated by coupling to fields, the measurement rate also corresponds to the rate for coherent feedback that is mediated by fields. Finally, we note that the time delay in the feedback loop and the bandwidth of the control are primarily relevant for measurement-based feedback. We have not included quantum dots in the table, since neither measurement-based quantum feedback nor field-mediated coherent feedback has been realized for those systems (see Table 2).

5.1. Quantum optics

5.1.1. Measurement-based feedback

Adaptive phase measurement (2002): The first experimental demonstration [312] of quantum feedback in optics was the realization of the adaptive phase measurement. The limited interactions available to detect light, or in fact any physical system, makes it impractical to exactly measure optical phase. If one has a good idea of the phase prior to the measurement, then homodyne detection can be used to provide good effect, since the quadrature to measure can be chosen using this information. But if the phase is completely unknown beforehand, this is not possible, and it was widely believed prior to 1995 that heterodyne detection gave the best possible phase measurement in that case [399]. In 1995, it is shown [298] that the use of homodyne detection, when combined with feedback used to modify the quadrature being measured during the measurement, could realize a more accurate phase measurement than heterodyne detection. For a pulse of light with no more than one photon, this adaptive phase measurement realizes exactly a measurement of canonical phase, as defined by the Pegg–Barnett phase operator.

In Fig. 15, we show a diagram of the experimental setup in Ref. [312]. The signal consists of noisy weak coherent light from a single-mode continuous-wave Nd:YAG laser, which first passes through a high-finesse Fabry–Perot cavity (not shown in the figure) with a ringdown time of 16 μs and shot-noise limit of 50 kHz. This cavity squeezes out the intensity noise in the signal beam. This beam is then fed into a Mach–Zehnder interferometer (MZI) to generate interference between the signal light and a local oscillator to implement homodyne detection. The local oscillator (LO) has a power of 230 μW and is frequency-shifted by an acousto-optic modulator (AOM), which is driven by an RF synthesizer (RF_1). The signal beam corresponds to a frequency sideband induced by an electro-optic modulator (EOM) driven by another RF synthesizer (RF_2). The two RF synthesizers RF_1 and RF_2 are phase-locked to each other to achieve synchronization between the local oscillator and the signal light. By changing the amplitude and switching RF_2 on and off, the power of the signal beam can be tuned between 5 fW and 5 pW and a pulse generated with a duration of about 50 μs. The two output ports of the MZI are measured by two photon detectors and the difference between their respective photocurrents realizes a homodyne or heterodyne measurement, depending on how the phase of the local oscillator is modulated. In the experiment, the shot noise in the difference photocurrent is about 6 dB above the noise floor in the range 1 kHz–10 MHz.

To realize an adaptive homodyne measurement, the phase of the local oscillator, Φ, is modified via RF_2 by a feedback signal as the measurement of the pulse proceeds. It is this phase that determines the quadrature that is measured. The feedback bandwidth, being the maximum rate at which the phase of the local oscillator can be changed, is about 1.5 MHz, and is mainly limited by the maximum slew rate of RF_2. The value of Φ as specified by the adaptive measurement protocol is [300]

$$\Phi(t) = \frac{\pi}{2} + \hat{\phi}(t) \equiv \frac{\pi}{2} + \int_0^t \frac{I(s)}{\sqrt{s}} ds, \tag{5.1}$$

where $I(s)$ is the measurement output signal at time s and $t \in [0, 1]$ is the normalized time scale such that the control pulse has duration 1. $\hat{\phi}(t)$ is the estimated phase at time t. The integral of the photocurrent is calculated by a field programmable gate array (FPGA). The final estimated phase is given by

$$\hat{\phi} = \hat{\phi}(1) = \int_0^1 \frac{I(s)}{\sqrt{s}} ds. \tag{5.2}$$

In fact, as shown in Fig. 15, the measurement output signal $I(t)$ is just the difference between the photocurrents at the two output ports of the beam splitter BS_2, and thus can be represented by

$$I(t)dt = 2\mathrm{Re}\left[\alpha e^{-i\Phi(t)}\right] dt + dW = 2|\alpha| e^{\phi - \Phi(t)} dt + dW, \tag{5.3}$$

where α is the complex amplitude of the signal beam, ϕ is the estimated phase, dW is white (Wiener) noise. In this adaptive measurement protocol [300], the phase of the local oscillator is chosen as $\Phi(t) = \pi/2 + \hat{\phi}(t)$, and $\hat{\phi}(t)$ is updated by the phase of the following complex quantity

$$A_t = \int_0^t I(s) e^{i\Phi(s)} ds, \tag{5.4}$$

i.e., $\hat{\phi}(t) \equiv \arg(A_t)$. By substituting Eq. (5.3) into Eq. (5.4), we have

$$\hat{\phi} \equiv \hat{\phi}(1) = \arg\left[\int_0^1 I(s) e^{i\Phi(s)} ds\right] = \arg\left[|\alpha| e^{i\phi} + \int_0^1 dW\right] \approx \arg\left[|\alpha| e^{i\phi}\right] = \phi,$$

which means that $\hat{\phi}$ is a good estimate of ϕ. Additionally, from $A_t = |A_t| e^{i\hat{\phi}(t)}$ and $\Phi(t) = \pi/2 + \hat{\phi}(t)$, it can be shown that

$$dA_t = I(t) e^{i\Phi(t)} dt = i \frac{A_t}{|A_t|} I(t) dt. \tag{5.5}$$

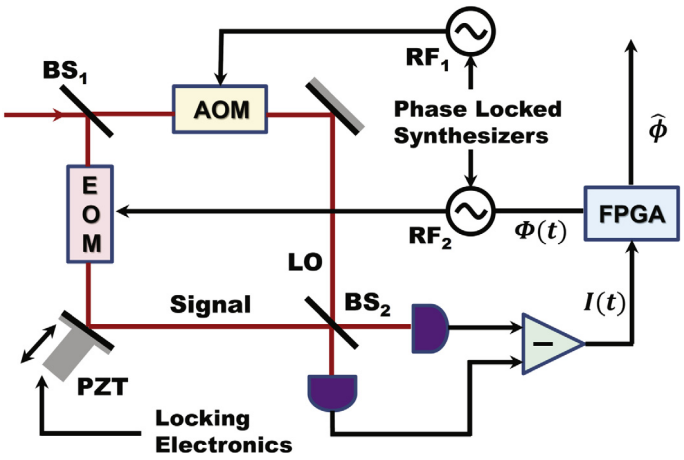

Fig. 15. Diagram of the adaptive homodyne measurement of an optical phase is performed by Armen et al. [312]. Optical beams are indicated by red lines and electronic beams by black lines. The AOM and EOM represent the acousto-optic modulator and electro-optic modulator. BS and RF are the beam splitter and the radio-frequency synthesizer. PZT is the piezoelectric transducer and FPGA is the field programmable gate array.

Using the Ito calculus, we have

$$d|A_t|^2 = (A_t^* d)A_t + (dA_t *)A_t + (dA_t^*)(dA_t) = dt,$$

which means that $|A_t| = \sqrt{t}$. By substituting this equation into Eq. (5.5), we have

$$d\hat{\phi}(t) = \mathrm{Im}(d \ln A_t) = \mathrm{Im}(dA_t/A_t) = \frac{I(t)dt}{\sqrt{t}}, \tag{5.6}$$

by which we can recover Eqs. (5.1) and (5.2).

The experiment demonstrated the superiority of the adaptive measurement scheme. In fact, the authors of Ref. [312] were able to use the protocol in Ref. [300] to obtain a phase estimate whose error was below that achievable with heterodyne detection. Here the error is given by the variance of the estimated phase. This is reasonable because only current-time information of the output signal is used for heterodyne detection. However, the whole history of the measurement output is considered in the adaptive homodyne detection. It means that more information is used for adaptive homodyne detection compared with the heterodyne detection which decreases the uncertainty of the measurement. The experimental results in Ref. [312] also show that heterodyne detection is better than adaptive homodyne detection in the sense that the variance of the unknown phase estimated by the heterodyne detection is smaller when the number of photons in the probe field is large enough. The authors of Ref. [312] attribute it to the excess technical noise in the feedback loop.

Adaptive phase estimation (2007): While the previous adaptive measurement was concerned with measuring phase as accurately as possible for low-power beams, the 2007 adaptive measurement of Higgins et al. was concerned with measuring a classical parameter, in this case a phase shift applied to a beam of light, with the most efficient use of resources [313]. The resources in question are the number of photons in the beam. Due to the relationship between amplitude and phase, the more photons in the beam the more sharply the phase is defined, and thus the more accurately can an applied phase shift be determined. If the beam is in a coherent state, then the error in the measured phase is proportional to $1/\sqrt{N}$, where N is the average number of photons. But by using nonclassical states, and in particular highly entangled states [314], the error can be reduced to $1/N$, which is known as the Heisenberg limit. The experimental and theoretical work by Higgins et al. showed that entanglement was not necessary to reach the Heisenberg limit, which could instead be achieved by applying the phase shift to one photon at a time, and using an adaptive measurement when measuring the sequence of photons [313].

There have been a number of further experiments that have also demonstrated a phase measurement below the standard quantum limit without using entangled input states [315,316,318]. For example, in Ref. [315], Xiang et al. use two n-photon states as the two inputs in a Michelson interferometer, use Bayesian analysis and optimal adaptive feedback to make full use of these multiphoton states.

Adaptive phase estimation with smoothing (2010): The phase estimation experiments we have described so far are concerned with estimating a single phase shift. This next experiment [154] involves estimating a time-varying phase shift. To estimate the phase shift ϕ at some time t, $\phi(t)$, we can use the stream of measurement results obtained up until that time. The procedure of processing the measurement results up until time t to produce an estimate of a signal at that time is called *filtering*. If we are prepared to wait until time $(t+\tau)$ for our estimate, then we can use the measurement results up until time $t+\tau$ to obtain our estimate of $\phi(t)$. The process of obtaining an estimate from measurement results obtained both before and after the time of the estimate is called *smoothing*. In Ref. [154], Wheatley et al. use an adaptive homodyne measurement procedure, combined with smoothing, to estimate a time-varying phase shift. They then compare this adaptive smoothing

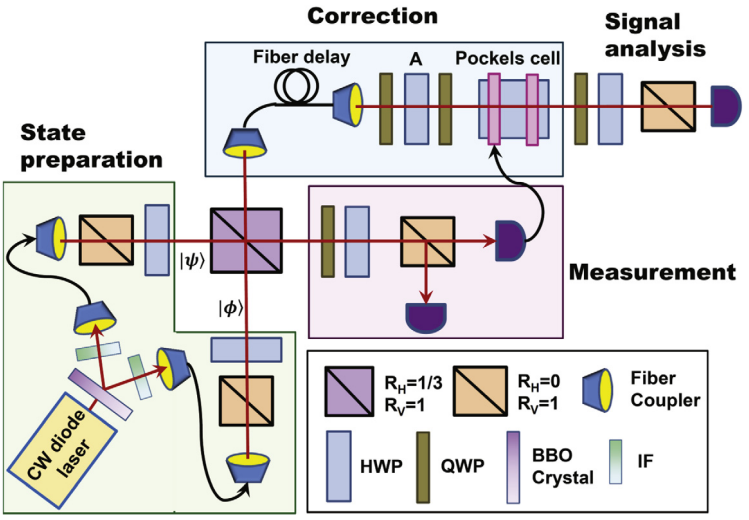

Fig. 16. Schematic diagram of the experimental setup of Gillett et al. [288]. A photon pair composed of a primary (or "signal") photon and an auxiliary photon is prepared by spontaneous parametric down conversion in a BBO crystal. The primary and auxiliary photons are then prepared in specific initial states by transmitting through the polarization beam splitters and half-wave plates (HWP). The two photons are combined at a partially-polarizing beam splitter which applies a controlled phase gate between the two (conditioned on there being only one photon in each output). A succeeding projective measurement in the $+/-$ basis on the auxiliary photon realizes a weak measurement on the primary. The measurement output is then fed into a Pockels cell to rotate the signal photon conditional on the measurement outcome. The acronym QWP labels the quarter-wave plate and IF labels the interference filter.

measurement with the performance of a nonadaptive (filtering) measurement referred to as "dual-homodyne" (or "eight-port homodyne") measurement (which is equivalent to heterodyne measurement). They show that the adaptive smoothing measurement can achieve a mean-square phase error that is smaller than that of the nonadaptive filtering measurement by a factor of $2\sqrt{2}$. As an extension of the results in Ref. [312] (presented in the first paragraph of this subsection), the authors of Ref. [154] show that adaptive measurement reduces the mean-square phase error by a factor of $\sqrt{2}$ over nonadaptive measurement, both for filtering and smoothing. They also show that smoothing reduces this error by a factor of 2 over filtering. Thus the total reduction in the mean-square phase error provided by adaptive smoothing over nonadaptive filtering is a factor of $2\sqrt{2}$.

Adaptive phase estimation with squeezed light (2012): One way to beat the standard quantum limit for phase estimation is to use squeezed light, since the phase error in this light is less than $1/\sqrt{N}$, where N is the number of photons. The experiment of Yonezawa et al. [317] implemented this method using a continuous beam of squeezed light. The experiment achieved a phase estimation error that was $15\% \pm 4\%$ below the ideal limit achievable with a coherent beam.

Correcting a single-photon state (2010): So far all the experiments we have described in linear optics are adaptive measurements of optical phase. This next experiment is an exception. Here Gillett et al. [288] use a weak measurement to optimally correct the state of a single qubit which is initially prepared in one of two non-orthogonal states. In this case, the qubit is encoded in the polarization of a single photon. This correction procedure was suggested and analyzed in Ref. [287]. Recall that a weak measurement is one in which the measurement operators are not rank-1 projectors, so it does not reduce a mixed state to a pure state, and does not provide full information about the final state (see Fig. 16).

In this experiment, the two states of the qubit are labeled as $|H\rangle \equiv |1\rangle$ (horizontal polarization) and $|V\rangle \equiv |0\rangle$ (vertical polarization). To make a weak, single-shot measurement of one of these qubits, Gillett et al. perform a gate that partially entangles the qubit with a second "probe" qubit, and then perform a projective measurement on the probe. The experiment is driven by an 820 nm Ti:sapphire laser. A 410 nm beam is created from this using second-harmonic generation, so that a pair of 820 nm photons can be created from this 410 nm beam using spontaneous parametric down conversion. Each photon in the pair is then fed into a single-mode fiber. One of these photons carries the qubit to be corrected – the "primary" photon – and the other will be used as the probe. The primary is prepared in one of the two (non-orthogonal) states

$$|\psi_{\pm}\rangle = \cos\frac{\theta}{2}|\pm\rangle \pm \sin\frac{\theta}{2}|-\rangle$$

by transmitting through a polarizing beam splitter with reflectivity $R_H = 0$ and $R_V = 1$ followed by a half-wave plate (HWP). Here 2θ is the angle between these two states on the Bloch sphere and

$$|\pm\rangle = \frac{1}{\sqrt{2}}\left(|0\rangle \pm |1\rangle\right).$$

The probe photon is to be detected, and is prepared in the state

$$|\phi\rangle = \cos\frac{\chi}{2}|+\rangle + \sin\frac{\chi}{2}|-\rangle,$$

where the parameter χ ranges from 0 to $\pi/2$ and represents the strength of the measurement that we will introduce below. The primary and probe photons are now interfered through a partially-polarizing beam splitter with reflectivity $R_H = 1/3$ and $R_V = 1$. Conditional on there being only one photon in each mode, the partially-polarizing beam splitter executes a control-Z gate (given by $|0\rangle\langle 0| \otimes \mathbf{1} + |1\rangle\langle 1| \otimes Z$), between the qubits with the probe as the control [400–402].

The primary qubit is next subjected to a dephasing error with probability p, which leads to the following two error states

$$\rho'_{\pm} = (1-p)\,|\psi_{\pm}\rangle\langle\psi_{\pm}| + pZ|\psi_{\pm}\rangle\langle\psi_{\pm}|Z.$$

To correct this error as best as possible, the probe qubit is measured in the basis $\{|\pm\rangle\}$. This measurement is implemented by rotating the polarization basis and transmitting through a polarizing beam splitter with reflectivity $R_H = 0$ and $R_V = 1$. This results in a weak measurement on the primary qubit described by the measurement operators [see Eq. (2.16)]

$$M_+ = \cos\frac{\chi}{2}|0\rangle\langle 0| + \sin\frac{\chi}{2}|1\rangle\langle 1|, \quad M_- = \sin\frac{\chi}{2}|0\rangle\langle 0| + \cos\frac{\chi}{2}|1\rangle\langle 1|, \tag{5.7}$$

where M_+ and M_- are the measurement operator to weakly extract information for the states $|0\rangle$ and $|1\rangle$, respectively. From the above equations, we can see that the parameter χ characterizes the strength of the measurement, with 0 equivalent to a projective measurement (with fully discriminative post-selective states) and $\pi/2$ equivalent to no measurement (with non-discriminative post-selective states). A unitary rotation is then performed on the primary qubit depending on the result of the measurement. This is implemented using a Pockels cell, which applies a rotation on the Bloch sphere through an angle of 4η around the axis of $\sigma_y = i(|0\rangle\langle 1| - |1\rangle\langle 0|)$ if a photon is detected in the transmission output of the polarization beam splitter. Combined with a fixed rotation of $-\eta$, the results are rotations of $\pm\eta$, i.e., rotation operations $Y_{\pm\eta} = \exp\left(\pm i\eta\sigma_y\right)$, corresponding to the measurement result $M_\pm$. Prior to this feedback operation, the primary photon passes through a 50 m fiber to allow time for the quantum weak measurement, as well as a set of plates to compensate the polarization rotation introduced by this fiber.

After the weak measurement and feedback correction, we can obtain the following two states

$$\tilde{\rho}_{\pm} = (Y_{+\eta}M_+)|\psi_{\pm}\rangle\langle\psi_{\pm}|(Y_{+\eta}M_+)^\dagger + (Y_{-\eta}M_-)|\psi_{\pm}\rangle\langle\psi_{\pm}|(Y_{-\eta}M_-)^\dagger. \tag{5.8}$$

Then we can define the average fidelity as

$$F_{\mathcal{C}} = \frac{1}{2}\langle\psi_+|\tilde{\rho}_+|\psi_+\rangle + \frac{1}{2}\langle\psi_-|\tilde{\rho}_-|\psi_-\rangle, \tag{5.9}$$

which approaches 1 for perfect correction. The average fidelity can be optimized over the correction angle η as

$$F_{\mathcal{C}}^{\text{opt}} = \frac{1}{2} + \frac{1}{2}\left\{\left[1-(1-(1-2p)\sin\chi)\cos^2\theta\right]^2 + \cos^2\chi\cos^2\theta\right\}^{1/2}, \tag{5.10}$$

and the corresponding optimized angle is

$$\eta_{\text{opt}} = \tan^{-1}\frac{\cos\chi\cos\theta}{1-\{1-[1-2p]\sin\chi\}\cos^2\theta}. \tag{5.11}$$

5.1.2. Coherent feedback

Noise cancellation (2008): The first all-optical demonstration of a coherent feedback scenario was performed by Mabuchi [356], and was a realization of a noise-cancellation loop suggested by James [61]. A diagram of the experimental setup is shown in Fig. 17. The primary system (the "plant") is a four-mirror ring cavity (top) as is the auxiliary (the "controller"). The experiment is driven by an 852 nm diode laser, and an external "noise" signal is injected into the plant cavity at the input w. The output of the primary, y, that is reflected from the plant input coupler, acts as the error signal, which is processed by the controller to generate a control signal u. This control signal is then fed back into the plant cavity again to attempt to cancel, as well as possible, the effect of the noise on the plant output, z. The goal of the feedback loop is to minimize the ratio of the optical power at the output z to that of the "noise" input w. This quantity can also be described as the magnitude of the closed-loop transfer function [see Eq. (1.7)]. In fact, the open-loop transfer function of the plant from the input w to the output z can be represented by

$$G_{zw} = -\frac{2\sqrt{k_1 k_4}}{s+\gamma_p}, \tag{5.12}$$

where k_1 and k_4 are the partial transmission rates of the input and output couplers, $\gamma_p = c(t_1^2+t_2^2+t_3^2+t_4^2+l^2)/(4\pi L_p)$, where c is the speed of light, L_p is the round-trip cavity length, t_i^2 is the transmission coefficient of ith mirror, and l^2 are denotes all other intracavity loss. When the feedback loop is implemented as shown in Fig. 17, the overall close-loop transfer function from w to z becomes

$$G_f = G_{zw} + G_{zu}(1-K_{uy}G_{uy})^{-1}K_{uy}G_{yw}, \tag{5.13}$$

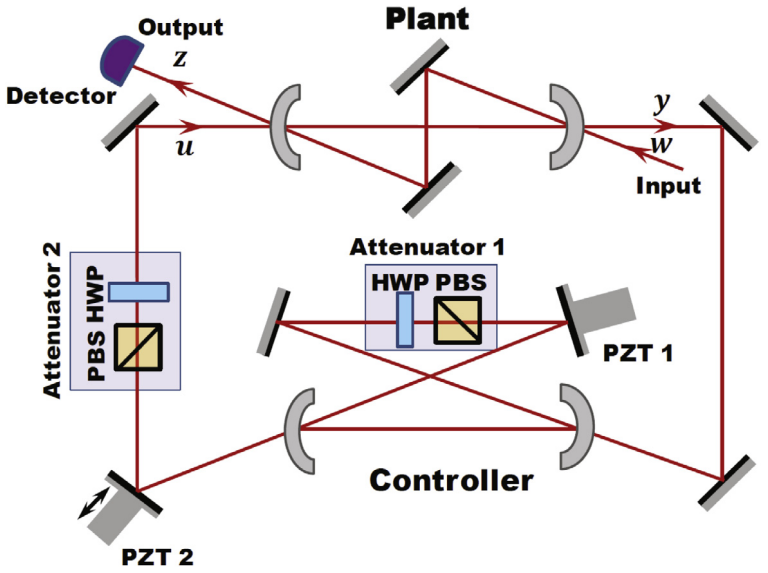

Fig. 17. Diagram of the experimental setup of Mabuchi [356]. Two four-mirror ring resonators couple with each other by a transmitting optical field, which work as the plant cavity and controller, respectively. The control goal is to tailor the behaviors of the controller to minimize the power detected at the system output z, when a "noise" signal w is fed into the plant cavity. This can be achieved by tuning the parameters via the two variable attenuators, i.e., attenuator 1 and attenuator 2, and the two piezoelectric transducers (PZTs), i.e., PZT 1 and PZT 2.

where the additional transfer functions are $G_{yu} = G_{zw}$, $G_{zu} = G_{zw}$, $G_{zu} = 1 - 2k_4/(s + \gamma_p)$, and $G_{yw} = 1 - 2k_1/(s + \gamma_p)$. The transfer function of the optical resonator that acts as the controller is K_{uy}, and is given by

$$K_{uy} = \frac{2\sqrt{\eta_K}\sqrt{k_1 k_4}}{s + \gamma_p - 2(k_1 + k_4) + \eta_\gamma}, \tag{5.14}$$

where η_K and η_γ are the two control parameters that can be tuned. The problem of disturbance rejection is to design the controller so as to minimize the magnitude of the closed-loop transfer function G_f.

Four practical ways to tune the parameters of the controller to achieve the noise cancellation (disturbance rejection) are: (i) adjust the resonance frequency using the actuator PZT 1; (ii) adjust the phase of the transfer function using the actuator PZT 2; (iii) adjust the decay rate using the intracavity variable attenuator (attenuator 1); and (iv) adjust the magnitude of the transfer function using an attenuator 2. By optimizing these parameters, Mabuchi was able to reduce the noise in the output by approximately 7 dB.

Squeezing light (2012): The experiment by S.Iida et al. [359] realized a coherent feedback loop to enhance the squeezing of an optical beam. This was an implementation of a protocol devised in Ref. [358]. The experimental setup is shown in Fig. 18. The optical parametric oscillator (OPO) generates squeezed light, and it is the job of the feedback loop to enhance this squeezing. As such, the primary system is the OPO and auxiliary system is the "control beam splitter" (CBS), which acts as a beam splitter whose reflectivity can be adjusted. The CBS also acts as the output port through which the squeezed light exits the combined system, and is then evaluated by a homodyne measurement.

This experiment is probably the most sophisticated coherent feedback loop realized to date. The feedback loop can be a little hard to read from the diagram, because there are additional classical locking loops that share the same mirrors as the coherent feedback loop, but are separate from it. The feedback loop is surrounded by the green dashed line, and consists of the OPO, a Mach–Zehnder interferometer that acts as the controlled beam splitter (CBS), and a loop that connects them. You will notice that multiple beams (or *branches*) are split off from the single Ti:sapphire laser that drives the experiment. The first branch is fed into a frequency-doubler to generate a second-order harmonic beam of 430 nm, which is used as the beam that pumps the OPO to produce squeezed light at 860 nm. The second branch is used as the local oscillator to implement the homodyne detection on the squeezed output. The third branch, the one that goes through the half-wave plate (HWP) is used to lock the Mach–Zehnder and the coherent feedback loop. The final branch works as the "probe" beam, which is injected into the OPO as the "seed" that sets the phase of the squeezed light. Photodetectors (PDs) and piezoelectric transducers (PZTs) are used in a classical phase-locking loop to fix the relative phase between the probe and the pump beams.

The authors were able to demonstrate a squeezing enhancement from -1.64 ± 0.15 to -2.20 ± 0.15 dB, in which the corresponding enhancement of the antisqueezing was from 1.52 ± 0.15 to 2.75 ± 0.15 dB.

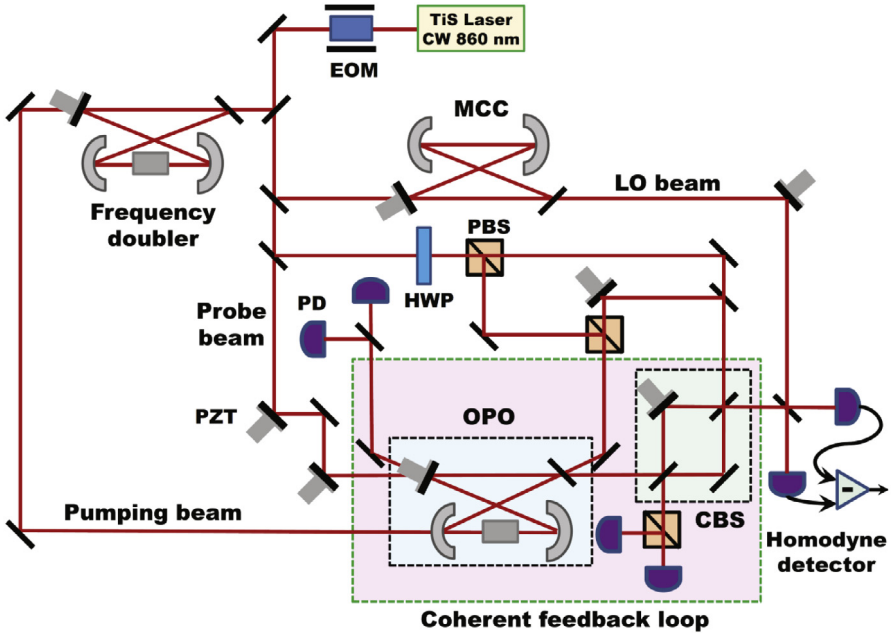

Fig. 18. Schematic diagram of the experimental setup of S.Iida et al. [359], in which coherent feedback is used to enhance optical squeezing. The coherent feedback control loop consists of the optical parametric oscillator (OPO) and a Mach–Zehnder interferometer that acts as a beam splitter with a tunable reflectivity (the "controlled beam splitter" (CBS)). The various labels denote the following optical elements: MCC (mode-cleaning cavity); EOM (electro-optic modulator); PD (photodetector); PZT (piezoelectric transducer); HWP (half-wave plate); PBS (polarized beam splitter); LO (local oscillator).

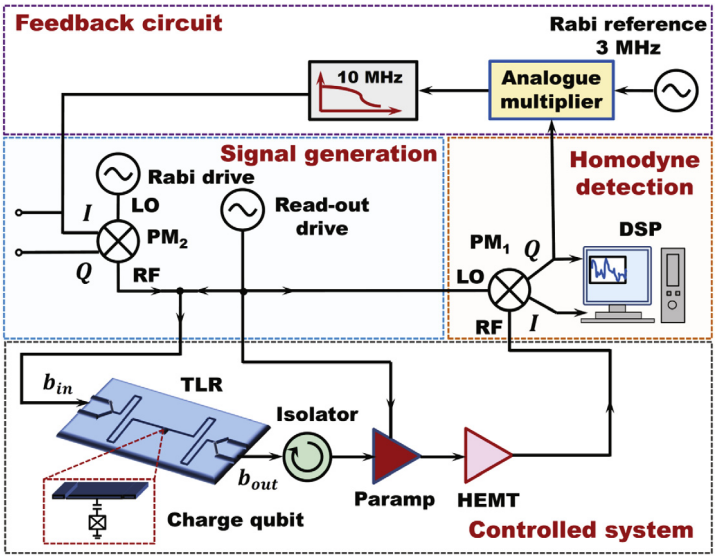

Fig. 19. Diagram of the experimental setup of Vijay et al. [194]. The Rabi drive at the ac stark-shifted qubit frequency and the read-out drive at frequency 7.2749 GHz are both fed into the weakly-coupled input port of a three-dimensional microwave cavity, which is dispersively coupled to a capacitively-shunted Josephson junction working as a superconducting qubit. The output signals leave from the strongly-coupled port of cavity and are then transmitted through two isolators. Afterwards, the output signals are amplified by a parametric amplifier (paramp) and a high-electron-mobility transistor (HEMT) amplifier, and then measured by a homodyne detection setup. The amplified quadrature Q is then sent to the feedback circuit to be compared to the 3 MHz Rabi reference signal and filtered by a 10 MHz low-pass filter. The output signal is then fed back to correct the Rabi frequency imposed on the qubit by the Rabi drive. LO and RF represent the local oscillator and radio frequency. PM_1 and PM_2 are the two photonmultipliers. I and Q are the in-phase component and quadrature component respectively.

5.2. Superconducting circuits

5.2.1. Measurement-based feedback

Stabilizing the state of a single qubit (2012): It is only very recently that measurement-based feedback has been realized in mesoscopic circuits, because it is only recently that amplifiers with sufficiently low noise have been devised [403–406]. The first two experiments to demonstrate measurement-based feedback control of a single superconducting qubit were those by Vijay et al. [194] and Riste et al. [193], and this field progressed very fast recently [407].

In Fig. 19, we show the experimental setup used in Ref. [194]. In this experiment, the authors use a continuous measurement and feedback process to keep the qubit undergoing Rabi oscillations under its free Hamiltonian. To do this, the feedback has to continually purify the state of the qubit and the feedback has to keep it within a given plane of the Bloch sphere. The qubit is a capacitively-shunted Josephson junction [408,409] with a transition frequency of $\omega_q/2\pi = 5.4853$ GHz. This qubit is dispersively coupled to a three-dimensional microwave cavity with a cavity resonant frequency of $\omega_c/2\pi = 7.2756$ GHz. Electrical signals that enable the measurement and feedback control are fed into the cavity via the weakly-coupled input port, and the measurement output leaves the cavity via the strongly-coupled port with decay rate $\kappa/2\pi = 13.4$ MHz. The qubit is dispersively coupled to the cavity with a strength of $\chi/2\pi = 0.687$ MHz, with the result that the qubit induces a phase shift of the cavity light that depends on the qubit's internal state, and this state is therefore measured by making a homodyne measurement of the output signal from the cavity. This is a "cavity-mediated" (or "oscillator-mediated") measurement as described in [86,214].

The cavity mode is driven at the frequency of $\omega_r = 2\pi \times 7.2749$ GHz $\approx \omega_c - \chi$ to control the mean cavity photon occupation which sets the measurement strength. The qubit is driven by the "Rabi drive" in Fig. 19 chosen to give a Rabi frequency of $\Omega_R/2\pi = 3$ MHz. At the output port of the cavity, the output quantum field is sent through two isolators to protect the qubit from the strong-field driving of the parametric amplifier (or "paramp"). It is then fed through the paramp (a near-noiseless phase-sensitive quantum amplifier [410,411]), and through the high-electron-mobility transistor (HEMT) amplifier to produce a macroscopic signal that can easily be manipulated without significant noise. It is then measured by homodyne detection. This measurement procedure achieves an efficiency of $\eta = 0.40$. The dynamical equation for the superconducting qubit with feedback can be expressed as

$$\begin{aligned}
d\langle\sigma_x\rangle &= -\left(\Gamma_{\rm env} + \frac{\Gamma_1}{2} + \frac{(\Delta I)^2}{4}\right)\langle\sigma_x\rangle\, dt - \frac{\Delta I}{\sqrt{2}}\langle\sigma_x\rangle\langle\sigma_z\rangle dW,\\
d\langle\sigma_y\rangle &= -\left[\left(\Gamma_{\rm env} + \frac{\Gamma_1}{2} + \frac{(\Delta I)^2}{4}\right)\langle\sigma_y\rangle + \Omega_R\langle\sigma_z\rangle\right] dt - \frac{\Delta I}{\sqrt{2}}\langle\sigma_y\rangle\langle\sigma_z\rangle dW,\\
d\langle\sigma_z\rangle &= \left(-\Omega_R\langle\sigma_y\rangle - \Gamma_1\langle\sigma_z\rangle\right) dt - \frac{\Delta I}{2\sqrt{2}}(1-\langle\sigma_z\rangle^2) dW,
\end{aligned} \tag{5.15}$$

where Ω_R is the Rabi frequency, $\Gamma_{\rm env}$ is the environmental dephasing rate, and Γ_1 is the relaxation rate. The measurement output signal is given by

$$dI(t) = \left(\frac{I_0 + I_1}{2} + \frac{\Delta I}{2}\langle\sigma_z\rangle\right) dt + dW, \tag{5.16}$$

where I_0 and I_1 are the average output signals for the qubit in the ground and excited states, respectively, and $\Delta I = I_1 - I_0$. When we omit the environmental dephasing and relaxation (that is, we set $\Gamma_{\rm env} = \Gamma_1 = 0$), the state of the qubit state will remain pure if the initial state is pure. If we further assume that the initial state satisfies $\langle\sigma_x\rangle(0) = 0$, then the evolving state can be described by a single parameter, being the polar angle $\theta(t)$ on the Bloch sphere:

$$\langle\sigma_x\rangle = 0, \quad \langle\sigma_y\rangle = \sin\theta(t), \quad \langle\sigma_z\rangle = \cos\theta(t). \tag{5.17}$$

The goal of the feedback is to keep oscillating as $\theta(t) = \Omega_0 t$ with a fixed frequency Ω_0. If we denote the phase difference between the reference and the homodyne output, $\theta_{\rm err} = \theta - \Omega_0 t$, the dynamical equation for the state of the qubit is given by

$$d\,\theta_{\rm err} = \left[-\frac{(\Delta I)^2}{4}\sin\theta(t)\cos\theta(t) + \Omega_{\rm fb}(t)\right] dt - \Delta I \sin\theta(t) dW, \tag{5.18}$$

where $\Omega_{\rm fb} = \Omega_R(t) - \Omega_0$ is the feedback-induced modulated part of the Rabi frequency. The feedback protocol used in the experiment is motivated by a classical phase-locked loop. As shown in Fig. 19, the output of the homodyne detection is compared with a 3-MHz Rabi reference signal and low-pass filtered to generate a signal proportional to the sine of the phase difference, $\theta_{\rm err}$. This error signal is then fed back to modulate the amplitude of the Rabi drive, $\Omega_{\rm fb}$, by

$$\frac{\Omega_{\rm fb}}{\Omega_0} = -F\sin(\theta_{\rm err}), \tag{5.19}$$

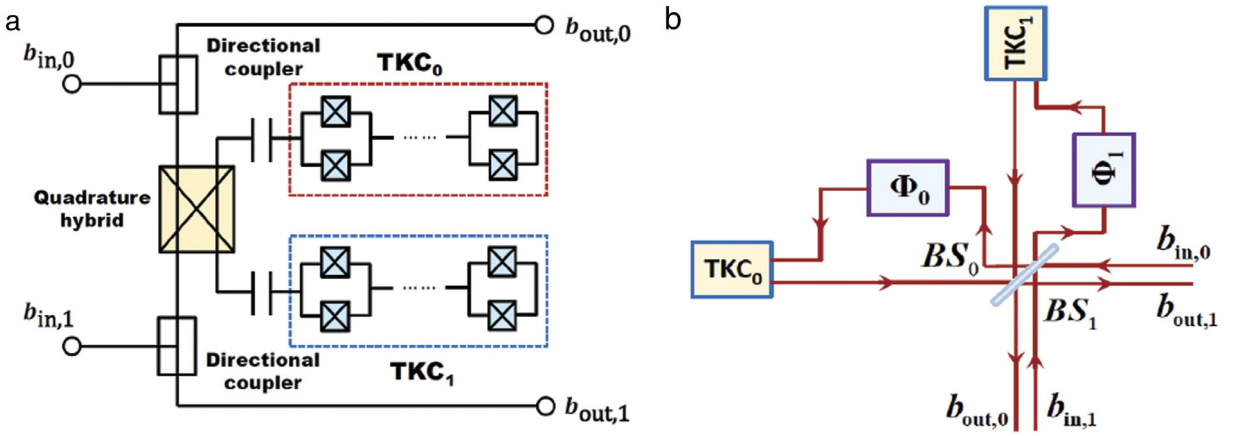

Fig. 20. (a) Diagram of the two-port coherent feedback circuit used by Kerckhoff and Lehnert [64]. The input fields are $b_{in,0}$ and $b_{in,1}$ and the output fields are $b_{out,0}$, $b_{out,1}$. The two flux-biased tunable Kerr circuits (TKC$_0$, TKC$_1$) are connected via a beam splitter which is the "quadrature hybrid". Each TKC is composed of a quarter-wave transmission line resonator interrupted by a series array of 40 Josephson junction SQUIDs, and one end of the transmission line resonator is capacitively coupled to the beam splitter. The two directional couplers merely separate the input and output fields. The entire system is housed in a dilution refrigerator which provides an ambient temperature of ∼50 mK. (b) Equivalent diagram of the two-port coherent feedback circuit.

where F is the dimensionless feedback gain. Under this feedback control, we have $\theta_{\rm err} \to 0$ when $t \to \infty$. This is a Markovian quantum feedback process. The performance is mainly limited by the efficiency of the measurement and the time delay in the feedback loop. There is a tradeoff between the rate at which the feedback can be performed (the feedback bandwidth) and the noise introduced by the feedback signal, which results in an optimal measurement strength. With a finite feedback bandwidth of 10 MHz and loop delay of 250 ns, the optimal measurement strength was found to be $\Gamma_\phi/2\pi = 0.134$ MHz.

Preparing entanglement between two qubits (2013): The experiment by Riste et al. [275] demonstrated the stabilization of entanglement between two superconducting qubits using measurement-based feedback control. In Ref. [275], a Bell state is prepared with a fidelity of 88% by using a parity measurement, which is a joint measurement on both qubits. By introducing a feedback loop incorporating the parity measurement, the probabilistic preparation of the Bell state was replaced by a deterministic preparation with a fidelity of 66%.

5.2.2. Coherent feedback

Engineering dynamics (2012): Kerckhoff and Lehnert [64] used a coherent feedback network to implement a bistable superconducting circuit, also known as a latch, useful in classical information processing. This was an experimental realization [64] of a scheme devised in Ref. [63], in which two oscillators with Kerr nonlinearities, when coupled in a loop via a beam splitter, generate both bistable and astable dynamics.

A diagram of the experimental configuration used in Ref. [64] is shown in Fig. 20(a). The system is an input–output circuit with two input fields $b_{in,0}$, $b_{in,1}$ and two output fields $b_{out,0}$, $b_{out,1}$. The central components of the coherent feedback loop are two tunable Kerr circuits, TKC$_0$ and TKC$_1$. Each TKC is composed of a quarter-wave transmission line resonator generated by a coplanar waveguide. In the center of the coplanar waveguide, a series array of 40 Josephson-junction superconducting quantum interference devices (Josephson-junction SQUIDs) interrupt the waveguide and generate a Kerr nonlinearity for the transmission line resonator [412]. One end of each resonator is capacitively coupled to the 4–8 GHz commercial quadrature hybrid which acts as a 50:50 microwave beam splitter. The two directional couplers merely separate the input fields from the output fields.

The above nonlinear coherent feedback network exhibits optical phenomena that neither of the Kerr resonators exhibit by themselves. For example, as shown in Ref. [64], if the two TKCs have central frequencies equal to $\omega_0/2\pi = 6.408$ GHz, and we drive them with probe fields at the frequency $\omega_p/2\pi = 6.39$ GHz, the output fields of the coherent feedback network exhibit a bistability phenomenon, an effect in which a system has two distinct equilibrium states. The bistable system can rest in either of these two states, and will transit from one stable state to the other if it is given enough activation energy to penetrate the barrier. If the two uncoupled TKCs are individually driven at the same detuning, neither would be bistable. Note that the bistable system has various interesting applications. As an example, it could act as an on-chip microwave switch, designed to sit in either the "on" or "off" positions. Since the TKCs and the feedback control circuits typically contain an average of about 1000 photons, the experimental results fit very well with a mean-field model using a semiclassical approximation. Further, purely quantum effects such as sub-Poisson statistics could potentially be observed in this feedback circuit.

The above phenomena can be explained using the language of quantum feedback networks presented in Section 3.2.1. The dynamics of a TKC is represented in the language of "SLH" (Eq. (3.5)) by

$$\mathbf{S}_{\mathrm{TKC}} = 1, \quad \mathbf{L}_{\mathrm{TKC}} = -i\sqrt{2\kappa}a, \quad H_{\mathrm{TKC}} = \Delta a^\dagger a + \frac{\chi}{2}a^{\dagger 2}a^2, \tag{5.20}$$

where a is the annihilation operator for the TKC resonator mode, $\Delta = \omega_0 - \omega_p$ is the detuning between the TKC resonance frequency ω_0 and the frequency of the driving field ω_p, κ is the field decay rate, and $\chi < 0$ is the Kerr coefficient induced by the SQUID array. The beam splitter is expressed as $\mathrm{BS} = (\mathbf{S}_{\mathrm{BS}}, \mathbf{L}_{\mathrm{BS}}, H_{\mathrm{BS}})$ where

$$\mathbf{S}_{\mathrm{BS}} = \begin{pmatrix} \mu & -\nu^* \\ \nu & \mu \end{pmatrix}, \quad \mathbf{L}_{\mathrm{BS}} = 0, \quad H_{\mathrm{BS}} = 0, \tag{5.21}$$

and $|\mu|^2 + |\nu|^2 = 1$. The phase shifter can be denoted as $\Phi = (\mathbf{S}_\phi, \mathbf{L}_\phi, H_\phi)$ where

$$\mathbf{S}_\phi = e^\phi, \quad \mathbf{L}_\phi = 0, \quad H_\phi = 0 \tag{5.22}$$

and the coherent drive $W_\alpha = (\mathbf{S}_{W_\alpha}, \mathbf{L}_{W_\alpha}, H_{W\alpha})$ where

$$\mathbf{S}_{W_\alpha} = 1, \quad \mathbf{L}_{W_\alpha} = \alpha, \quad H_{W_\alpha} = 0. \tag{5.23}$$

The dynamics of the quantum coherent feedback network shown in Fig. 20(b) is then represented by

$$N = (\mathbf{S}_N, \mathbf{L}_N, H_N) = \left\{P_{(0,1)} \lhd [(I_2 \boxplus (\mathrm{TKC}_0 \lhd \Phi_0)) \lhd [(I_3 \boxplus (\mathrm{TKC}_1 \lhd \Phi_1)) \lhd (BS_0 \boxplus BS_1)]]\right\} \lhd (W_{\alpha_0} \boxplus W_{\alpha_1}), \tag{5.24}$$

where

$$\begin{aligned}
\mathbf{S}_N &= \frac{1}{3}\begin{pmatrix} 2\sqrt{2}i & 1 \\ 1 & 2\sqrt{2}i \end{pmatrix}, \\
\mathbf{L}_N &= \frac{1}{3}\begin{pmatrix} -\sqrt{2\kappa}a_0 + i2\sqrt{\kappa}a_1 + i2\sqrt{2}\beta_0 - \beta_1 \\ -\sqrt{2\kappa}a_1 + i2\sqrt{\kappa}a_0 - i2\sqrt{2}\beta_1 + \beta_0 \end{pmatrix}, \\
H_N &= \Delta_0 a_0^\dagger a_0 + \Delta_1 a_1^\dagger a_1 + \frac{\chi_0}{2}a_0^{\dagger 2}a_0^2 + \frac{\chi_1}{2}a_1^{\dagger 2}a_1^2 \\
&\quad + \left(-\frac{\sqrt{\kappa}}{3}a_0^\dagger\beta_0 + i\frac{\sqrt{2\kappa}}{6}a_0^\dagger\beta_1 - i\frac{\sqrt{2\kappa}}{6}a_1^\dagger\beta_0 + \frac{\sqrt{\kappa}}{3}a_1^\dagger\beta_1 + \mathrm{h.c.}\right).
\end{aligned} \tag{5.25}$$

Here we have set $\nu_i = 1/\sqrt{2}$ and $\mu_i = i/\sqrt{2}$. The symbols a_i, Δ_i, and χ_i in Eq. (5.25) are, respectively, the annihilation operator, the detuning frequency, and effective Kerr coefficient of the ith tunable Kerr circuit TKC_i. The coherent driving amplitude for the input i is denoted by β_i. We then introduce the semiclassical approximation, letting $\langle a_i\rangle = \alpha_i$ and $\langle a_i^\dagger a_i\rangle = |\alpha_i|^2$. The resulting dynamical equation for the TKC resonator modes is

$$\begin{aligned}
\dot{\alpha}_0 &= -\left(i\Delta_0 + \frac{\kappa}{3}\right)\alpha_0 - i\chi_0\alpha_0^*\alpha_0^2 - 2i\frac{\sqrt{2\kappa}}{3}\alpha_1 + \frac{\sqrt{2\kappa}}{3}(\sqrt{2}i\beta_0 + \beta_1), \\
\dot{\alpha}_1 &= -\left(i\Delta_1 + \frac{\kappa}{3}\right)\alpha_1 - i\chi_1\alpha_1^*\alpha_1^2 - 2i\frac{\sqrt{2\kappa}}{3}\alpha_0 + \frac{\sqrt{2\kappa}}{3}(\beta_0 + \sqrt{2}i\beta_1).
\end{aligned} \tag{5.26}$$

The bistable effects can be extracted by analyzing this nonlinear differential equation.

Controlling qubits with a cavity controller (2012, 2013): The experiment of Shankar et al. [413] demonstrated the use of a continuous coherent feedback process to maintain superconducting circuits in an entangled state. The system consists of the two qubits and a superconducting cavity that is used as the feedback controller. The qubits are coupled dispersively to the cavity, so that the states of the qubits shift the energy of the states of the cavity, and vice versa. This means that many of the joint states of the qubits and cavity are distinguished by their energy, so that a joint Hamiltonian can be engineered by driving the system with signals that will drive selected transitions. The authors apply six driving fields that implement concurrently the two classic parts of coherent feedback [57,59,86]. The first correlates the qubits with the cavity, so that the cavity acts as a measuring device for the qubits. The second applies a different unitary operation to the qubits for each of the relevant cavity states, thus applying an action that is equivalent to an operation conditional on the result of a measurement. The cavity is continually reset to its ground state via its own damping. The end result can be thought of as sideband cooling, in which the entangled state of the qubits is the "ground state" to which the qubits are "cooled". Two further examples of coherent feedback in which a cavity is used to prepare a qubit in a pure state are given in Refs. [414,415].

5.3. Other physical setups

Cooling macroscopic mechanical resonators (1999–2012): A number of experiments have demonstrated cooling of macroscopic mechanical resonators using measurement and feedback, but this approach to cooling has not yet reached the quantum regime [229–232,416,417]. One possible example along this line is the experiment by Kleckner and Bouwmeester [232]. In this experiment, the authors were able to cool the cantilever from room temperature to 135 mK. This indicates that if their cantilever was at the temperature of a dilution refrigerator, they would be able to get close to the ground state. Of course, at that point, the back-action noise and any other sources of classical noise in the feedback system might provide further obstacles to reaching the ground state. Another example of feedback cooling of a macroscopic mechanical resonator is the experiment by Gavartin et al. [417]. Here the resonator is a doubly-clamped nanobeam of Si_3N_4 that has a resonance frequency of $\Omega_M/2\pi = 2.88$ MHz. The beam is placed in the evanescent field of a toroidal "microdisk" optical cavity. The movement of the mechanical resonator changes the frequency of the toroidal cavity mode, an effect which is described as an "optomechanical" coupling [418–420]. The phase of the light that is output from the toroidal cavity provides a readout of the motion of the mechanical resonator. To obtain the position spectrum, the authors used a demodulation technique described by Poot et al. [421], which is not limited by the bandwidth of the digital signal processor, and can therefore be applied to cooling resonators in MHz and even GHz range. The authors were able to cool the resonator to 0.7 K. We note finally that, while the nominal purpose of this experiment, as described by the authors, was to improve force detection, it has in fact been shown that force detection cannot be improved by any linear feedback applied to a resonator [422–424].

The first paper to operate feedback in a regime where quantum back action noise is really suppressed is demonstrated by Kippenberg's group in 2015 [425]. In this work, a position sensor that is capable of resolving the zero-point motion of a solid-state nanomechanical oscillator in the timescale of its thermal decoherence is introduced to fulfill a weak continuous position measurement with imprecision back-action noise that is within a factor of five of the Heisenberg uncertainty limit. A succeeding experiment shows that measurement-based feedback can be used to improve the visibility of quantum correlations [426] in which both squeezing of the meter field fluctuations below the vacuum level in a homodyne measurement and sideband asymmetry in a heterodyne measurement are demonstrated.

Cooling of mechanical resonators using "resolved-sideband cooling", a coherent feedback method, has been realized experimentally [227,228,234,236,242,243]. Not only that, this method has already achieved cooling to a mean energy below a single phonon, in experiments performed by Teufel et al. [242] and Chan et al. [243] in 2011. In resolved-sideband cooling, the mechanical resonator is coupled to an "auxiliary" resonator that may be electrical or optical. The frequency of the auxiliary is high enough that it sits in its ground state at the ambient temperature. The coupling is modulated at the frequency difference between the mechanical and auxiliary resonators, which provides the energy required to convert the mechanical quanta to electrical or optical quanta, and vice versa. The interaction therefore transfers energy and entropy between the two resonators, and since the auxiliary has neither, energy is transferred out of the mechanics. So long as the damping rate of the auxiliary is sufficiently fast, this energy is removed from the auxiliary quickly so that energy can continue to be sucked out of the mechanics.

Stabilization of a quantum state in a cavity-QED system (2002): The first demonstration of quantum feedback control of an atom-optical system was that performed by Smith et al. [204]. (Earlier experiments in atom-optical systems, while reported as quantum feedback at the time, were not in fact quantum feedback because they could be described by classical analyses [427–429]. The reason for this is that the quantum noise was insignificant compared to the classical noise [22].) The system to be controlled consists of a stream of atoms interacting with a single mode of an optical cavity, as shown in Fig. 21. If we denote the average number of atoms interacting with the cavity at any given time by N, and if the interaction is sufficiently weak that only one of the atoms is excited at any given time, then the system settles down to a steady state given by

$$|\psi_{ss}\rangle \approx |0\rangle|g\rangle + \lambda\left(|1\rangle|g\rangle - \frac{2g\sqrt{N}}{\gamma}|0\rangle|e\rangle\right). \tag{5.27}$$

In this equation, the kets $|0\rangle$ and $|1\rangle$ denote the states of the cavity with 0 and 1 photons, respectively. The ket $|g\rangle$ denotes the state in which all the atoms are in their ground states, and $|e\rangle$ denotes the symmetric state in which one and only one of the atoms is in the excited state. The parameter λ is determined by the intensity of the laser driving the cavity mode.

The state of the system is changed upon the detection of a photon leaving the cavity. If a photon is detected at the time $t = 0$ and no photon is detected between $t = 0$ and a time $t = \tau$, the state of the system at $t = \tau$ conditioned on the photondetection at $t = 0$ is given by

$$|\psi_c(\tau)\rangle = |0\rangle|g\rangle + \lambda\left[\xi(\tau)|1\rangle|g\rangle - \theta(\tau)\frac{2g\sqrt{N}}{\gamma}|0\rangle|e\rangle\right], \tag{5.28}$$

where ξ and θ are functions that oscillate at the Rabi frequency. We now note that when τ is such that $\xi(\tau) = \theta(\tau)$, then the conditioned state $|\psi_c(\tau)\rangle$ is precisely the steady state $|\psi_{ss}\rangle$, but with a different value of λ. Thus if we suddenly switch the intensity of the driving field by the right amount, the conditioned state *becomes* the new steady state, and the evolution

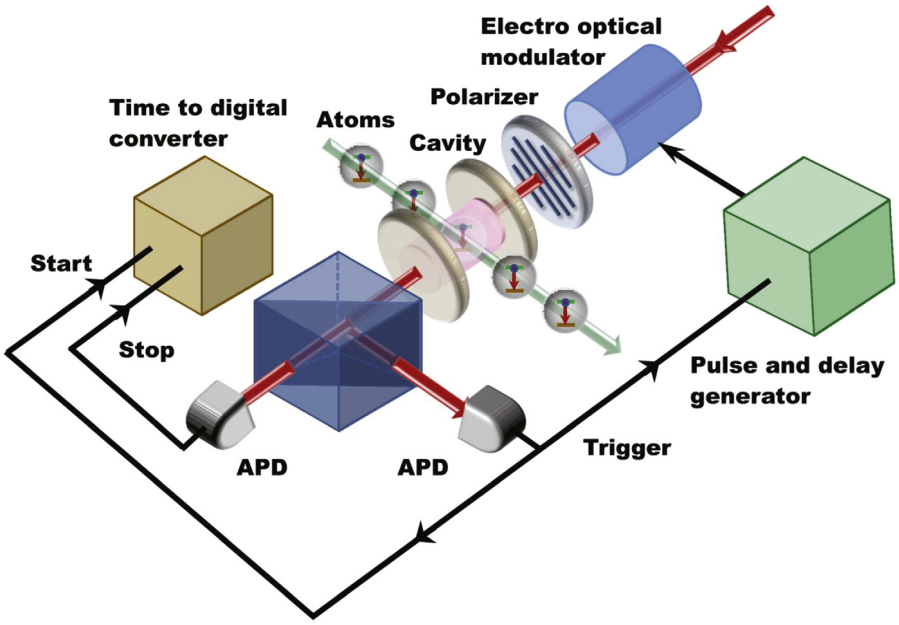

Fig. 21. Diagram of the experimental setup of Smith et al. [204] to capture and release quantum state by feedback. Here, APD denotes an avalanche photodiode.

of the system is frozen until we change the driving laser back to its original value. Switching the driving laser so as to freeze the evolution is a feedback process, because one must first detect a single photon emitted by the cavity, and perform the switch based on this detection. The experiment in Ref. [204] did just that, and read out the change in the evolution of the system by measuring the intensity autocorrelation function of the light output from the cavity.

Referring again to Fig. 21, the central component of the experiment is an optical cavity composed of two high-reflectivity curved mirrors with separation $l = 880\ \mu\text{m}$. A thermal beam of Rb^{85} atoms is produced by an effusive oven heated to 440 K. The cavity field is driven by an Ar^{+}-pumped titanium sapphire (Ti:sapphire) laser which excites the Rb^{85} transition between the states $5S_{1/2}, F = 3$ and $5P_{3/2}, F = 4$. The coupling strength between the atom and the cavity, the decay rate of the cavity, and the decay rate of the atom are $(g, \kappa, \gamma/2)\ /2\pi = (5.1, 3.7, 3.0)$ MHz. The output field from the cavity is split by a beam splitter and detected by two ("start" and "stop") avalanche photodiodes (APDs). The output signal from the start detector is also split into two branches. One branch enters the start channel and is fed into a time-to-digital converter (TDC) used to measure the second-order correlation function $g^{(2)}(\tau)$, and the other is sent to a delay generator and then fed back to control the strength of the driving laser using an electro-optical modulator. The delay between the detection of the single photon emitted from the cavity, and the switch of the power of the driving laser is just 45 ns.

Preparation of Fock states in a cavity-QED system (2011): The experiment of Sayrin et al. [430] uses feedback based on a sequence of weak measurements to prepare a single cavity mode in a Fock state (a state with a precise number of photons and no phase). The diagram of the experimental systems are presented in Fig. 22. Each weak measurement is made by passing a two-level atom through the cavity and then measuring the internal state of the atom. This state is measured using a field-ionization detector which gives a detection efficiency of 35%. The resulting measurement on the cavity mode is given by the measurement operators [see Eq. (2.16)]

$$M_e = \cos\left[\frac{1}{2}\left(\phi_r + \phi_0\left(a^\dagger a + \frac{1}{2}\right)\right)\right], \quad M_g = \sin\left[\frac{1}{2}\left(\phi_r + \phi_0\left(a^\dagger a + \frac{1}{2}\right)\right)\right], \tag{5.29}$$

where the phase ϕ_0 is determined by the initial state of the atom and the effective basis in which the atomic state is measured. The operator M_e (M_g) corresponds to the measurement result in which the atom is detected to be in the state $|e\rangle$ ($|g\rangle$). The operator a is the annihilation operator of the cavity mode. The initial state of the atom is set by an interaction with an auxiliary cavity, and the effective basis in which the atomic state is measured is set by a second auxiliary cavity. Since the measurement operators commute with the number operator $a^\dagger a$, each measurement provides information about the number of photons without disturbing it. After each measurement, the state of the cavity mode is estimated by the mapping

$$\rho \to \rho_j = \frac{M_j \rho M_j^\dagger}{\text{tr}(M_j \rho M_j^\dagger)}, \quad j = e, g, \tag{5.30}$$

where ρ_e (ρ_g) corresponds to a detection of the atomic state $|e\rangle$ ($|g\rangle$). The measurement result is used to modify the amplitude of the coherent light driving the cavity. This coherent light by itself cannot create a Fock state, and will in general take the

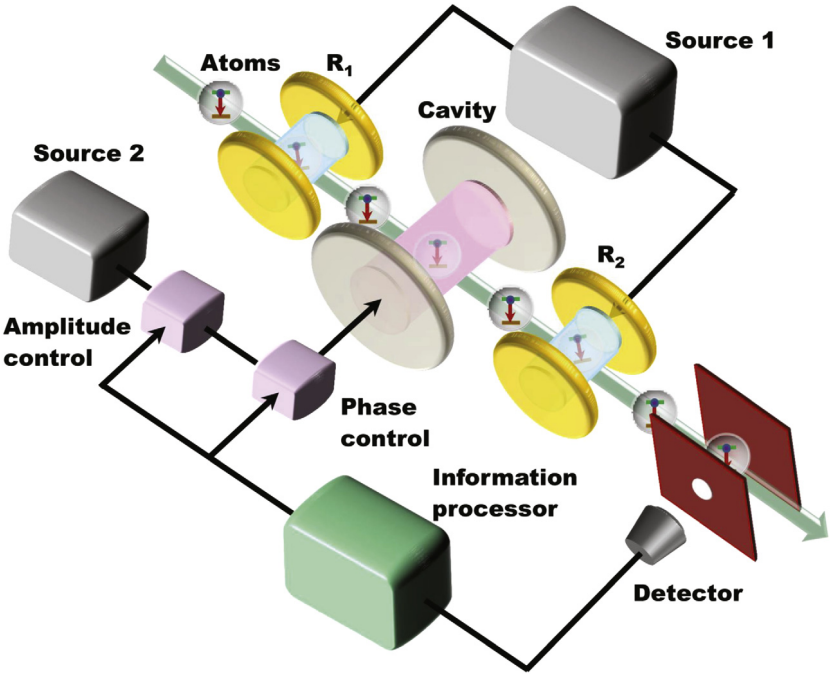

Fig. 22. Diagram of the experimental setup of Sayrin et al. [430]. The state of the cavity mode C is weakly measured by an atomic beam. The atoms in this beam are resonant with the two cavities R_1 and R_2, which form an "atomic Ramsey interferometer" by setting the initial state in which the atoms are prepared before entering the cavity, and the effective basis in which the atomic state is measured by the field-ionization detector. The output of the measurement is fed into the information processor to execute the state estimation and determine the phase and intensity of the laser that drives the cavity mode, source 2.

mode further from a Fock state, by which we can obtain a new cavity state

$$\tilde{\rho}_j = D(\alpha_j)\,\rho_j\,D(-\alpha_j), \quad j = e, g, \tag{5.31}$$

where $D(\alpha) = \exp(\alpha a^\dagger - \alpha^* a)$ is the displacement operator of the cavity mode. To generate a state $\tilde{\rho}_j$ that is as close as possible to the target state $|n_t\rangle\langle n_t|$, one seeks the choice of driving amplitude α_j that minimizes the distance

$$d(\tilde{\rho}_j, |n_t\rangle\langle n_t|) = 1 - \langle n_t|\tilde{\rho}_j|n_t\rangle. \tag{5.32}$$

In practice, the calculation of $d(\tilde{\rho}_j, |n_t\rangle\langle n_t|)$ is time-consuming, and thus the following second-order approximation is introduced

$$\tilde{\rho}_j = D(\alpha_j)\rho_j D(-\alpha_j) \approx \rho_j - \alpha_j[\rho_j, a^\dagger - a] + \frac{\alpha_j^2}{2}[[\rho_j, a^\dagger - a], a^\dagger - a], \tag{5.33}$$

by which we have

$$d(\tilde{\rho}_j, |n_t\rangle\langle n_t|) \approx d(\rho_j, |n_t\rangle\langle n_t|) + \alpha_j \mathrm{tr}([|n_t\rangle\langle n_t|, a^\dagger - a]\rho_j) - \frac{\alpha_j^2}{2}\mathrm{tr}([[|n_t\rangle\langle n_t|, a^\dagger - a], a^\dagger - a]\rho_j). \tag{5.34}$$

In the fact, in the control process, the role of the coherent light is merely to help keep the average number of photons in the cavity constant, while it is the job of the measurement to narrow the distribution of photons towards a Fock state.

A diagram of the experiment is shown in Fig. 22, in which R_1 and R_2 label the auxiliary cavities, each of which performs a chosen unitary operation on the internal state of the atoms. The central component is the microwave cavity, for which the mode in question has a frequency of 51 GHz and a damping time of $T_c = 65$ ms. The feedback delay in each round is approximately 83 ns. The experiment was able to stabilize Fock states up to $n = 4$. The time taken by the feedback loop to converge to a steady state with $n = 3$ was 50 ms, which was 5 times faster than that resulting from an optimized trial-and-error projection method using the same apparatus.

It would clearly be an improvement over the above experiment if the feedback was able to add or subtract a photon from the cavity, instead of merely shifting the state in phase-space, because this kind of feedback would not degrade Fock states. In fact, the atoms that are passed through the cavity provide a means to do just this, and a feedback protocol using this method was demonstrated by Zhou et al. [431]. The experimental setup is very similar to that in Fig. 22, and the only difference is that the result of the measurement now controls the initial state of the atoms prior to entering the central

cavity. The atomic beam works both as a quantum nondemolition probe and a means to add or subtract a single photon to the cavity mode. In this work, the authors demonstrated the stabilization of Fock states with up to seven photons.

Classical feedback control of atomic states (2012, 2013): Here we examine some nice experiments that push the boundaries of feedback control in quantum systems, but are nevertheless not examples of quantum feedback, under our definition. While the present review concerns solely quantum feedback, the experiments here are instructive in helping us to explain more clearly what constitutes quantum feedback.

Recall that our definition of measurement-based quantum feedback is that quantum measurement theory is required to correctly describe it. This means that the change in the state of the system caused by the measurement is (i) important in describing the behavior under the feedback loop, and (ii) that this change is not the same as the change that would be predicted by Bayesian inference. Condition (ii) is often stated by saying that the measurement induces "quantum back-action".

We now describe two ways in which a measurement on a quantum system can be effectively classical, meaning that the measurement has no dynamical effect on the system, and can therefore be described purely by Bayesian inference. The first of these is when the observable being measured commutes at every time with the density matrix of the system. In this case, the state of the system is merely a classical probability distribution of the eigenstates of the observable. Since the measurement does not disturb these eigenstates, the only change is to the probability distribution, and since this distribution is classical, this change obeys Bayesian inference. An experiment that uses this kind of measurement to control the populations of atomic energy levels is that by Brakhane et al. [276]. Because the transitions between the levels are incoherent, the density matrix remains diagonal in the same basis as the measurement operators, and the feedback is classical.

The second way in which a quantum measurement can avoid back-action is if the controller has many identical systems that are all in the same state, $|\psi\rangle$, and undergoing the same evolution. In this case, the controller can learn $|\psi\rangle$ by extracting only a very tiny amount of information from each system. As a result, the quantum state $|\psi\rangle$ has been transformed into a set classical parameters that can be measured without disturbing them. Feedback that uses this kind of measurement process to control the internal state of an (ensemble of) atoms is realized in the experiments by Vanderbruggen et al. [432] and Inoue et al. [433].

Controlling the motion of trapped particles (2002–2009): Feedback has now been applied to cooling the motion of single trapped ions [245] electrons [246], nanoparticles [247], and atoms [225,226,248]. Only one of these, however, has reached the quantum domain in the trapped-ion experiment [245]. The experiment in Ref. [248] uses an ensemble of atoms in identical states, and thus an effectively classical measurement. The experiments in Refs. [225,226,246,247] make measurements on single particles, but the effect of the back-action is negligible. Nevertheless these experiments are interesting as they represent the state of the art in applying feedback control to microscopic systems.

6. Summary and outlook

We have seen in this review that continuous-time feedback can be implemented with or without measurements, and in the latter case can be implemented either with direct Hamiltonian coupling between the system and controller, or with couplings mediated by irreversible one-way quantum fields. We have also seen that the range of applications of feedback in quantum systems is rather broad, and further applications are yet to be discovered.

Measurement-based feedback control of quantum systems was first demonstrated in quantum optics, and for some time there was no other field in which this kind of feedback could be realized. It is only very recently, in 2012, that experimental technology has allowed measurement-based feedback to be achieved in superconducting circuits [193,194]. This was possible because of recent breakthroughs in quantum-limited amplifiers [403–405]. We expect this development to open the door to many more implementations of measurement-based feedback in both electrical and electromechanical systems.

The situation regarding coherent feedback control is a little different. Experiments implementing coherent feedback had been realized for some time – for example those involving the laser cooling of atoms and ions – before the theoretical notion of coherent feedback was articulated. This notion provides a new way to think about interacting quantum systems, especially those coupled via irreversible fields. As pointed out in Ref. [64], coherent feedback provides not only a tool for controlling quantum systems, but also for changing the dynamics of a system and thus engineering new dynamics.

While measurement-based feedback control has been studied theoretically for a little over 20 years, coherent feedback has been much less studied, and there are still many basic questions that remain, particularly to do with the relationship between the various kinds of feedback. A basic question regarding any kind of control process is just how well it can perform, given a set of limitations on the physical control resources, such as the measurement strength, coupling constant(s), and the speed and nature of the available control Hamiltonian. Since the dynamics of most measured quantum systems is nonlinear, and since the question of the limits to control is essentially one about optimality of control protocols, it may not be possible to obtain exact answers, or even numerical answers to these questions for measurement-based feedback. The connection between measurement-based feedback and coherent feedback however might provide a new way to analyze such questions.

There is one question regarding the limits to coherent feedback control that has been recently answered, at least with considerable confidence, and that is the limit to the fidelity of state preparation given a bound on the rate of the coupling between the system and auxiliary components [434]. This was only solved, however, in the regime of good control, where the coupling is fast compared to the noise in the system, and in the regime of weak coupling in which the coupling rate is small

compared to the energy scale of the system (the gaps between the energy levels of the system). The reason for the weak-coupling restriction is that without it, the master equation that describes the noise, even for Markovian weak-damping, is no longer independent of the control Hamiltonian. The reason that the noise depends on the control Hamiltonian for strong coupling is that in this case the energy levels of the system are altered by the coupling, and the noise that a system experiences usually depends on the energy levels of the system. As an example, thermal noise depends on a system's energy levels because the thermal steady state depends on these levels. Since the control Hamiltonian is usually time dependent, strong control Hamiltonians imply that the master equation will be time dependent. Because of this, up until very recently, theoretical treatments of quantum control were restricted to the regime of weak coupling/weak control. Modeling strongly-controlled systems is an important challenge in quantum control, either by using methods for exact simulation of open-system dynamics (see e.g. [435–438]) or by obtaining approximate master equations that correctly model noise for time-dependent systems [439].

A key question regarding the relationship between various kinds of feedback is whether one kind is superior to the others for certain applications, or under certain kinds of constraints. Some results along these lines have already been obtained [59,65–68]. It appears that under a constraint on the speed (equivalently the norm) of the interaction Hamiltonian between the system and controller, coherent feedback is fundamentally more powerful than measurement-based feedback, because it allows a larger class of joint evolutions [59]. It is not known whether the same is true under a bound on the measurement strength, equivalent to a bound on the input–output rate to a field or a damping rate into a Markovian bath. What is fairly clear is that a constraint on an irreversible Markovian damping rate is not equivalent to a constraint on the norm of an interaction Hamiltonian. This further suggests that while continuous-time measurement-based feedback can be compared directly with field-mediated coherent feedback, this may not be possible with coherent feedback implemented via direct coupling. Nevertheless the relationship between various forms of feedback raises questions that are both fundamental and relevant to potential applications.

Systems driven by white noise obey Markovian master equations, meaning that the time derivative of the density matrix depends only on the density matrix at the current time. One way in which analyses of feedback control are being extended is to include systems coupled to baths that induce non-Markovian evolution, or feedback implemented via fields with a finite or tailored bandwidth. It turns out that the standard input–output formalism that we introduced in Section 3.2.1, and which is used to treat field-mediated feedback networks can be extended without difficulty to couplings with arbitrary bandwidths [353,354]. Interestingly, with this extension the resulting formalism can handle strong damping and coupling, something that the standard formalism cannot. For nonlinear networks, the input–output equations must be converted to master equations to be solved, and these require considerable numerical resources. For linear systems, the input–output formalism provides an efficient means of solution, and thus appears to be a powerful method for analyzing non-Markovian feedback for linear systems. It can also be used to describe feedback in which there is a time delay in the feedback control process. With the implementation of feedback in superconducting circuits, and beyond that to spins in, e.g., nitrogen-vacancy centers in diamond or quantum dots, the analysis of non-Markovian evolution will become increasingly important.

When feedback was introduced into quantum theory in the late 80s and early 90s, the number of physical systems in which feedback could be implemented were extremely limited, and such experiments were very difficult, especially for measurement-based feedback. With recent breakthroughs in the construction and measurement of mesoscopic circuits [440–442], the number of experimental applications for feedback control has greatly increased. We anticipate that the field of quantum feedback control will expand considerably due to these developments, and feedback will be realized in an increasing range of mesoscopic systems, including, e.g., superconducting circuits, quantum dots, and silicon-based on-chip optical devices [443–449].

Acknowledgments

We would like to thank Prof. T.J. Tarn and Dr. W. Cui for helpful discussions and Prof. G.Y. Xiang for providing related materials. Y.-X. Liu and J. Zhang are supported by the National Basic Research Program of China (973 Program) under Grant No. 2014CB921401, the Tsinghua University Initiative Scientific Research Program, and the Tsinghua National Laboratory for Information Science and Technology (TNList) Cross-discipline Foundation. J. Zhang and R.B. Wu are supported by the National Natural Science Foundation of China under Grant Nos. 61622306, 11674194, 61134008, 60904034, and Y.-X. Liu is supported by this foundation under Grant Nos. 10975080, 4361025022, 60836010. K. Jacobs was partially supported by the US National Science Foundation projects PHY-1005571 and PHY-1212413. F. Nori was partially supported by the RIKEN iTHES Project, MURI Center for Dynamic Magneto-Optics via the AFOSR Award No. FA9550-14-1-0040, the Japan Society for the Promotion of Science (KAKENHI), the IMPACT program of JST, JSPS-RFBR grant No. 17-52-50023, CREST grant No. JPMJCR1676, and the John Templeton Foundation.

References

[1] H. Mabuchi, N. Khaneja, Principles and applications of control in quantum systems, Internat. J. Robust Nonlinear Control 15 (2005) 647–667.
[2] D. D'Alessandro, Introduction to Quantum Control and Dynamics, Chapman and Hall, Boca Raton, LA, 2007.
[3] P. Rouchon, Quantum systems and control, Arima 9 (2008) 325–357.
[4] D.Y. Dong, I.R. Petersen, Quantum control theory and applications: a survey, IET Control Theory Appl. 4 (2010) 2651–2671.

[5] C. Altafini, F. Ticozzi, Modeling and control of quantum systems: an introduction, IEEE Trans. Automat. Control 57 (2012) 1898–1917.
[6] G. Huang, T.J. Tarn, J.W. Clark, On the controllability of quantum-mechanical systems, J. Math. Phys. 24 (1983) 2608–2618.
[7] J. Bechhoefer, Feedback for physicists: A tutorial essay on control, Rev. Modern Phys. 77 (2005) 783–836.
[8] C. Brif, R. Chakrabarti, H. Rabitz, Control of quantum phenomena: past, present and futures, New J. Phys. 12 (2010) 075008.
[9] N. Wiener, Cybernetics: or Control and Communication in the Animal and the Machine, second ed., The MIT Press, Cambridge, 1965.
[10] W.J. Rugh, Linear System Theory, second ed., Prentice Hall, New Jersey, 1996.
[11] R.E. Kalman, Y.C. Ho, K.S. Narendra, Controllability of linear dynamical systems, Contrib. Differ. Equ. 1 (1963) 189–213.
[12] R. Bellman, Introduction to Matrix Analysis, McGrw-Hill Book Company, New York, 1960.
[13] M. Athans, P. Falb, Optimal Control: An Introduction to the Theory and its Applications, 2006.
[14] A. Isidori, Nonlinear Control Systems, third ed., Springer, London, 1995.
[15] Y. Kang, D.H. Zhai, G.P. Liu, Y.B. Zhao, P. Zhao, Stability analysis of a class of hybrid stochastic retarded systems under asynchronous switching, IEEE Trans. Automat. Control 59 (2014) 1511–1523.
[16] Y. Kang, D.H. Zhai, G.P. Liu, Y.B. Zhao, On input-to-state stability of switched stochastic nonlinear systems under extended asynchronous switching, IEEE Trans. Cybern. 46 (2015) 1092–1105.
[17] M.A. Nielsen, I.L. Chuang, Quantum Computation and Quantum Information, Cambridge University Press, Cambridge, England, 2000.
[18] H. Diels, Antike Technik, Teubner, Berlin, 1920.
[19] O. Mayr, The Origins of Feedback Control, The M.I.T. Press, 1970.
[20] A.M. Lepschy, Feedback control in ancient water and mechanical clocks, IEEE Trans. Educ. 35 (1992) 3–10.
[21] J.C. Maxwell, On governors, Proc. R. Soc. Lond. 16 (1868) 270–283.
[22] H.M. Wiseman, G.J. Milburn, Quantum Measurement and Control, Cambridge University Press, Cambridge, United Kingdom, 2010.
[23] M.R. James, Control Theory: From Classical to Quantum Optimal, Stochastic, and Robust Control, Australian National University, 2005.
[24] H. Mabuchi, A.C. Doherty, Cavity quantum electrodynamics: Coherence in context, Science 298 (2002) 1372–1377.
[25] S. Habib, K. Jacobs, H. Mabuchi, Quantum feedback control: How can we control quantum systems without disturbing them? Los Alamos Sci. 27 (2002) 126–135.
[26] G. Zhang, M.R. James, Quantum feedback networks and control: A brief survey, Chin. Sci. Bull. 5 (2012) 2200–2214.
[27] A. Serafini, Feedback control in quantum optics: an overview of experimental breakthroughs and areas of application, ISRN Opt. 2012 (2012) 275016.
[28] M.D. Srinivas, E.B. Davies, Photon counting probabilities in quantum optics, J. Modern Opt. 28 (1981) 981.
[29] E.B. Davies, Quantum stochastic processes, Comm. Math. Phys. 15 (1969) 277–304.
[30] E.B. Davies, Quantum stochastic processes II, Comm. Math. Phys. 19 (1970) 83–105.
[31] E.B. Davies, Quantum stochastic processes III, Comm. Math. Phys. 22 (1971) 51–70.
[32] H.J. Carmichael, S. Singh, R. Vyas, P.R. Rice, Photoelectron waiting times and atomic state reduction in resonance fluorescence, Phys. Rev. A 39 (1989) 1200–1218.
[33] H.J. Carmichael, Statistical Methods in Quantum Optics 2: Non-Classical Fields, Springer, New York, 2008.
[34] J. Dalibard, Y. Castin, K. Mølmer, Wave-function approach to dissipative processes in quantum optics, Phys. Rev. Lett. 68 (1992) 580–583.
[35] G.C. Hegerfeldt, T.S. Wilser, Ensemble or individual system, collapse or no collapse: a description of a single radiating atom, in: H.D. Doebner, W. Scherer, F. Schroeck (Eds.), Classical and Quantum Systems, in: Proceedings of the Second International Wigner Symposium, 1992, pp. 104–115.
[36] N. Gisin, Quantum measurements and stochastic processes, Phys. Rev. Lett. 52 (1984) 1657–1660.
[37] L. Diosi, Stochastic pure state representation for open quantum systems, Phys. Lett. A 114 (1986) 451–454.
[38] A. Barchielli, G. Lupieri, Quantum stochastic calculus, operation valued stochastic processes and continual measurements in quantum mechanics, J. Math. Phys. 26 (1985) 2222.
[39] V.P. Belavkin, Non-demolition measurement and control in quantum dynamical systems, in: A. Blaquiere, S. Diner, G. Lochak (Eds.), Information, Complexity and Control in Quantum Physics, in: Proceedings of the 4th International Seminar on Mathematical Theory of Dynamical Systems and Microphysics, Springer-Verlag, New York, 1987, pp. 331–336.
[40] L. Diosi, Continuous quantum measurement and Ito formalism, Phys. Lett. A 129 (1988) 419.
[41] L. Diosi, Localized solution of a simple non-linear quantum Langevin equation, Phys. Lett. A 132 (1988) 233.
[42] H.M. Wiseman, G.J. Milburn, Quantum theory of field-quadrature measurements, Phys. Rev. A 47 (1993) 642–662.
[43] H.M. Wiseman, G.J. Milburn, Quantum theory of optical feedback via homodyne detection, Phys. Rev. Lett. 70 (1993) 548–551.
[44] P.S. Maybeck, Stochastic Models, Estimation and Control (I and II), Academic Press, New York, 1982.
[45] V.P. Belavkin, Quantum stochastic calculus and quantum nonlinear filtering, J. Multivariate Anal. 42 (1992) 171–202.
[46] V.P. Belavkin, Quantum continual measurements and a posteriori collapse on CCR, Comm. Math. Phys. 146 (1992) 611–635.
[47] V.P. Belavkin, Theory of the control of observable quantum systems, Autom. Remote Control 44 (1983) 178–188.
[48] H.M. Wiseman, Quantum theory of continuous feedback, Phys. Rev. A 49 (1994) 2133–2150.
[49] M. Yanagisawa, H. Kimura, A control problem for Gaussian states, in: Y. Yamamoto, S. Hara (Eds.), Learning, Control and Hybrid Systems, in: Lecture Notes in Control and Information Sciences, vol. 241, Springer-Verlag, New York, 1998, pp. 249–313.
[50] A.C. Doherty, K. Jacobs, Feedback control of quantum systems using continuous state estimation, Phys. Rev. A 60 (1999) 2700–2711.
[51] H.M. Wiseman, G.J. Milburn, All-optical versus electro-optical quantum-limited feedback, Phys. Rev. A 49 (1994) 4110–4125.
[52] I. Kenyon, The Light Fantastic: A Modern Introduction to Classical and Quantum Optics, 2011.
[53] C.W. Gardiner, M.J. Collett, Input and output in damped quantum systems: Quantum stochastic differential equations and the master equation, Phys. Rev. A 31 (1985) 3761–3774.
[54] C.W. Gardiner, P. Zoller, Quantum Noise, third ed., Springer-Verlag, Berlin, 2004.
[55] C.W. Gardiner, Driving a quantum system with the output field from another driven quantum system, Phys. Rev. Lett. 70 (1993) 2269–2272.
[56] H.J. Carmichael, Quantum trajectory theory for cascaded open systems, Phys. Rev. Lett. 70 (1993) 2273–2276.
[57] S. Lloyd, Coherent quantum feedback, Phys. Rev. A 62 (2000) 022108.
[58] R.J. Nelson, Y. Weinstein, D. Cory, S. Lloyd, Experimental demonstration of fully coherent quantum feedback, Phys. Rev. Lett. 85 (2000) 3045–3048.
[59] K. Jacobs, X. Wang, H.M. Wiseman, Coherent feedback that beats all measurement-based feedback protocols, New J. Phys. 16 (2014) 073036.
[60] B. Qi, L. Guo, Is measurement-based feedback still better for quantum control systems? Syst. Control Lett. 59 (2010) 333–339.
[61] M.R. James, H.I. Nurdin, I.R. Petersen, H^{∞} Control of Linear Quantum Stochastic Systems, IEEE Trans. Automat. Control 53 (2008) 1787–1803.
[62] J.E. Gough, M.R. James, The series product and its application to quantum feedforward and feedback networks, IEEE Trans. Automat. Control 54 (2009) 2530–2544.
[63] H. Mabuchi, Nonlinear interferometry approach to photonic sequential logic, Appl. Phys. Lett. 99 (2011) 153103.
[64] J. Kerckhoff, K.W. Lehnert, Superconducting microwave multivibrator produced by coherent feedback, Phys. Rev. Lett. 109 (2012) 153602.
[65] J. Zhang, R.B. Wu, Y.-X. Liu, C.W. Li, T.J. Tarn, Quantum coherent nonlinear feedbacks with applications to quantum optics on chip, IEEE Trans. Automat. Control 57 (2012) 1997–2008.
[66] Z.-P. Liu, H. Wang, J. Zhang, Y.-X. Liu, R.-B. Wu, C.-W Li, F. Nori, Feedback-induced nonlinearity and superconducting on-chip quantum optics, Phys. Rev. A 88 (2013) 063851.
[67] H.I. Nurdin, M.R. James, I.R. Petersen, Coherent quantum LQG control, Automatica 45 (2009) 1837–1846.
[68] R. Hamerly, H. Mabuchi, Advantages of coherent feedback for cooling quantum oscillators, Phys. Rev. Lett. 109 (2012) 173602.
[69] A. Pechen, C. Brif, R.-B. Wu, R. Chakrabarti, H. Rabitz, General unifying features of controlled quantum phenomena, Phys. Rev. A 82 (2010) 030101(R).
[70] K. Maruyama, F. Nori, V. Vedral, The physics of Maxwell's demon and information, Rev. Mod. Phys. 81 (2009) 1–23.
[71] T. Sagawa, M. Ueda, Second law of thermodynamics with discrete quantum feedback control, Phys. Rev. Lett. 100 (2008) 080403.
[72] T. Sagawa, M. Ueda, Nonequilibrium thermodynamics of feedback control, Phys. Rev. E 85 (2012) 021104.

[73] D. Abreu, U. Seifert, Thermodynamics of genuine nonequilibrium states under feedback control, Phys. Rev. Lett. 108 (2012) 030601.
[74] K. Jacobs, Second law of thermodynamics and quantum feedback control: Maxwell's demon with weak measurements, Phys. Rev. A 80 (2009) 012322.
[75] P.W. Shor, Scheme for reducing decoherence in quantum computer memory, Phys. Rev. A 52 (1995) R2493–R2496.
[76] A.M. Steane, Multiple-particle interference and quantum error correction, Proc. R. Soc. Lond. Ser. A Math. Phys. Eng. Sci. 452 (1996) 2551–2577.
[77] E. Knill, R. Laflamme, Theory of quantum error-correcting codes, Phys. Rev. A 55 (1997) 900–911.
[78] J.I. Cirac, T. Pellizzari, P. Zoller, Enforcing coherent evolution in dissipative quantum dynamics, Science 273 (1996) 1207–1210.
[79] W.H. Zurek, R. Laflamme, Quantum logical operations on encoded qubits, Phys. Rev. Lett. 77 (1996) 4683–4686.
[80] L.M. Duan, G.C. Guo, Preserving coherence in quantum computation by pairing quantum bits, Phys. Rev. Lett. 79 (1997) 1953–1956.
[81] S. Lloyd, J.J.E. Slotine, Analog quantum error correction, Phys. Rev. Lett. 80 (1998) 4088–4091.
[82] K. Jacobs, Twenty open problems in quantum control, arXiv:1304.0819v2.
[83] M.J. Collett, C.W. Gardiner, Squeezing of intracavity and traveling-wave light fields produced in parametric amplification, Phys. Rev. A 30 (1984) 1386–1391.
[84] R.I. Hudson, K.R. Parthasarathy, Quantum Ito's formula and stochastic evolution, Comm. Math. Phys. 93 (1984) 301–323.
[85] K. Jacobs, Stochastic Processes for Physicists: Understanding Noisy Systems, Cambridge University Press, Cambridge, 2010.
[86] K. Jacobs, Quantum Measurement Theory and its Applications, Cambridge University Press, Cambridge, 2014.
[87] D. Wineland, H. Dehmelt, Proposed $10^{14}\Delta\nu < \nu$ laser fluorescence spectroscopy on Tl^{+} mono-ion oscillator, Bull. Amer. Math. Soc. 20 (1975) 637.
[88] F. Diedrich, J.C. Bergquist, W.M. Itano, D.J. Wineland, Laser cooling to the zero-point energy of motion, Phys. Rev. Lett. 62 (1989) 403–406.
[89] F. Golnaraghi, B.C. Kuo, Automatic Control Systems, eighth ed., Wiley, New York, 2009.
[90] K. Zhou, J. Doyle, K. Glover, Robust and Optimal Control, Prentice Hall, Englewood Cliffs, New Jersey, 1995.
[91] C. Ahn, A.C. Doherty, A.J. Landahl, Continuous quantum error correction via quantum feedback control, Phys. Rev. A 65 (2002) 042301.
[92] C. Ahn, H.M. Wiseman, G.J. Milburn, Quantum error correction for continuously detected errors, Phys. Rev. A 67 (2003) 052310.
[93] M.B. Plenio, P.L. Knight, The quantum-jump approach to dissipative dynamics in quantum optics, Rev. Mod. Phys. (1998) 101–144.
[94] K. Jacobs, D.A. Steck, A straightforward introduction to continuous quantum measurement, Contemp. Phys. 47 (2006) 279–303.
[95] K. Mølmer, Y. Castin, J. Dalibard, Monte Carlo wave-function method in quantum optics, J. Opt. Soc. Amer. B 10 (1993) 524–538.
[96] N. Gisin, I.C. Percival, The quantum-state diffusion model applied to open systems, J. Phys. A: Math. Gen. 25 (1992) 5677–5691.
[97] I.C. Percival, Quantum State Diffusion, Cambridge University Press, Cambridge, 1998.
[98] C.W. Gardiner, A.S. Parskins, P. Zoller, Wave-function quantum stochastic differential equations and quantum-jump simulation methods, Phys. Rev. A 46 (1992) 4363–4381.
[99] U. Leonhardt, Measuring the Quantum State of Light, Cambridge University Press, Cambridge, 2005.
[100] H.M. Wiseman, G.J. Milburn, Interpretation of quantum jump and diffusion processes illustrated on the Bloch sphere, Phys. Rev. A 47 (1993) 1652–1666.
[101] P. Warszawski, H.H. Wiseman, Quantum trajectories for realistic photodetection: I. General formalism, J. Opt. B 5 (2003) 1–14.
[102] P. Warszawski, H.H. Wiseman, Quantum trajectories for realistic photodetection: II. Application and analysis, J. Opt. B 5 (2003) 15–28.
[103] H.M. Wiseman, L. Diósi, Complete parameterization, and invariance, of diffusive quantum trajectories for Markovian open systems, Chem. Phys. 268 (2001) 91–104.
[104] Y. Aharonov, D.Z. Albert, L. Vaidman, How the result of a measurement of a component of the spin of a spin-1/2 particle can turn out to be 100, Phys. Rev. Lett. 60 (1988) 1351–1354.
[105] Y. Aharonov, L. Vaidman, Properties of a quantum system during the time interval between two measurements, Phys. Rev. A 41 (1990) 11–20.
[106] A.G. Kofman, S. Ashhab, F. Nori, Noperturbative theory of weak pre- and post-selected measurements, Phys. Rep. 520 (2012) 43–133.
[107] A.J. Scott, G.J. Milburn, Quantum nonlinear dynamics of continuously measured systems, Phys. Rev. A 63 (2001) 042101.
[108] J. Gough, A. Sobolev, Continuous measurement of canonical observables and limit stochastic Schrodinger equations, Phys. Rev. A 69 (2004) 032107.
[109] U. Leonhardt, H. Paul, Phase measurement and Q function, Phys. Rev. A 47 (1993) 2460(R).
[110] L. Bouten, R. van Handel, M.R. James, An introduction to quantum filtering, SIAM J. Control Optim. 46 (2007) 2199–2241.
[111] A.C. Doherty, S. Habib, K. Jacobs, H. Mabuchi, S.M. Tan, Quantum feedback control and classical control theory, Phys. Rev. A 62 (2000) 012105.
[112] D.A. Steck, K. Jacobs, H. Mabuchi, T. Bhattacharya, S. Habib, Quantum feedback control of atomic motion in an optical cavity, Phys. Rev. Lett. 92 (2004) 223004.
[113] D.A. Steck, K. Jacobs, H. Mabuchi, S. Habib, T. Bhattacharya, Feedback cooling of atomic motion in cavity QED, Phys. Rev. A 74 (2006) 012322.
[114] K. Jacobs, J. Finn, S. Vinjanampathy, Real-time feedback control of a mesoscopic superposition, Phys. Rev. A 83 (2011) 041801.
[115] J. Wang, H.M. Wiseman, Feedback-stabilization of an arbitary pure state of a two-level atom, Phys. Rev. A 64 (2001) 063810.
[116] H.F. Hofmann, O. Hess, G. Mahler, Quantum control by compensation of quantum fluctuations, Opt. Exp. 2 (1998) 339–346.
[117] H.F. Hofmann, G. Mahler, O. Hess, Quantum control of atomic systems by homodyne detection and feedback, Phys. Rev. A 57 (1998) 4877–4888.
[118] J. Wang, H.M. Wiseman, G.J. Milburn, Dynamical creation of entanglement by homodyne-mediated feedback, Phys. Rev. A 71 (2005) 042309.
[119] J.-G. Li, J. Zou, B. Shao, J.-F. Cai, Steady atomic entanglement with different quantum feedbacks, Phys. Rev. A 77 (2008) 012339.
[120] N. Yamamoto, Parametrization of the feedback Hamiltonian realizing a pure steady state, Phys. Rev. A 72 (2005) 024104.
[121] S. Mancini, J. Wang, Towards feedback control of entanglement, Eur. Phys. J. D 32 (2005) 257–260.
[122] Y. Li, B. Luo, H. Guo, Entanglement and quantum discord dynamics of two atoms under practical feedback control, Phys. Rev. A 84 (2011) 012316.
[123] A.R.R. Carvalho, M. Busse, O. Brodier, C. Viviescas, A. Buchleitner, Optimal dynamical characterization of entanglement, Phys. Rev. Lett. 98 (2007) 190501.
[124] C. Viviescas, I. Guevara, A.R.R. Carvalho, M. Busse, A. Buchleitner, Entanglement dynamics in open two-qubit systems via diffusive quantum trajectories, Phys. Rev. Lett. 105 (2010) 210502.
[125] A.R.R. Carvalho, J.J. Hope, Stabilizing entanglement by quantum-jump-based feedback, Phys. Rev. A 76 (2007) 010301(R).
[126] A.R.R. Carvalho, A.J.S. Reid, J.J. Hope, Controlling entanglement by direct quantum feedback, Phys. Rev. A 78 (2008) 012334.
[127] S.C. Hou, X.L. Huang, X.X. Yi, Suppressing decoherence and improving entanglement by quantum-jump-based feedback control in two-level systems, Phys. Rev. A 82 (2010) 012336.
[128] R.N. Stevenson, A.R.R. Carvalho, J.J. Hope, Production of entanglement in Raman three-level systems using feedback, Eur. Phys. J. D 61 (2011) 523–529.
[129] L.C. Wang, J. Shen, X.X. Yi, Effect of feedback control on the entanglement evolution, Eur. Phys. J. D 56 (2010) 435–440.
[130] D. Xue, J. Zou, J.-G. Li, W.-Y. Chen, B. Shao, Controlling entanglement between two separated atoms by quantum-jump-based feedback, J. Phys. B: At. Mol. Opt. Phys. 43 (2010) 045503.
[131] J. Song, Y. Xia, X.-D. Sun, Noise-induced quantum correlation via quantum feedback control, J. Opt. Soc. Amer. B 29 (2012).
[132] P. Tombesi, D. Vitali, Macroscopic coherence via quantum feedback, Phys. Rev. A 51 (1995) 4913–4917.
[133] P. Goetsch, P. Tombesi, D. Vitali, Effect of feedback on the decoherence of a Schrodinger-cat state: A quantum trajectory description, Phys. Rev. A 54 (1996) 4519–4527.
[134] D. Vitali, P. Tombesi, G.J. Milburn, Controlling the decoherence of a 'meter' via stroboscopic feedback, Phys. Rev. Lett. 79 (1997) 2442–2445.
[135] D. Vitali, P. Tombesi, G.J. Milburn, Quantum-state protection in cavities, Phys. Rev. A 57 (1998).
[136] M. Fortunato, J.M. Raimond, P. Tombesi, D. Vitali, Autofeedback scheme for preservation of macroscopic coherence in microwave cavities, Phys. Rev. A 60 (1999) 1687–1697.
[137] H.M. Wiseman, G.J. Milburn, Squeezing via feedback, Phys. Rev. A 49 (1994) 1350–1366.
[138] H.M. Wiseman, G.J. Milburn, Reduction in laser-intensity fluctuations by a feedback-controlled output mirror, Phys. Rev. A 46 (1992) 2853–2858.
[139] A. Liebman, G.J. Milburn, Quantum-noise reduction in a driven cavity with feedback, Phys. Rev. A 47 (1993) 634–638.
[140] P. Tombesi, D. Vitali, Physical realization of an environment with squeezed quantum fluctuations via quantum-nondemolition-mediated feedback, Phys. Rev. A 50 (1994).

[141] H.M. Wiseman, M.S. Taubman, H.-A. Bachor, Feedback-enhanced squeezing in second-harmonic generation, 51 (1995) 3227–3233.
[142] H.M. Wiseman, In-loop squeezing is like real squeezing to an in-loop atom, Phys. Rev. Lett. 81 (1998) 3840–3843.
[143] R. Ruskov, K. Schwab, A.N. Korotkov, Squeezing of a nanomechanical resonator by quantum nondemolition measurement and feedback, Phys. Rev. B 71 (2005) 235407.
[144] A. Vinante, P. Falferi, Feedback-enhanced parametric squeezing of mechanical motion, Phys. Rev. Lett. 111 (2013) 207203.
[145] L.K. Thomsen, S. Mancini, H.M. Wiseman, Spin squeezing via quantum feedback, Phys. Rev. A 65 (2002) 061801(R).
[146] J.K. Stockton, R. van Handel, H. Mabuchi, Deterministic Dicke-state preparation with continuous measurement and control, Phys. Rev. A 70 (2004) 022106.
[147] J. Zhang, Y.X. Liu, R.B. Wu, C.W. Li, T.J. Tarn, Transition from weak to strong measurements by nonlinear quantum feedback control, Phys. Rev. A 82 (2010) 022101.
[148] V. Giovannetti, P. Tombesi, D. Vitali, Non-Markovian quantum feedback from homodyne measurements: The effect of a nonzero feedback delay time, Phys. Rev. A 60 (1999).
[149] K. Nishio, K. Kashima, J. Imura, Effects of time delay in feedback control of linear quantum systems, Phys. Rev. A 79 (2009) 062105.
[150] C. Emary, Delayed feedback control in quantum transport, Phil. Trans. R. Soc. A 371 (2013) 1999.
[151] M. Sarovar, H.-S. Goan, T.P. Spiller, G.J. Milburn, High-fidelity measurement and quantum feedback control in circuit QED, Phys. Rev. A 72 (2005) 062327.
[152] Z. Liu, L.L. Kuang, K. Hu, L.T. Xu, S.H. Wei, L.Z. Guo, X.Q. Li, Deterministic creation and stabilization of entanglement in circuit QED by homodyne-mediated feedback control, Phys. Rev. A 82 (2010) 032335.
[153] W. Feng, P.Y. Wang, X.M. Ding, L.T. Xu, X.Q. Li, Generating and stabilizing the Greenberger-Horne-Zeilinger state in circuit QED: Joint measurement, Zeno effect, and feedback, Phys. Rev. A 83 (2011) 042313.
[154] T.A. Wheatley, D.W. Berry, H. Yonezawa, D. Nakane, H. Arao, D.T. Pope, T.C. Ralph, H.M. Wiseman, A. Furusawa, E.H. Huntington, Adaptive optical estimation using time-symmetric quantum smoothing, Phys. Rev. Lett. 104 (2010) 093601.
[155] H.M. Wiseman, S. Mancini, J. Wang, Bayesian feedback versus Markovian feedback in a two-level atom, Phys. Rev. A 66 (2002) 013807.
[156] H.M. Wiseman, A.C. Doherty, Optimal unravellings for feedback control in linear quantum systems, Phys. Rev. Lett. 94 (2005) 070405.
[157] N. Yamamoto, Robust oberver for uncertain linear quantum systems, Phys. Rev. A 74 (2006) 032107.
[158] N. Yamamoto, Relation between fundamental estimation limit and stability in linear quantum systems with imperfect measurement, Phys. Rev. A 76 (2007) 034102.
[159] A. Chia, H.M. Wiseman, Quantum theory of multiple-inputmultiple-output Markovian feedback with diffusive measurements, Phys. Rev. A 84 (2011) 012120.
[160] A. Chia, H.M. Wiseman, Complete parametrizations of diffusive quantum monitorings, Phys. Rev. A 84 (2011) 012119.
[161] P. Goetsch, R. Graham, F. Haake, Schrodinger cat states and single runs for the damped harmonic oscillator, Phys. Rev. A 51 (1995) 136–142.
[162] H.M. Wiseman, L.K. Thomsen, Reducing the linewidth of an atom laser by feedback, Phys. Rev. Lett. 86 (2001) 1143–1147.
[163] L.K. Thomsen, H.M. Wiseman, Atom-laser coherence and its control via feedback, Phys. Rev. A 65 (2002) 063607.
[164] M. Sarovar, C. Ahn, K. Jacobs, G.J. Milburn, Practical scheme for error control using feedback, Phys. Rev. A 69 (2004) 052324.
[165] B.A. Chase, A.J. Landahl, J.M. Geremia, Efficient feedback controllers for continuous-time quantum error correction, Phys. Rev. A 77 (2008) 032304.
[166] H. Mabuchi, Continuous quantum error correction as classical hybrid control, New J. Phys. 11 (2009) 105044.
[167] K. Keane, A.N. Korotkov, Simplified quantum error detection and correlation for superconducting qubits, Phys. Rev. A 86 (2012) 012333.
[168] S.S. Szigeti, A.R.R. Carvalho, J.G. Morley, M.R. Hush, Ignorance is bliss: general and robust cancellation of decoherence via no-knowledge quantum feedback, Phys. Rev. Lett. 113 (2014) 020407.
[169] M.J. Biercuk, H. Uys, A.P. VanDevender, N. Shiga, W.M. Itano, J.J. Bollinger, Optimized dynamical decoupling in a model quantum memory, Nature 458 (2009) 996–1000.
[170] L. Viola, E. Knill, S. Lloyd, Dynamical decoupling of open quantum systems, Phys. Rev. Lett. 82 (1999) 2417–2421.
[171] P. Zanardi, Symmetrizing evolutions, Phys. Lett. A 258 (1999) 77–82.
[172] T. Green, H. Uys, M.J. Biercuk, High-order noise filtering in nontrivial quantum logic gates, Phys. Rev. Lett. 109 (2012) 020501.
[173] F. Ticozzi, L. Viola, Single-bit feedback and quantum-dynamical decoupling, Phys. Rev. A 74 (2006) 052328.
[174] J. Zhang, R.-B. Wu, C.-W. Li, T.-J. Tarn, Protecting coherence and entanglement by quantum feedback controls, IEEE Trans. Automat. Control 55 (2010) 619–633.
[175] N. Ganesan, T.-J. Tarn, Decoherence control in open quantum systems via classical feedback, Phys. Rev. A 75 (2007) 032323.
[176] A. Hopkins, K. Jacobs, S. Habib, K. Schwab, Feedback cooling of a nanomechanical resonator, Phys. Rev. B 68 (2003) 235328.
[177] J. Zhang, Y.-X. Liu, F. Nori, Cooling and squeezing the fluctuations of a nanomechanical beam by indirect quantum feedback control, Phys. Rev. A 79 (2009) 052102.
[178] M.J. Woolley, A.C. Doherty, G.J. Milburn, Continuous quantum nondemolition measurement of Fock states of a nanoresonator using feedback-controlled circuit QED, Phys. Rev. B 82 (2010) 094511.
[179] R. Ruskov, A.N. Korokov, Quantum feedback control of a solid-state qubit, Phys. Rev. B 6 (2002) 041401(R).
[180] A.N. Korotkov, Quantum feedback of a double-dot qubit, Microelectron. J. 36 (2005) 253–255.
[181] A.N. Korotkov, Simple quantum feedback of a solid-state qubit, Phys. Rev. B 71 (2005) 201305(R).
[182] Q. Zhang, R. Ruskov, A.N. Korotkov, Continuous quantum feedback of coherent oscillations in a solid-state qubit, Phys. Rev. B 72 (2005) 245322.
[183] A.N. Jordan, A.N. Korotkov, Qubit feedback and control with kicked quantum nondemolition measurements: a quantum Bayesian analysis, Phys. Rev. B 74 (2006) 085307.
[184] A.N. Korotkov, Selective quantum evolution of a qubit state due to continuous measurement, Phys. Rev. B 63 (2001) 115403.
[185] A.N. Korotkov, Continuous quantum measurement of a double dot, Phys. Rev. B 60 (1999) 5737–5742.
[186] W. Cui, N. Lambert, Y. Ota, X.-Y.L., Z.-L. Xiang, J.Q. You, F. Nori, Confidence and backaction in the quantum filter equation, Phys. Rev. A 86 (2012) 052320.
[187] H.-S. Goan, G.J. Milburn, H.M. Wiseman, H.B. Sun, Continuous quantum measurement of two coupled quantum dots using a point contact: a quantum trajectory approach, Phys. Rev. B 63 (2001) 125326.
[188] N.P. Oxtoby, P. Warszawski, H.M. Wiseman, H.-B. Sun, R.E.S. Polkinghorne, Quantum trajectories for the realistic measurement of a solid-state charge qubit, Phys. Rev. B 71 (2005) 165317.
[189] N.P. Oxtoby, H.M. Wiseman, H.-B. Sun, Sensitivity and back action in charge qubit measurements by a strongly coupled single-electron transistor, Phys. Rev. B 74 (2006) 045328.
[190] J.S. Jin, X.Q. Li, Y.J. Yan, Quantum coherence control of solid-state charge qubit by means of a suboptimal feedback algorithm, Phys. Rev. B 73 (2006) 233302.
[191] W. Cui, F. Nori, Feedback control of Rabi oscillations in circuit QED, Phys. Rev. A 88 (2013) 063823.
[192] R.D. Wilson, A.M. Zagoskin, S. Savel'ev, M.J. Everitt, F. Nori, Feedback-controlled adiabatic quantum computation, Phys. Rev. A 86 (2012) 052306.
[193] D. Riste, C.C. Bultink, K.W. Lehnert, L. DiCarlo, Feedback control of a solid-state qubit using high-fidelity project measurement, Phys. Rev. Lett. 109 (2012) 240502.
[194] R. Vijay, C. Macklin, D.H. Slichter, S.J. Weber, K.W. Murch, R. Naik, A.N. Korotkov, I. Siddiqi, Stabilizing Rabi oscillations in a superconducting qubit using quantum feedback, Nature 490 (2012) 77–80.
[195] P. Campagne-Ibarcq, E. Flurin, N. Roch, D. Darson, P. Morfin, M. Mirrahimi, M.H. Devoret, F. Mallet, B. Huard, Persistent control of a superconducting qubit by stroboscopic measurement feedback, Phys. Rev. X 3 (2013) 021008.
[196] S. Gustavsson, M. Studer, R. Leturcq, T. Ihn, K. Ensslin, D.C. Driscoll, A.C. Gossard, Frequency-selective single-photon detection using a double quantum dot, Phys. Rev. Lett. 99 (2007) 206804.

[197] S.-H. Ouyang, C.-H. Lam, J.Q. You, Backaction of a charge detector on a double quantum dot, Phys. Rev. B 81 (2010) 075301.
[198] Z.-Z. Li, C.-H. Lam, T. Yu, J.Q. You, Detector-induced backaction on the counting statistics of a double quantum dot, Sci. Rep. 3 (2013) 3026.
[199] R. van Handel, J.K. Stochton, H. Mabuchi, Feedback control of quantum state reduction, IEEE Trans. Automat. Control 50 (2005) 768–780.
[200] C. Altafini, Feedback stabilization of isospectral control systems on complex flag manifolds: application to quantum ensembles, IEEE Trans. Automat. Control 52 (2007) 2019–2028.
[201] R. van Handel, J.K. Stockton, H. Mabuchi, Modelling and feedback control design for quantum state preparation, J. Opt. B: Quantum Semiclass. Opt 7 (2005) S179–S197.
[202] B. Qi, H. Pan, L. Guo, Further results on stabilizing control of quantum systems, IEEE Trans. Automat. Control 58 (2013) 1349–1354.
[203] M. Mirrahimi, R. van Handel, Stabilizing feedback controls for quantum systems, SIAM J. Control Optim. 46 (2007) 445–467.
[204] W.P. Smith, J.E. Reiner, L.A. Orozco, S. Kuhr, H.M. Wiseman, Capture and release of a conditional state of a cavity QED system by quantum feedback, Phys. Rev. Lett. 89 (2002) 133601.
[205] J.E. Reiner, H.M. Wiseman, H. Mabuchi, Quantum jumps between dressed states: A proposed cavity-QED test using feedback, Phys. Rev. A 67 (2003) 042106.
[206] J.E. Reiner, W.P. Smith, L.A. Orozco, H.M. Wiseman, J. Gambetta, Quantum feedback in a weakly driven cavity QED system, Phys. Rev. A 70 (2004) 023819.
[207] R.I. Karasik, H.M. Wiseman, How many bits does it take to track an open quantum system, Phys. Rev. Lett. 106 (2011) 020406.
[208] R.I. Karasik, H.M. Wiseman, Tracking an open quantum system using a finite state machine: stability analysis, Phys. Rev. A 84 (2011) 052120.
[209] J. Ma, X. Wang, C.P. Sun, F. Nori, Quantum spin squeezing, Phys. Rep. 509 (2011) 89.
[210] F. Xue, Y.X. Liu, C.P. Sun, F. Nori, Two-mode squeezed states and entangled states of two mechanical resonators, Phys. Rev. B 76 (2007) 064305.
[211] A.M. Zagoskin, E. Il'ichev, M.W. McCutcheon, J. Young, F. Nori, Controlled generation of squeezed states of microwave radiation in a superconducting resonant circuit, Phys. Rev. Lett. 101 (2008) 253602.
[212] P.D. Nation, J.R. Johansson, M.P. Blencowe, F. Nori, Stimulating uncertainty: amplifying the quantum vacuum with superconducting circuits, Rev. Modern Phys. 84 (2012) 1–24.
[213] V.B. Braginsky, Y.I. Vorontsov, K.S. Thorne, Quantum nondemolition measurements, Science 209 (1980) 547–557.
[214] A.A. Clerk, F. Marquardt, K. Jacobs, Back-action evasion and squeezing of a mechanical resonator using a cavity detector, New J. Phys. 10 (2008) 095010.
[215] A. Szorkovszky, A.C. Doherty, G.I. Harris, W.P. Bowen, Mechanical squeezing via parametric amplification and weak measurement, Phys. Rev. Lett. 107 (2011) 213603.
[216] A. Szorkovszky, A.A. Clerk, A.C. Doherty, W.P. Bowen, Detuned mechanical parametric amplification as a quantum non-demolition measurement, New J. Phys. 16 (2014) 043023.
[217] A. Szorkovszky, G.A. Brawley, A.C. Doherty, W.P. Bowen, Strong thermomechanical squeezing via weak measurement, Phys. Rev. Lett. 110 (2013) 184301.
[218] A. Pontin, M. Bonaldi, A. Borrielli, F.S. Cataliotti, F. Marino, G.A. Prodi, E. Serra, F. Marin, Squeezing a thermal mechanical oscillator by stabilized parametric effect on the optical spring, Phys. Rev. Lett. 112 (2014) 023601.
[219] I.D. Leroux, M.H. Schleier-Smith, V. Vuletić, Implementation of cavity squeezing of a collective atomic spin, Phys. Rev. Lett. 104 (2010) 073602.
[220] M.H. Schleier-Smith, I.D. Leroux, V. Vuletić, States of an ensemble of two-Level atoms with reduced quantum uncertainty, Phys. Rev. Lett. 104 (2010) 073604.
[221] H. Zhang, R. McConnell, S. Ćuk, Q. Lin, M.H. Schleier-Smith, I.D. Leroux, V. Vuletić, Collective state measurement of mesoscopic ensembles with single-atom resolution, Phys. Rev. Lett. 109 (2012) 133603.
[222] K. Xia, J. Evers, Ground-state cooling of a nanomechanical resonator coupled to two interacting flux qubits, Phys. Rev. B 82 (2010) 184532.
[223] K. Xia, J. Evers, Ground state cooling of a nanomechanical resonator in the nonresolved regime via quantum interference, Phys. Rev. Lett. 103 (2009) 227203.
[224] F. Xue, Y.D. Wang, Y.X. Liu, F. Nori, Cooling a micromechanical beam by coupling it to a transmission line, Phys. Rev. B 76 (2007) 205302.
[225] A. Kubanek, M. Koch, C. Sames, A. Ourjoumtsev, P.W.H. Pinkse, K. Murr, G. Rempe, Photon-by-photon feedback control of a single-atom trajectory, Nature 462 (2009) 898–901.
[226] T. Fischer, P. Maunz, P.W.H. Pinkse, T. Puppe, G. Rempe, Feedback on the motion of a single atom in an optical cavity, Phys. Rev. Lett. 88 (2002) 163002.
[227] O. Arcizet, P.F. Cohadon, T. Briant, M. Pinard, A. Heidmann, Radiation-pressure cooling and optomechanical instability of a micromirror, Nature 444 (2006) 71–74.
[228] S. Gigan, H.R. Bohm, M. Paternostro, F. Blaser, G. Langer, J.B. Hertzberg, K.C. Schwab, D.Bauerle, M. Aspelmeyer, A. Zeilinger, Self-cooling of a micromirror by radiation pressure, Nature 444 (2006) 67–70.
[229] T. Corbitt, C. Wipf, T. Bodiya, D. Ottaway, D. Sigg, N. Smith, S. Whitcomb, N. Mavalvala, Optical dilution and feedback cooling of a gram-scale oscillator to 6.9 mK, Phys. Rev. Lett. 99 (2007) 160801.
[230] P.F. Cohadon, A. Heidmann, M. Pinard, Cooling of a mirror by radiation pressure, Phys. Rev. Lett. 83 (1999) 3174–3177.
[231] O. Arcizet, P.F. Cohadon, T. Briant, M. Pinard, A. Heidmann, J.M. Mackowski, C. Michel, L. Pinard, O. Francais, L. Rousseau, High-sensitivity optical monitoring of a micromechanical resonator with a quantum-limited optomechanical sensor, Phys. Rev. Lett. 97 (2006) 133601.
[232] D. Kleckner, D. Bouwmeester, Sub-Kelvin optical cooling of a micromechanical resonator, Nature 444 (2006) 75–78.
[233] J.D. Thompson, B.M. Zwickl, A.M. Jayich, F. Marquardt, S.M. Girvin, J.G.E. Harris, Strong dispersive coupling of a high-finesse cavity to a micromechanical membrane, Nature 452 (2008) 72–75.
[234] A. Schliesser, R. Rivière, G. Anetsberger, O. Arcizet, T.J. Kippenberg, Resolved-sideband cooling of a micromechanical oscillator, Nat. Phys. 5 (2008) 415–419.
[235] S. Gröblacher, J.B. Hertzberg, M.R. Vanner, G.D. Cole, S. Gigan, K.C. Schwab, M. Aspelmeyer, Demonstration of an ultracold micro-optomechanical oscillator in a cryogenic cavity, Nat. Phys. 5 (2009) 485–488.
[236] A. Schliesser, O. Arcizet, R. Rivière, G. Anetsberger, T.J. Kippenberg, Resolved-sideband cooling and position measurement of a micromechanical oscillator close to the Heisenberg uncertainty limit, Nat. Phys. 5 (2009) 509–514.
[237] S. Gröblacher, K. Hammerer, M.R. Vanner, M. Aspelmeyer, Observation of strong coupling between a micromechanical resonator and an optical cavity field, Nature 460 (2009) 724–727.
[238] G. Anetsberger, O. Arcizet, Q.P. Unterreithmeier, R. Rivière, A. Schliesser, E.M. Weig, J.P. Kotthaus, T.J. Kippenberg, Near-field cavity optomechanics with nanomechanical oscillators, Nat. Phys. 5 (2009) 909–914.
[239] M. Eichenfield, R. Camacho, J. Chan, K.J. Vahala, O. Painter, A picogram- and nanometre-scale photonic-crystal optomechanical cavity, Nature 459 (2009) 550–555.
[240] M. Eichenfield, J. Chan, R.M. Camacho, K.J. Vahala, O. Painter, Optomechanical crystals, Nature 462 (2009) 78–82.
[241] J.D. Teufel, D. Li, M.S. Allman, K. Cicak, A.J. Sirois, J.D. Whittaker, R.W. Simmonds, Circuit cavity electromechanics in the strong-coupling regime, Nature 471 (2011) 204–208.
[242] J.D. Teufel, T. Donner, D. Li, J.W. Harlow, M.S. Allman, K. Cicak, A.J. Sirois, J.D. Whittaker, K.W. Lehnert, R.W. Simmonds, Sideband cooling of micromechanical motion to the quantum ground state, Nature 475 (2011) 359–363.
[243] J. Chan, T.P.M. Alegre, A.H. Safavi-Naeini, J.T. Hill, A. Krause, S. Groeblacher, M. Aspelmeyer, O. Painter, Laser cooling of a nanomechanical oscillator into its quantum ground state, Nature 478 (2011) 89–92.
[244] S.G. Hofer, D.V. Vasilyev, M. Aspelmeyer, K. Hammerer, Time-continuous Bell measurements, Phys. Rev. Lett. 111 (2013) 170404.
[245] P. Bushev, D. Rotter, A. Wilson, F. Dubin, C. Becher, J. Eschner, R. Blatt, V. Steixner, P. Rabl, P. Zoller, Feedback cooling of a single trapped ion, Phys. Rev. Lett. 96 (2006) 043003.

[246] B. D'Urso, B. Odom, G. Gabrielse, Feedback cooling of a one-electron oscillator, Phys. Rev. Lett. 90 (2003) 043001.
[247] J. Gieseler, B. Deutsch, R. Quidant, L. Novotny, Subkelvin parametric feedback cooling of a laser-trapped nanoparticle, Phys. Rev. Lett. 109 (2012) 103603.
[248] N.V. Morrow, S.K. Dutta, G. Raithel, Feedback control of atomic motion in an optical lattice, Phys. Rev. Lett. 88 (2002) 093003.
[249] A.J. Berglund, H. Mabuchi, Feedback controller design for tracking a single fluorescent molecule, Appl. Phys. B 78 (2004) 653–659.
[250] A.J. Berglund, K. McHale, H. Mabuchi, Feedback localization of freely diffusing fluorescent particles near the optical shot-noise limit, Opt. Lett. 32 (2007) 145–147.
[251] A.J. Berglund, K. McHale, H. Mabuchi, Fluctuations in close-loop fluorescent particle tracking, Opt. Express 15 (2007) 7752–7773.
[252] K.W. Murch, K.L. Moore, S. Gupta, D.M. Stamper-Kurn, Observation of quantum-measurement backaction with an ultracold atomic gas, Nature Phys. 4 (2008) 561–564.
[253] T.P. Purdy, D.W.C. Brooks, T. Botter, N. Brahms, Z.-Y. Ma, D.M. Stamper-Kurn, Tunable cavity optomechanics with ultracold atoms, Phys. Rev. Lett. 105 (2010) 133602.
[254] S.S. Szigeti, M.R. Hush, A.R.R. Carvalho, J.J. Hope, Continuous measurement feedback control of a Bose–Einstein condensate using phase-contrast imaging, Phys. Rev. A 80 (2009) 013614.
[255] S.S. Szigeti, M.R. Hush, A.R.R. Carvalho, J.J. Hope, Feedback control of an interacting Bose–Einstein condensate using phase-contrast imaging, Phys. Rev. A 82 (2010) 043632.
[256] M.R. Hush, S.S. Szigeti, A.R.R. Carvalho, J.J. Hope, Controlling spontaneous-emission noise in measurement-based feedback cooling of a Bose–Einstein condensate, New J. Phys. 15 (2013) 113060.
[257] S.S. Szigeti, S.J. Adlong, M.R. Hush, A.R.R. Carvalho, J.J. Hope, Robustness of system-filter separation for the feedback control of a quantum harmonic oscillator undergoing continuous position measurement, Phys. Rev. A 87 (2013) 013626.
[258] M.Y. Vilensky, I.Sh. Averbukh, Y. Prior, Laser cooling in a feedback-controlled optical shaker, Phys. Rev. A 73 (2006) 063402.
[259] Y. Kishimoto, J.K. Koga, T. Tajima, D.L. Fisher, Phase space control and consequences for cooling by using a laser-undulator beat wave, Phys. Rev. E 55 (1997) 5948–5963.
[260] G.-C. Zhang, J.-L. Shen, J.-H. Dai, Cooling charged particles in a Paul trap by feedback control, Phys. Rev. A 60 (1999) 704–707.
[261] J.A. Dunningham, H.M. Wiseman, D.F. Walls, Manipulating the motion of a single atom in a standing wave via feedback, Phys. Rev. A 55 (1997) 1398–1411.
[262] S. Mancini, P. Tombesi, Atomic localization in the presence of optical feedback, Phys. Rev. A 56 (1997) 2466–2469.
[263] S. Mancini, D. Vitali, P. Tombesi, Stochastic phase-space localization for a single trapped particle, Phys. Rev. A 61 (2000) 053404.
[264] S.D. Wilson, A.R.R. Carvalho, J.J. Hope, M.R. James, Effects of measurement backaction in the stabilization of a Bose–Einstein condensate through feedback, Phys. Rev. A 76 (2007) 013610.
[265] G. Kießlich, G. Schaller, C. Emary, T. Brandes, Charge qubit purification by an electronic feedback loop, Phys. Rev. Lett. 107 (2011) 050501.
[266] G. Kießlich, C. Emary, G. Schaller, T. Brandes, Reverse quantum state engineering using electronic feedback loops, New J. Phys. 14 (2012) 123036.
[267] T. Brandes, Feedback control of quantum transport, Phys. Rev. Lett. 105 (2010) 060602.
[268] C. Poltl, C. Emary, T. Brandes, Feedback stabilization of pure states in quantum transport, Phys. Rev. B 84 (2011) 085302.
[269] S. Schneider, G.J. Milburn, Entanglement in the steady state of a collective-angular-momentum (Dicke) model, Phys. Rev. A 65 (2002) 042107.
[270] W.K. Wootters, Entanglement of formation of an arbitrary state of two qubits, Phys. Rev. Lett. 80 (1998) 2245–2248.
[271] A. Chia, A.S. Parkins, Entangled-state cycles of atomic collective-spin states, Phys. Rev. A 77 (2008) 033810.
[272] N. Yamamoto, K. Tsumura, S. Hara, Feedback control of quantum entanglement in a two-spin system, Automatica 43 (2007) 981–992.
[273] R.N. Stevenson, J.J. Hope, A.R.R. Carvalho, Engineering steady states using jump-based feedback for multipartite entanglement generation, Phys. Rev. A 84 (2011) 022332.
[274] J. Song, Y. Xia, X.-D. Sun, H.-S. Song, Dissipative preparation of multibody entanglement via quantum feedback control, Phys. Rev. A 86 (2012) 034303.
[275] D. Riste, M. Dukalski, C.A. Watson, G. de Lange, M.J. Tiggelman, Ya.M. Blanter, K.W. Lehnert, R.N. Schouten, L. DiCarlo, Deterministic entanglement of superconducting qubits by parity measurement and feedback, Nature 502 (2013) 350–354.
[276] S. Brakhane, W. Alt, T. Kampschulte, M. Martinez-Dorantes, R. Reima, Bayesian feedback control of a two-atom spin-state in an atom–cavity system, Phys. Rev. Lett. 109 (2012) 173601.
[277] S. Mancini, Markovian feedback to control continuous-variable entanglement, Phys. Rev. A 73 (2006) 010304(R).
[278] G.-X. Li, H.-T. Tan, S.-S. Ke, Quantum-feedback-induced enhancement of continuous-variable entanglement in a self-phase-locked type-II nondegenerate optical parameter oscillator, Phys. Rev. A 74 (2006) 012304.
[279] S.-S. Ke, G.-P. Cheng, L.-H. Zhang, G.-X. Li, Enhancement of entanglement in the nonlinear optical coupler by homodyne-mediated feedback, J. Phys. B: At. Mol. Opt. Phys. 40 (2007) 2827–2839.
[280] S. Mancini, H.M. Wiseman, Optimal control of entanglement via quantum feedback, Phys. Rev. A 75 (2007) 012330.
[281] M.G. Genoni, S. Mancini, A. Serafini, Optimal feedback control of linear quantum systems in the presence of thermal noises, Phys. Rev. A 87 (2013) 042333.
[282] A. Serafini, S. Mancini, Determination of maximal Gaussian entanglement achievable by feedback-controlled dynamics, Phys. Rev. Lett. 104 (2010) 220501.
[283] M. Yanagisawa, Quantum feedback control for deterministic entangled photon generation, Phys. Rev. Lett. 97 (2006) 190201.
[284] N. Yamamoto, H.I. Nurdin, M.R. James, I.R. Petersen, Avoiding entanglement sudden death via measurement feedback control in a quantum network, Phys. Rev. A 78 (2008) 042339.
[285] H.I. Nurdin, N. Yamamoto, Distributed entanglement generation between continuous-mode Gaussian fields with measurement-feedback enhancement, Phys. Rev. A 86 (2012) 034303.
[286] L. Vandenberghe, S. Boyd, Semidefinite programming, SIAM Rev. 38 (1996) 49–95.
[287] A.M. Brańczyk, P.E.M.F. Mendonca, A. Gilchrist, A.C. Doherty, S.D. Bartlett, Quantum control of a single qubit, Phys. Rev. A 75 (2007) 012329.
[288] G.G. Gillett, R.B. Dalton, B.P. Lanyon, M.P. Almeida, M. Barbieri, G.J. Pryde, J.L. O'Brien, K.J. Resch, S.D. Bartlett, A.G. White, Experimental feedback control of quantum systems using weak measurements, Phys. Rev. Lett. 104 (2010) 080503.
[289] B.L. Higgins, B.M. Booth, A.C. Doherty, S.D. Bartlett, H.M. Wiseman, G.J. Pryde, Mixed state discrimination using optimal control, Phys. Rev. Lett. 103 (2009) 220503.
[290] V. Giovannetti, S. Guha, S. Lloyd, L. Maccone, J.H. Shapiro, H.P. Yuen, Classical capacity of the lossy bosonic channel: the exact solution, Phys. Rev. Lett. 92 (2004) 27902.
[291] S. Guha, J.L. Habif, M. Takeoka, Approaching Helstrom limits to optical pulse-position demodulation using single photon detection and optical feedback, J. Modern Opt. 58 (2011) 257–265.
[292] K. Tsujino, D. Fukuda, G. Fujii, S. Inoue, M. Fujiwara, M. Takeoka, M. Sasaki, Phys. Rev. Lett. 106 (2011) 250503.
[293] J. Chen, J.L. Habif, Z. Dutton, R. Lazarus, S. Guha, Optical codeword demodulation with error rates below the standard quantum limit using a conditional nulling receive, Nature Photon. 6 (2012) 374–379.
[294] F.E. Becerra, J. Fan, G. Baumgartner, J. Goldhar, J.T. Kosloski, A. Migdall, Experimental demonstration of a receiver beating the standard quantum limit for multiple nonorthogonal state discrimination, Nature Photon. 7 (2013) 147–152.
[295] C.W. Helstrom, Quantum Detection and Estimation Theory, Mathematics in Science and Engineering, Academic Press, New York, 1976.
[296] B.C. Sanders, G.J. Milburn, Optimal quantum measurements for phase estimation, Phys. Rev. Lett. 75 (1995) 2944–2947.
[297] B.C. Sanders, G.J. Milburn, Z. Zhang, Optimal quantum measurements for phase-shift estimation in optical interferometry, J. Modern Opt. 44 (1997) 1309–1320.
[298] H.M. Wiseman, Adaptive phase measurement of optical modes: going beyond the marginal Q distribution, Phys. Rev. Lett. 75 (1995) 4587–4590.
[299] H.M. Wiseman, R.B. Killip, Adaptive single-shot phase measurements: A semiclassical approach, Phys. Rev. A 56 (1997) 944–957.

[300] H.M. Wiseman, R.B. Killip, Adaptive single-shot phase measurements: The full quantum theory, Phys. Rev. A 57 (1998) 2169–2185.
[301] T.C. Ralph, A.P. Lund, H.M. Wiseman, Adaptive phase measurements in linear optical quantum computation, J. Opt. B: Quantum Semiclass. Opt. 7 (2005) S245–S249.
[302] D.W. Berry, H.M. Wiseman, Phase measurements at the theoretical limit, Phys. Rev. A 63 (2000) 013813.
[303] D.T. Pope, H.M. Wiseman, N.K. Lanford, Adaptive phase estimation is more accurate than nonadaptive phase estimation for continuous beams of light, Phys. Rev. A 70 (2004) 043812.
[304] D.W. Berry, H.M. Wiseman, Optimal states and almost optimal adaptive measurements for quantum interferometry, Phys. Rev. Lett. 85 (2000) 5098–5101.
[305] D.W. Berry, H.M. Wiseman, J.K. Breslin, Optimal input states and feedback for interferometric phase estimation, Phys. Rev. A 63 (2001) 053804.
[306] D.W. Berry, H.M. Wiseman, Adaptive quantum measurements of a continuously varying phase, Phys. Rev. A 65 (2002) 043803.
[307] D.T. Pegg, S.M. Barnett, Unitary phase operator in quantum mechanics, Europhys. Lett. 6 (1988) 483–487.
[308] D.T. Pegg, S.M. Barnett, Phase properties of the quantized single-mode electromagnetic-field, Phys. Rev. A 39 (1989) 1665–1675.
[309] M. Tsang, Time-symmetric quantum theory of smoothing, Phys. Rev. Lett. 102 (2009) 250403.
[310] M. Tsang, Optimal waveform estimation for classical and quantum systems via time-symmetric smoothing, Phys. Rev. A (2009) 033840.
[311] M. Tsang, Optimal waveform estimation for classical and quantum systems via time-symmetric smoothing. II. Applications to atomic magnetometry and Hardy's paradox, Phys. Rev. A 81 (2010) 013824.
[312] M.A. Armen, J.K. Au, J.K. Stockton, A.C. Doherty, H. Mabuchi, Adaptive homodyne measurement of optical phase, Phys. Rev. Lett. 89 (2002) 133602.
[313] B.L. Higgins, D.W. Berry, S.D. Bartlett, H.M. Wiseman, G.J. Pryde, Entanglement-free Heisenberg-limited phase estimation, Nature 450 (2007) 393–396.
[314] J.P. Dowling, Quantum optical metrology–the lowdown on high-NooN states, Contemp. Phys. 49 (2008) 125.
[315] G.Y. Xiang, B.L. Higgins, D.W. Berry, H.M. Wiseman, G.J. Pryde, Entanglement-enhanced measurement of a completely unknown optical phase, Nature Photon. 5 (2011) 43–47.
[316] G.Y. Xiang, T.C. Ralph, A.P. Lund, N. Walk, G.J. Pryde, Heralded noiseless linear amplification and distillation of entanglement, Nature Photon. 4 (2010) 316–319.
[317] H. Yonezawa, D. Nakane, T.A. Wheatley, K. Iwasawa, S. Takeda, H. Arao, K. Ohki, K. Tsumura, D.W. Berry, T.C. Ralph, H.M. Wiseman, E.H. Huntington, A. Furusawa, Quantum-enhanced optical-phase tracking, Science 337 (2012) 1514–1517.
[318] R. Okamoto, M. Iefuji, S. Oyama, K. Yamagata, H. Imai, A. Fujiwara, S. Takeuchi, Experimental demonstration of adaptive quantum state estimation, Phys. Rev. Lett. 109 (2012) 130404.
[319] F. Verstraete, A.C. Doherty, H. Mabuchi, Sensitivity optimization in quantum parameter estimation, Phys. Rev. A 64 (2001) 032111.
[320] J. Gambetta, H.M. Wiseman, State and dynamical parameter estimation for open quantum systems, Phys. Rev. A 64 (2001) 042105.
[321] P. Warszawski, J. Gambetta, H.M. Wiseman, Dynamical parameter estimation using realistic photondetection, Phys. Rev. A 69 (2004) 042104.
[322] B.A. Chase, J.M. Geremia, Single-shot parameter estimation via continuous quantum measurement, Phys. Rev. A 79 (2009) 022314.
[323] J.F. Ralph, K. Jacobs, C.D. Hill, Frequency tracking and parameter estimation for robust quantum state estimation, Phys. Rev. A 84 (2011) 052119.
[324] J.K. Stockton, J.M. Geremia, A.C. Doherty, H. Mabuchi, Robust quantum parameter estimation: Coherent magnetometry with feedback, Phys. Rev. A 69 (2004) 032109.
[325] K. Jacobs, How to project qubits faster using quantum feedback, Phys. Rev. A 67 (2003) 030301(R).
[326] J. Combes, K. Jacobs, Rapid state reduction of quantum systems using feedback control, Phys. Rev. Lett. 96 (2006) 010504.
[327] H.M. Wiseman, J.F. Ralph, Reconsidering rapid qubit purification by feedback, New J. Phys. 8 (2006) 90.
[328] C. Hill, J. Ralph, Weak measurement and rapid state reduction in entangled bipartite quantum systems, New J. Phys. 9 (2007) 151.
[329] E.J. Griffith, C.D. Hill, J.F. Ralph, H.M. Wiseman, K. Jacobs, Rapid-state purification protocols for a Cooper pair box, Phys. Rev. B 7 (2007) 014511.
[330] C. Hill, J.F. Ralph, Weak measurement and control of entanglement generation, Phys. Rev. A 77 (2008) 014305.
[331] H.M. Wiseman, L. Bouten, Optimality of feedback control strategies for qubit purification, Quantum Inf. Process. 7 (2008) 71–83.
[332] J. Combes, H.M. Wiseman, K. Jacobs, Rapid measurement of quantum systems using feedback control, Phys. Rev. Lett. 100 (2008) 160503.
[333] J. Combes, H.M. Wiseman, A.J. Scott, Replacing quantum feedback with open-loop control and quantum filtering, Phys. Rev. A 80 (2010) 020301(R).
[334] J. Combes, H.M. Wiseman, K. Jacobs, A.J. O'Connor, Rapid purification of quantum systems by measuring in a feedback-controlled unbiased basis, Phys. Rev. A 82 (2010) 022307.
[335] J. Combes, H.M. Wiseman, Maximum information gain in weak or continuous measurements of qudits: complementarity is not enough, Phys. Rev. X 1 (2011) 011012.
[336] K. Maruyama, F. Nori, Entanglement purification without controlled-NOT gates by using the natural dynamics of spin chains, Phys. Rev. A 78 (2008) 022312.
[337] T. Tanamoto, K. Maruyama, Y.X. Liu, X. Hu, F. Nori, Efficient purification protocols using iSWAP gates in solid-state qubits, Phys. Rev. A 78 (2008) 062313.
[338] A. Pechen, N. Il'in, F. Shuang, H. Rabitz, Quantum control by von Neumann measurements, Phys. Rev. A 74 (2006) 052102.
[339] F. Shuang, M. Zhou, A. Pechen, R. Wu, O.M. Shir, H. Rabitz, Control of quantum dynamics by optimized measurements, Phys. Rev. A 78 (2008) 063422.
[340] S. Ashhab, J.Q. You, F. Nori, The information about the state of a qubit gained by a weakly coupled detector, New J. Phys. 11 (2009) 083017.
[341] S. Ashhab, J.Q. You, F. Nori, The information about the state of a charge qubit gained by a weakly coupled quantum point contact, Phys. Scr. T 137 (2009) 014005.
[342] S. Ashhab, J .Q. You, F. Nori, Weak and strong measurement of a qubit using a switching-based detector, Phys. Rev. A 79 (2009) 032317.
[343] S. Ashhab, F. Nori, Control-free control: manipulating a quantum system using only a limited set of measurements, Phys. Rev. A 82 (2010) 062103.
[344] H.M. Wiseman, Quantum control: Squinting at quantum systems, Nature 470 (2011) 178–179.
[345] M.S. Blok, C. Bonato, M.L. Markham, D.J. Twitchen, V.V. Dobrovitski, R. Hanson, Manipulating a qubit through the backaction of sequential partial measurements and real-time feedback, Nat. Phys. 10 (2014) 189–193.
[346] K. Jacobs, Feedback control using only quantum back-action, New J. Phys. 12 (2010) 043005.
[347] M. Yanagisawa, H. Kimura, Transfer function approach to quantum control-part I: dynamics of quantum feedback systems, IEEE Trans. Automat. Control 48 (2003) 2107.
[348] M. Yanagisawa, H. Kimura, Transfer function approach to quantum control-part II: control concepts and applications, IEEE Trans. Automat. Control 48 (2003) 2121.
[349] J.E. Gough, R. Gohm, M. Yanagisawa, Linear quantum feedback networks, Phys. Rev. A 78 (2008) 062104.
[350] J.E. Gough, M.R. James, H.I. Nurdin, Squeezing components in linear quantum feedback networks, Phys. Rev. A 81 (2010) 023804.
[351] G. Zhang, M.R. James, Direct and indirect couplings in coherent feedback control of linear quantum systems, IEEE Trans. Automat. Control 56 (2011) 1535–1550.
[352] G. Zhang, H.W.J. Lee, B. Huang, H. Zhang, Coherent feedback control of linear quantum optical systems via squeezing and phase shift, SIAM J. Control Optim. 50 (2012) 2130–2150.
[353] L. Diosi, Non-Markovian open quantum systems: Input–output fields, memory, and monitoring, Phys. Rev. A 85 (2012) 034101.
[354] J. Zhang, Y.-X. Liu, R.-B. Wu, K. Jacobs, F. Nori, Non-Markovian quantum input–output networks, Phys. Rev. A 87 (2013) 032117.
[355] S.-B. Xue, R.-B. Wu, W.-M. Zhang, J. Zhang, C.-W. Li, T.-J. Tarn, Decoherence suppression via non-Markovian coherent feedback control, Phys. Rev. A 86 (2012) 052304.
[356] H. Mabuchi, Coherent-feedback quantum control with a dynamical compensator, Phys. Rev. A 78 (2008) 032323.
[357] C. Emary, J.E. Gough, Coherent feedback control in quantum transport, Phys. Rev. B 90 (2014) 205436.
[358] J.E. Gough, S. Wildfeuer, Enhancement of field squeezing using coherent feedback, Phys. Rev. A 80 (2009) 042107.

[359] S. Iida, M. Yukawa, H. Yonezawa, N. Yamamoto, A. Furusawa, Experimental demonstration of coherent feedback control on optical field squeezing, IEEE Trans. Automat. Control 57 (2012) 2045–2050.
[360] J. Kerckhoff, H.I. Nurdin, D.S. Pavlichin, H. Mabuchi, Designing quantum memories with embedded control: photonic circuits for autonomous quantum error correction, Phys. Rev. Lett. 105 (2010) 040502.
[361] J. Kerckhoff, D.S. Pavlichin, H. Chalabi, H. Mabuchi, Design of nanophotonic circuits for autonomous subsystem quantum error correction, New J. Phys. 13 (2011) 055022.
[362] H. Mabuchi, Cavity-QED models of switches for attojoule-scale nanophotonic logic, Phys. Rev. A 80 (2009) 045802.
[363] J. Kerckhoff, L. Bouten, A. Silverfarb, H. Mabuchi, Physical model of continuous two-qubit parity measurement in a cavity-QED network, Phys. Rev. A 79 (2009) 024305.
[364] F. Marquardt, J.P. Chen, A.A. Clerk, S.M. Girvin, Quantum theory of cavity-assisted sideband cooling of mechanical motion, Phys. Rev. Lett. 99 (2007) 093902.
[365] I. Wilson-Rae, N. Nooshi, W. Zwerger, T.J. Kippenberg, Theory of ground state cooling of a mechanical oscillator using dynamical backaction, Phys. Rev. Lett. 99 (2007) 093901.
[366] L. Tian, Ground state cooling of a nanomechanical resonator via parametric linear coupling, Phys. Rev. B 79 (2009) 193407.
[367] N. Yang, J. Zhang, H. Wang, Y.X. Liu, R.B. Wu, L.Q. Liu, C.W. Li, F. Nori, Noise suppression of on-chip mechanical resonators by chaotic coherent feedback, Phys. Rev. A 92 (2015) 033812.
[368] X.T. Wang, S. Vinjanampathy, F.W. Strauch, K. Jacobs, Ultraefficient cooling of resonators: beating sideband cooling with quantum control, Phys. Rev. Lett. 107 (2011) 177204.
[369] J. Kerckhoff, R.W. Andrews, H.S. Ku, W.F. Kindel, K. Cicak, R.W. Simmonds, K.W. Lehnert, Tunable coupling to a mechanical oscillator circuit using a coherent feedback network, Phys. Rev. X 3 (2013) 021013.
[370] K. Jacobs, H. Nurdin, F.W. Strauch, M. James, Comparing resolved-sideband cooling and measurement-based feedback cooling on an equal footing: analytical results in the regime of ground-state cooling, Phys. Rev. A 91 (2015) 043812.
[371] M. Yanagisawa, Non-Gaussian state generation from linear elements via feedback, Phys. Rev. Lett. 103 (2009) 203601.
[372] M.F. Yanik, S. Fan, M. Soljacic, High-contrast all-optical bistable switching in photonic crystal microcavities, Appl. Phys. Lett. 83 (2003) 2739–2741.
[373] X. Yang, C. Husko, C.W. Wong, M. Yu, D.L. Kwong, Observation of femtojoule optical bistability involving Fano resonances in high-Q/Vm silicon photonic crystal nanocavities, Appl. Phys. Lett. 91 (2007) 051113.
[374] K. Nozaki, T. Tanabe, A. Shinya, S. Matsuo, T. Sato, H. Taniyama, M. Notomi, Sub-femtojoule all-optical switching using a photonic-crystal nanocavity, Nature Photon. 4 (2010).
[375] R. Kumar, L. Liu, G. Roelkens, E.-J. Geluk, T. de Vries, F. Karouta, P. Regreny, D. Van Thourhout, R. Baets, G. Morthier, 10-GHz all-optical gate based on a IIIcv/SOI microdisk, IEEE Photon. Technol. Lett. 22 (2010) 981–983.
[376] M. Armen, H. Mabuchi, Low-lying bifurcations in cavity quantum electrodynamics, Phys. Rev. A 73 (2006) 063801.
[377] M. Armen, A.E. Miller, H. Mabuchi, Spontaneous dressed-state polarization in the strong driving regime of cavity QED, Phys. Rev. Lett. 103 (2009) 173601.
[378] H. Mabuchi, Coherent-feedback control strategy to suppress spontaneous switching in ultralow power optical bistability, Appl. Phys. Lett. 98 (2011) 193109.
[379] Z. Zhou, C.J. Liu, Y.M. Fang, J. Zhou, R.T. Glasser, L.Q. Chen, J.T. Jing, W.P. Zhang, Optical logic gates using coherent feedback, Appl. Phys. Lett. 101 (2012) 191113.
[380] Z.H. Yan, X.J. Jia, C.D. Xie, K.C. Peng, Coherent feedback control of multipartite quantum entanglement for optical fields, Phys. Rev. A 84 (2011) 062304.
[381] P. van Loock, A. Furusawa, Detecting genuine multipartite continuous-variable entanglement, Phys. Rev. A 67 (2003) 052315.
[382] R.S. Judson, H. Rabitz, Teaching lasers to control molecules, Phys. Rev. Lett. 68 (1992) 1500–1503.
[383] R. Bartels, S. Backus, E. Zeek, L. Misoguti, G. Vdovin, I.P. Christov, M.M. Murnane, H.C. Kapteyn, Shaped-pulse optimization of coherent emission of high-harmonic soft X-rays, Nature 406 (2000) 164–166.
[384] H.A. Rabitz, M.M. Hsieh, C.M. Rosenthal, Quantum optimally controlled transition landscapes, Science 303 (2004) 1998–2001.
[385] C.H. Metzger, K. Karrai, Cavity cooling of a microlever, Nature 432 (2004) 1002–1005.
[386] S. De Liberato, N. Lambert, F. Nori, Quantum noise in photothermal cooling, Phys. Rev. A 83 (2011) 033809.
[387] A. Greilich, A. Shabaev, D.R. Yakovlev, Al.L. Efros, I.A. Yugova, D. Reuter, A.D. Wieck, M. Bayer, Nuclei-induced frequency focusing of electron-spin coherence, Nature 317 (2007) 1896–1899.
[388] S.G. Carter, A. Shavaev, S.E. Economou, T.A. Kennedy, A.S. Bracker, T.L. Reinecke, Directing nuclear spin flips in InAs quantum dots using detuned optical pulse trains, Phys. Rev. Lett. 102 (2009) 167403.
[389] X.D. Xu, W. Yao, B. Sun, D.G. Steel, A.S. Bracker, D. Gammon, L.J. Sham, Optically controlled locking of the nuclear field via coherent dark-state spectroscopy, Nature 459 (2009) 1105–1109.
[390] C. Latta, A. Hogele, Y. Zhao, A.N. Vamivakas, P. Maletinsky, M. Kroner, J. Dreiser, I. Carusotto, A. Badolato, D. Schuh, W. Wegscheider, M. Atature, A. Imamoglu, Confluence of resonant laser excitation and bidirectional quantum-dot nuclear-spin polarization, Nat. Phys. 5 (2009) 758–763.
[391] Ya. S. Greenberg, E. Il'ichev, F. Nori, Cooling a magnetic resonance force microscope via the dynamical back action of nuclear spins, Phys. Rev. B 80 (2009) 214423.
[392] T.D. Ladd, D. Press, K. De Greve, P.L. McMahon, B. Friess, C. Schneider, M. Kamp, S. Hofling, A. Forchel, Y. Yamamoto, Pulsed nuclear pumping and spin diffusion in a single charged quantum dot, Phys. Rev. Lett. 105 (2010) 107401.
[393] B. Sun, C.M.E. Chow, D.G. Steel, A.S. Bracker, D. Gammon, L.J. Sham, Persistent narrowing of nuclear-spin fluctuations in InAs quantum dots using laser excitation, Phys. Rev. Lett. 108 (2012) 187401.
[394] D.J. Reilly, J.M. Taylor, J.R. Petta, C.M. Marcus, M.P. Hanson, A.C. Gossard, Suppressing spin qubit dephasing by nuclear state preparation, Science 321 (2008) 817–821.
[395] I.T. Vink, K.C. Nowack, F.H.L. Koppens, J. Danon, Y.V. Nazarov, Locking electron spins into magnetic resonance by electron-nuclear feedback, Nat. Phys. 5 (2009) 764–768.
[396] H. Bluhm, S. Foletti, D. Mahalu, V. Umansky, A. Yacoby, Enhancing the coherence of a spin qubit by operating it as a feedback loop that controls its nuclear spin bath, Phys. Rev. Lett. 105 (2010) 216803.
[397] C. Barthel, J. Medford, H. Bluhm, A. Yacoby, C.M. Marcus, M.P. Hanson, A.C. Gossard, Relaxation and readout visibility of a singlet-triplet qubit in an Overhauser field gradient, Phys. Rev. B 85 (2012) 035306.
[398] W. Yao, Y. Luo, Feedback control of nuclear hyperfine fields in a double quantum dot, Europhys. Lett. 92 (2010) 17008.
[399] C.M. Caves, P.D. Drummond, Quantum limits on bosonic communication rates, Rev. Modern Phys. 66 (1994) 481.
[400] R. Okamoto, H.F. Hofmann, S. Takeuchi, K. Sasaki, Demonstration of an optical quantum controlled-NOT gate without path interference, Phys. Rev. Lett. 95 (2005) 210506.
[401] N. Kiesel, C. Schmid, U. Weber, R. Ursin, H. Weinfurter, Linear optics controlled-phase gate made simple, Phys. Rev. Lett. 95 (2005) 210505.
[402] N.K. Langford, T.J. Weinhold, R. Prevedel, K.J. Resch, A. Gilchrist, J.L. O'Brien, G.J. Pryde, A.G. White, Demonstration of a simple entangling optical gate and its use in Bell-state analysis, Phys. Rev. Lett. 95 (2005) 210504.
[403] M.A. Castellanos-Beltran, K.W. Lehnert, Widely tunable parametric amplifier based on a superconducting quantum interference device array resonator, Appl. Phys. Lett. 91 (2007) 083509.
[404] T. Yamamoto, K. Inomata, M. Watanabe, K. Matsuba, T. Miyazaki, W.D. Oliver, Y. Nakamura, J.S. Tsai, Flux-driven Josephson parametric amplifier, Appl. Phys. Lett. 93 (2008) 042510.
[405] N. Bergeal, R. Vijay, V.E. Manucharyan, I. Siddiqi, R.J. Schoelkopf, S.M. Girvin, M.H. Devoret, Analog information processing at the quantum limit with a Josephson ring modulator, Nat. Phys. 6 (2010) 296–302.

[406] S. Savelev, A.M. Zagoskin, A.L. Rakhmanov, A.N. Omelyanchouk, Z. Washington, F. Nori, Two-qubit parametric amplifier: Large amplification of weak signals, Phys. Rev. A 85 (2012) 013811.
[407] S.J. Weber, A. Chantasri, J. Dressel, A.N. Jordan, K.W. Murch, I. Siddiqi, Mapping the optimal route between two quantum states, Nature 511 (2014) 570–573.
[408] J.Q. You, X.D. Hu, S. Ashhab, F. Nori, Low-decoherence flux qubit, Phys. Rev. B 75 (2007) 140515.
[409] J. Koch, T.M. Yu, J. Gambetta, A.A. Houck, D.I. Schuster, J. Majer, A. Blais, M.H. Devoret, S.M. Girvin, R.J. Schoelkopf, Charge-insensitive qubit design derived from the Cooper pair box, Phys. Rev. A 76 (2007) 042319.
[410] C.M. Caves, Quantum limits on noise in linear amplifiers, Phys. Rev. D 26 (1982) 1817–1839.
[411] A.A. Clerk, M.H. Devoret, S.M. Girvin, F. Marquardt, R.J. Schoelkopf, Introduction to quantum noise, measurement, and amplification, Rev. Modern Phys. 82 (2010) 1155–1208.
[412] M.A. Castellanos-Beltran, K.D. Irwin, G.C. Hilton, L.R. Vale, K.W. Lehnert, Amplification and squeezing of quantum noise with a tunable Josephson metamaterial, Nat. Phys. 4 (2008) 928–931.
[413] S. Shankar, M. Hatridge, Z. Leghtas, K.M. Sliwa, A. Narla, U. Vool, S.M. Girvin, L. Frunzio, M. Mirrahimi, M.H. Devoret, Autonomously stabilized entanglement between two superconducting quantum bits, Nature 504 (2013) 419–422.
[414] K.W. Murch, U. Vool, D. Zhou, S.J. Weber, S.M. Girvin, I. Siddiqi, Cavity-assisted quantum bath engineering, Phys. Rev. Lett. 109 (2012) 183602.
[415] K. Geerlings, Z. Leghtas, I.M. Pop, S. Shankar, L. Frunzio, R.J. Schoelkopf, M. Mirrahimi, M.H. Devoret, Demonstrating a driven reset protocol for a superconducting qubit, Phys. Rev. Lett. 110 (2013) 120501.
[416] M. Poggio, C.L. Degen, H.J. Mamin, D. Rugar, Feedback Cooling of a Cantilever's Fundamental Mode below 5 mK, Phys. Rev. Lett. 99 (2007) 017201.
[417] E. Gavartin, P. Verlot, T.J. Kippenberg, A hybrid on-chip optomechanical transducer for ultrasensitive force measurements, Nature Nanotechnol. 7 (2012) 509–514.
[418] F. Monifi, J. Zhang, S.K. Ozdemir, B. Peng, Y.-X. Liu, F. Bo, F. Nori, L. Yang, Optomechanically induced stochastic resonance and chaos transfer between optical fields, Nature Photon. 10 (2016) 399–405.
[419] X.Y.L., Y. Wu, J.R. Johansson, H. Jing, J. Zhang, F. Nori, Squeezed optomechanics with phase-matched amplification and dissipation, Phys. Rev. Lett. 114 (2015) 093602.
[420] H. Jing, S.K. Ozdemir, Z. Geng, J. Zhang, X.Y.L., B. Peng, L. Yang, F. Nori, Optomechanically-Induced Transparency in parity-time-symmetric microresonators, Sci. Rep. 5 (2015) 9663.
[421] M. Poot, S. Etaki, H. Yamaguchi, H.S.J. van der Zant, Discrete-time quadrature feedback cooling of a radio-frequency mechanical resonator, Appl. Phys. Lett. 99 (2011) 013113.
[422] A. Vinante, M. Bonaldi, F. Marin, J.-P. Zendri, Dissipative feedback does not improve the optimal resolution of incoherent force detection, Nature Nanotechnol. 8 (2013) 470.
[423] G.I. Harris, D.L. McAuslan, T.M. Stace, A.C. Doherty, W.P. Bowen, Minimum requirements for feedback enhanced force sensing, Phys. Rev. Lett. 111 (2013) 103603.
[424] A. Pontin, M. Bonaldi, A. Borrielli, F.S. Cataliotti, F. Marino, G.A. Prodi, E. Serra, F. Marin, Detection of weak stochastic forces in a parametrically stabilized micro-optomechanical system, Phys. Rev. A 89 (2014) 023848.
[425] D.J. Wilson, V. Sudhir, N. Piro, R. Schilling, A. Ghadimi, T.J. Kippenberg, Measurement-based control of a mechanical resonator at its thermal decoherence rate, Nature 524 (2015) 325–329.
[426] V. Sudhir, D.J. Wilson, R. Schilling, H. Schütz, S.A. Fedorov, A.H. Ghadimi, A. Nunnenkamp, T.J. Kippenberg, Appearance and disappearance of quantum correlations in measurement-based feedback control of a mechanical oscillator, Phys. Rev. X 7 (2017) 011001.
[427] Y. Yamamoto, N. Imoto, S. Machida, Amplitude squeezing in a semiconductor laser using quantum nondemolition measurement and negative feedback, Phys. Rev. A 33 (1986) 3243–3261.
[428] H.A. Haus, Y. Yamamoto, Theory of feedback-generated squeezed states, Phys. Rev. A 34 (1986) 270–292.
[429] J.H. Shapiro, G. Saplakoglu, S.-T. Ho, P. Kumar, B.E.A. Saleh, M.C. Teich, Theory of light detection in the presence of feedback, J. Opt. Soc. Amer. B 4 (1987) 1604–1620.
[430] C. Sayrin, I. Dotsenko, X.X. Zhou, B. Peaudecerf, T. Rybarczyk, S. Gleyzes, P. Rouchon, M. Mirrahimi, H. Amini, M. Brune, J.-M. Raimond, S. Haroche, Real-time quantum feedback prepares and stabilizes photon number states, Nature 477 (2011) 73–77.
[431] X. Zhou, I. Dotsenko, B. Peaudecerf, T. Rybarczyk, C. Sayrin, S. Gleyzes, Field locked to a Fock state by quantum feedback with single photon corretions, Phys. Rev. Lett. 108 (2012) 243602.
[432] T. Vanderbruggen, R. Kohlhass, A. Bertoldi, S. Bernon, A. Aspect, A. Landragin, P. Bouyer, Feedback control of trapped coherent atomic ensembles, Phys. Rev. Lett. 110 (2013) 210503.
[433] R. Inoue, S.I.R. Tanada, R. Namiki, T. Sagawa, Y. Takahashi, Unconditional quantum-noise suppression via measurement-based quantum feedback, Phys. Rev. Lett. 110 (2013) 163602.
[434] X.T. Wang, S. Vinjanampathy, F.W. Strauch, K. Jacobs, Absolute dynamical limit to cooling weakly coupled quantum systems, Phys. Rev. Lett. 110 (2013) 157207.
[435] J. Prior, A.W. Chin, S.F. Huelga, M.B. Plenio, Efficient simulation of strong system-environment interactions, Phys. Rev. Lett. 105 (2010) 050404.
[436] A. Ishizaki, Y. Tanimura, Quantum dynamics of system strongly coupled to low-temperature colored noise bath: reduced hierarchy equations approach, J. Phys. Soc. Japan 74 (2005) 3131–3134.
[437] R. Bulla, N.-H. Tong, M. Vojta, Numerical renormalization group for bosonic systems and application to the subohmic spin-boson model, Phys. Rev. Lett. 91 (2003) 170601.
[438] M. Thorwart, P. Reimann, P. Jung, R.F. Fox, Quantum hysteresis and resonant tunneling in bistable systems, Chem. Phys. 235 (1998) 61–80.
[439] T. Albash, S. Boixo, D.A. Lidar, P. Zanardi, Quantum adiabatic Markovian master equations, New J. Phys. 14 (2012) 123016.
[440] J.Q. You, F. Nori, Superconducting circuits and quantum information, Phys. Today 58 (2005) 42–47.
[441] J.Q. You, F. Nori, Atomic physics and quantum optics using superconducting circuits, Nature 474 (2011) 589–597.
[442] Z.-L. Xiang, S. Ashhab, J.Q. You, F. Nori, Hybrid quantum circuits: Superconducting circuits interacting with other quantum systems, Rev. Modern Phys. 85 (2013) 623–653.
[443] K.J. Vahala, Optical microcavities, Nature 424 (2003) 839–846.
[444] T.J. Kippenberg, K.J. Vahala, Cavity optomechanics: back-action at the mesoscale, Science 321 (2008) 1172–1176.
[445] L. He, S.K. Ozdemir, L. Yang, Whispering gallery microcavity lasers, Laser Photonics Rev. 7 (2013) 60–82.
[446] B. Peng, S.K. Ozdemir, F.C. Lei, F. Monifi, M. Gianfreda, G.L. Long, S.H. Fan, F. Nori, C.M. Bender, L. Yang, Parity-time-symmetric whispering-gallery microcavities, Nat. Phys. 10 (2014) 394–398.
[447] H. Jing, S.K. Ozdemir, X.-Y.L., J. Zhang, L. Yang, F. Nori, PT-symmetric phonon laser, Phys. Rev. Lett. 113 (2014) 053604.
[448] Z.-P. Liu, J. Zhang, S.K. Ozdemir, B. Peng, H. Jing, X.-Y. Lü, C.-W. Li, L. Yang, F. Nori, Y.-X. Liu, Metrology with PT-symmetric cavities: enhanced sensitivity near the PT-phase transition, Phys. Rev. Lett. 117 (2016) 110802.
[449] K. Jacobs, I. Tittonen, H.M. Wiseman, S. Schiller, Quantum noise in the position measurement of a cavity mirror undergoing Brownian motion, Phys. Rev. A 60 (1999) 538.